COMPRESSIBILITY CHARACTERISTICS OF UNDISTURBED SNOW

Gunars Abele, et al

Cold Regions Research and Engineering Laboratory
Hanover, New Hampshire

May 1975

Research Report 336

COMPRESSIBILITY CHARACTERISTICS OF UNDISTURBED SNOW

Gunars Abele and Anthony J. Gow

May 1975

CORPS OF ENGINEERS, U.S. ARMY
COLD REGIONS RESEARCH AND ENGINEERING LABORATORY
HANOVER, NEW HAMPSHIRE

REPORT DOCUMENTATION PAGE

READ INSTRUCTIONS BEFORE COMPLETING FORM

1. REPORT NUMBER: Research Report 336
2. GOVT ACCESSION NO.:
3. RECIPIENT'S CATALOG NUMBER:

4. TITLE (and Subtitle): COMPRESSIBILITY CHARACTERISTICS OF UNDISTURBED SNOW
5. TYPE OF REPORT & PERIOD COVERED:
6. PERFORMING ORG. REPORT NUMBER:

7. AUTHOR(s): Gunars Abele and Anthony J. Gow
8. CONTRACT OR GRANT NUMBER(s):

9. PERFORMING ORGANIZATION NAME AND ADDRESS: U.S. Army Cold Regions Research and Engineering Laboratory, Hanover, New Hampshire 03755
10. PROGRAM ELEMENT, PROJECT, TASK AREA & WORK UNIT NUMBERS: DA Project 4A161101A91D, Work Unit 168

11. CONTROLLING OFFICE NAME AND ADDRESS: U.S. Army Cold Regions Research and Engineering Laboratory, Hanover, New Hampshire 03755
12. REPORT DATE: May 1975
13. NUMBER OF PAGES: 62

14. MONITORING AGENCY NAME & ADDRESS (if different from Controlling Office):
15. SECURITY CLASS. (of this report): Unclassified
15a. DECLASSIFICATION/DOWNGRADING SCHEDULE:

16. DISTRIBUTION STATEMENT (of this Report)

Approved for public release, distribution unlimited.

17. DISTRIBUTION STATEMENT (of the abstract entered in Block 20, if different from Report)

18. SUPPLEMENTARY NOTES

19. KEY WORDS (Continue on reverse side if necessary and identify by block number)

Compressive properties
Crystals
Mechanical properties
Snow
Stresses
Trafficability

20. ABSTRACT (Continue on reverse side if necessary and identify by block number)

The effects of snow temperature, rate of deformation, and initial density on the stress vs density and stress vs deformation relationships were investigated in the pressure range of 0.1 to 75 bars. The rate of deformation in the range of 0.027 to 27 cm sec^{-1} does not have a significant effect. A decrease in temperature in the range of 0° to –40°C increases the resistance to stress and deformation, the temperature effect increasing with applied pressure and initial density. The effect of initial density is significant. For any stress, an increase in the initial density results in an increase in the resulting density, particularly at low stress levels and at temperatures near 0°C. The texture of artificially compacted snow is significantly different from that of naturally compacted snow of the same density because of the very short recrystallization time period.

PREFACE

This study was conducted by Gunars Abele, Research Civil Engineer, Applied Research Branch, Experimental Engineering Division; Dr. Anthony J. Gow, Research Geologist, Snow and Ice Branch, Research Division, performed the microstructural analysis. The work was performed under DA Project 4A161101A91D, *In-House Laboratory Independent Research*, Work Unit 168.

Dr. Malcolm Mellor participated in the formulation of this study and the analysis of the results, and reviewed the report. Larry Gould designed the sample containers and assisted in the laboratory tests. The Materials Testing System was operated by Allen George.

The contents of this report are not to be used for advertising, publication, or promotional purposes. Citation of trade names does not constitute an official endorsement or approval of the use of such commercial products.

CONTENTS

ILLUSTRATIONS

NOMENCLATURE

		Range
w	Load (kg)	Up to 9500
v	Rate of deformation (cm sec^{-1})	0.027 to 27
T	Temperature (°C)	0 to -40
ρ_0	Initial snow density (g cm^{-3})	0.09 to 0.27
ρ	Density after load application (g cm^{-3})	To 0.9
d	Sample diameter (cm)	12.7, 20.3, 29.0
h_0	Sample height (cm)	2.5, 5.1, 7.6, 10.2, 12.7
z	Vertical deformation of sample (cm)	Up to 0.9 h_0
σ_1	Major principal stress (bar) (bar = 0.98 kg cm^{-2})	Up to 75

COMPRESSIBILITY CHARACTERISTICS OF UNDISTURBED SNOW

by

Gunars Abele and Anthony J. Gow

INTRODUCTION

The mechanical characteristic of snow that distinguishes it most strongly from typical engineering materials, including soils, is its high compressibility. Moderate bulk stress can produce large volumetric strain and, as a result, the resistance to deviatoric stress can change dramatically. An essential requirement for the advance of snow mechanics in general, and mobility/trafficability analysis in particular, is the definition of snow compressibility relationships for a wide range of loading rates and snow characteristics.

When bulk stress is plotted against density (i.e. the dimensional inverse of specific volume) with loading rate as a parameter, the family of curves is bounded at the upper limit by the Hugoniot (locus of final states for adiabatic shock compression), and at the lower limits by the locus of asymptotic values for slow isothermal creep under triaxial compression. At the present, these curves can only be roughly deduced from scattered data sources (Mellor 1974). It is desirable to have the curves clearly defined by direct experiment, since they represent "equations of state" that are important for the definition of shear strength and deviatoric stress-strain rate relationships.

The relevance to mobility/trafficability is two-fold. First, the data are pertinent to the compaction of snow under a track or a wheel, especially for the case of a finite snow layer on a rigid base. Secondly, compressibility relations provide the basis for subsequent systematic studies of shear strength. Regarding the latter, it is important to recognize that attempts to apply Mohr-Coulomb failure theory to snow become very confusing when the bulk stress, or normal stress, is high enough to collapse the snow and, in effect, change it into a different material.

DESCRIPTION OF STUDY

Sample preparation

Circular aluminum containers with the following dimensions were constructed:

Inside diameter d (cm)	12.7	12.7	20.3	20.3	29.0	29.0	29.0
Height h_0 (cm)	2.5	5.1	5.1	7.6	7.6	10.2	12.7

Each cylinder was removable from the baseplate, facilitating sample removal for final height measurements and preparation of thin sections for microstructure analysis. To eliminate any friction between the load plate and the inside of the cylinder, a radial clearance of 0.15 cm was provided (Fig. 1).

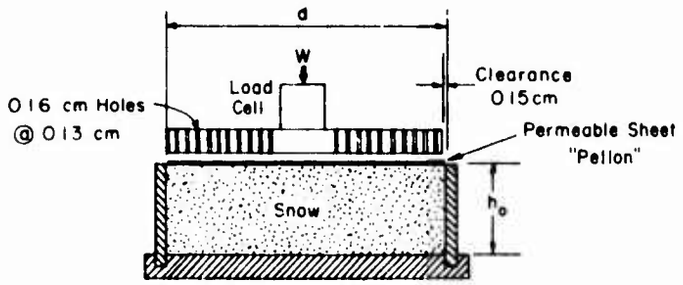

Figure 1. Test setup.

Initial trials at high deformation rates made it obvious that some provision had to be made to allow air to escape easily from the snow sample during compression. When a solid plate was used at a compression rate of 27 cm sec^{-1}, the air resistance itself was only approximately 0.07 kg cm^{-2}, but the escaping air had a tendency to blow some snow out through the peripheral clearance around the load plate. Small holes were drilled through the load plate, and a fitted sheet of Pellon, permeable to air but not snow particles, was placed between the surface of the snow sample and the load plate (Fig. 1)

Snow samples were collected by placing the containers outside during periods of snowfall. The samples were then placed in coldrooms at various temperatures, usually for a period of hours, to ensure that the snow temperature was the same as that in the test chamber. During the storage period, the containers with the snow samples were sealed in plastic bags. The sealing was done while the samples were still outside; some excess snow was left on top of each sample to compensate for any subsequent settlement that might occur before the test. The plastic bag was removed and the top surface of the snow shaved before the sample was placed in the test chamber.

Test equipment and procedure

The compression tests were conducted with a modern 10,000-kg load capacity servo-controlled MTS machine equipped with an environmental test chamber (temperature control to -50°C). The load vs ram displacement trace during the test was displayed and stored on an oscilloscope screen; a polaroid photograph of the trace was taken after each test (see Appendix). The load and deformation data were obtained from the photographs.

The MTS was equipped with a closely calibrated ram speed control and was capable of any rate of deformation from 0 to 27 cm sec^{-1}. (Subsequent to these tests, the ram travel speed was readjusted to produce a maximum of 40 cm sec^{-1}.)

After the snow sample was positioned in the test chamber, the load plate, which was attached to a load cell, was moved down to the top of the sample and the oscilloscope trace adjusted to the zero position. The MTS was set to the desired deformation rate, and the temperature in the chamber was checked.

Immediately after the test, the sample was transferred to a coldroom where the sample was measured and weighed. The initial density was determined from the sample weight and the known

initial volume (no snow was lost during the test). The final density was determined by measuring the height of the sample after the test. The density at any point during the test was computed from data from the load-deformation trace photograph.

All tests were performed to near the maximum load capability of the testing system. The maximum resulting pressure was therefore approximately 15 bars on the large diameter (29.0 cm) samples, 29 bars on the medium diameter (20.3 cm) samples, and 75 bars on the small diameter (12.7 cm) samples (1 bar = 0.98 kg cm^{-2}). The load scale of the oscilloscope readout was varied so that for some tests the entire load-deformation trace could be seen, while for other tests the scale was enlarged so that the behavior in the low stress region of the load-deformation trace could be observed in more detail, although this meant the loss of the trace in the higher stress regions. The deformation scale was also varied, depending on sample height. Photographs of the load-deformation traces are shown in the Appendix.

The rate of deformation and the snow (and test chamber) temperature were the controlled, preselected parameters. The inital snow density, however, could not be controlled. Those samples which were tested at the low temperatures (-20° to -40° C) required some time, usually several hours or overnight, to reach the desired temperature, since the snowfall during the collection period occurred at somewhat higher temperatures. This "cooling off" period generally resulted in some settlement and thus the samples had a higher density than those tested at near-ambient temperatures soon after collection. Some samples were stored at a constant temperature for several days prior to testing.

The temperature of the snow during any test was either near the ambient temperature observed during the collection period or at a lower temperature achieved during storage in a coldroom. In no case was a sample tested at a temperature higher than that at which it was stored.

Sections for the microscopic (thin section) inspection were taken from the samples after the volumetric measurements and stored at -35°C.

The comparison tests and the test conditions are listed in Table I.

DISCUSSION OF RESULTS

Stress-density relationship

The range of the test data is shown in Figure 2, superimposed on Mellor's (1974) Figure 13, which summarizes the results of various uniaxial strain experiments. It is interesting to note that the stress-density data, obtained at deformation rates between 0.027 and 27 cm sec^{-1}, coincide wtih the Hugoniot data (region F) for explosively generated shock waves at impact velocities 2 to 4 orders of magnitude higher. This implies that compression or strain rate is not a very influential parameter on the stress-density relationship in this range.

Mellor's (1974) calculated values for plane wave impact (region E in Fig. 2) could not be confirmed experimentally, at least not in the density region below 0.3 g cm^{-3}. This, however, does not imply disagreement; Mellor's values were calculated for impact at 20 to 40 m sec^{-1}, roughly 2 orders of magnitude higher than the maximum deformation rate in these experiments. At a density of 0.3 g cm^{-3} and above, tests on the snow samples with a low initial density (0.09 g cm^{-3}, tests 37, 38) did produce stress values comparable to those calculated by Mellor ($\sigma_1 \gtrsim 2$ bars). Mellor's most recent calculated values for avalanche impact pressures at 10 m sec^{-1} (line L in Fig. 2) show good agreement.

Table I. Summary of tests.

Test	Temp T (°C)	Rate of deform v (cm sec^{-1})	Sample size Diam d (cm)	Sample size Height h_0 (cm)	Initial density ρ_0 (g cm^{-3})	Final density ρ_f (g cm^{-3})	Final stress σ_f (bar)
1	− 7	27	20.3	7.5	0.15	0.88	29.5
2	− 7	27	20.3	7.5	0.14	0.83	29.5
3	− 7	27	20.3	7.5	0.39	0.72	28.8
4	Air resis-	27	20.3	7.5	Perforated plate		0.014
5	tance tests	27	20.3	7.5	Solid plate		0.067
6	− 7	27	20.3	7.5	0.20	0.76	29.5
7	−18	27	20.3	7.5	0.12	0.65	29.5
8	−18	27	20.3	7.5	0.18	0.71	26.0
9	−18	27	20.3	7.5	0.18	0.77	28.3
10	0	27	20.3	7.5	0.20	0.90	29.5
11	0	27	20.3	7.5	0.19	0.90	27.0
12	0	2.7	20.3	7.5	0.22	0.87	27.3
13	0	0.27	20.3	7.5	0.21	0.89	26.5
14	-30	27	29.0	7.6	0.18	0.61	13.8
15	−30	27	29.0	12.7	0.16	0.60	14.8
16	No oscilloscope trace						
17	−40	27	29	7.6	0.19	0.60	13.8
18	−40	27	29	10.2	0.14	0.60	14.5
19	−40	27	12.7	5.1	0.24	0.73	71.6
20	−30	27	12.7	2.5	0.27	0.74	69.1
21	-40	27	12.7	2.5	0.27	0.77	72.0
22	-40	0.27	12.7	2.5	0.25	0.75	72.0
23	−40	0.027	12.7	5.1	0.19	0.74	68.0
24	−20	27	12.7	2.5	0.22	0.80	72
25	−20	0.027	12.7	2.5	0.22	0.80	67
26	− 5	27	12.7	5.1	0.23	0.84	72
27	− 5	0.027	12.7	5.1	0.23	0.85	66
28	−35	27	29.0	7.6	0.14	0.59	14.5
29	−35	27	29.0	10.6	0.20	0.60	14.5
30	−35	0.027	29.0	10.2	0.18	0.58	13.8
31	-40	27	29.0	10.2	0.17	0.61	14.5
32	-20	27	29.0	7.6	0.17	0.60	14.5
33	− 1	27	29.0	10.2	0.11	0.60	14.5
34	− 1	0.27	29.0	10.2	0.12	0.56	14.5
35	− 1	0.027	29.0	10.2	0.13	0.57	14.5
36	− 1	27	12.7	5.1	0.13	0.90	75
37	− 1	0.27	12.7	5.1	0.09	0.89	75
38	− 1	0.027	12.7	5.1	0.09	0.88	75
39	− 1	27	12.7	5.1	0.18	0.90	75
40	−20	0.27	29	7.6	0.11	0.56	14.5
41	−20	0.027	29	7.6	0.11	0.55	14.5
42	−20	0.27	20.3	5.1	0.18	0.71	29.4
43	−20	0.027	20.3	5.1	0.10	0.66	29.4
44	−35	0.27	20.3	7.6	0.16	0.63	29.4
45	−35	0.027	20.3	7.6	0.17	0.68	29.4
46	−35	0.27	12.7	2.5	0.12	0.73	75.0
47	−35	0.027	12.7	2.5	0.12	0.74	75.0
48	− 3	27	12.7	2.5	0.10	0.88	75.0
49	− 3	0.027	12.7	2.5	0.11	0.86	75.0
50	− 3	0.027	20.3	7.6	0.14	0.66	29.4
51	− 3	27	29.0	12.7	0.13	0.63	14.5
52	−20	27	29.0	12.7	0.17	0.50	14.5
53	−20	0.027	29.0	7.6	0.23	0.60	14.5
54	−20	27	12.7	2.5	0.18	0.78	75
55	−20	0.027	12.7	5.1	0.18	0.74	75
56	−35	27	12.7	2.5	0.18	0.73	75
57	−35	0.027	12.7	2.5	0.18	0.73	75
58	−20	27	12.7	2.5	0.26	0.76	71.6
59	−35	27	20.3	7.5	0.14	0.67	29.4

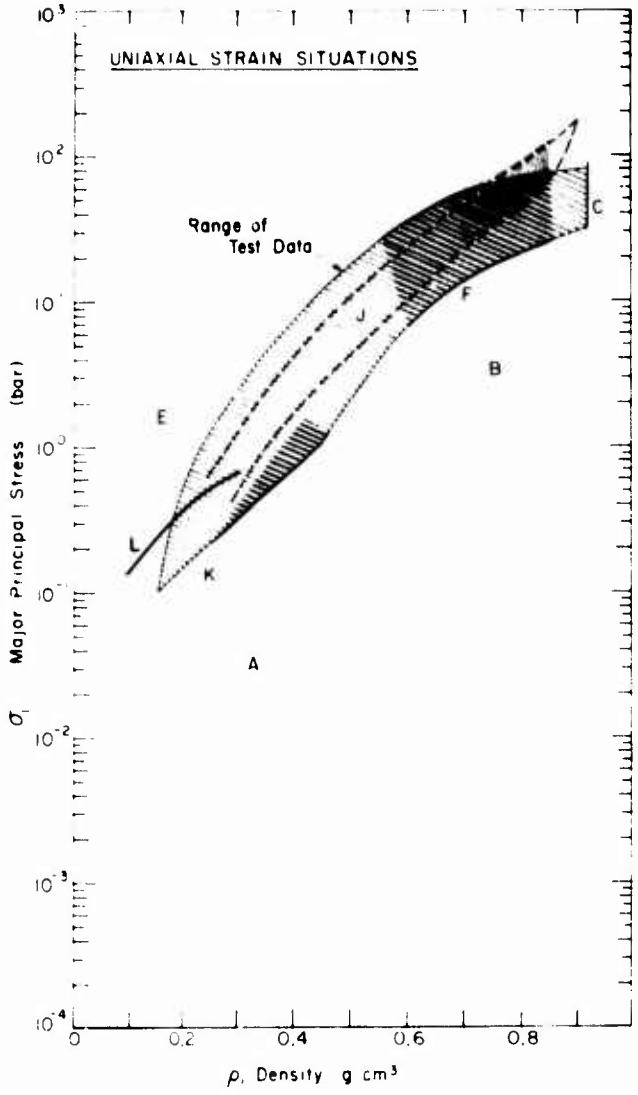

Compilation of data relating major principal stress to bulk density for compression in uniaxial strain at various rates and temperatures. (From Mellor 1974)
A: Natural densification of snow deposits, -1° to -48°C. Approximate average loading rates 10^{-10} to 10^{-8} bar/sec (data from depth/density curves for many sites). *B*: Slow natural compression of dense firn and porous ice. Approximate loading rates 10^{-10} to 10^{-9} bar/sec (from depth/density curves for polar ice caps). *C*: Slow compression of solid ice. *E*: Calculated values for plane wave impact at 20 to 40 m/sec. *F*: Hugoniot data for explosively generated shock waves (impact velocities 1 to 12 m/sec), -7° to -18°C. *J*: Compression at approximately constant strain rate, -7° to -18°C. Strain rate ≈ 10^{-4} sec^{-1} (Kinosita 1967). *K*: Compression in uniaxial strain - incremental loading to collapse, -2° to 3°C. *L*: Calculated values of avalanche impact pressures at 10 m sec^{-1} (Mellor in press).

Variable		*Range*
T_1	Temperature	0 to -40°C
ρ_0	Initial density	0.09 to 0.27 g cm^{-3}
$\dot{\nu}$	Rate of deformation	0.027 to 27 cm sec^{-1}
h_0	Sample height	2.5 to 12.7 cm
d	Sample diameter	12.7 to 29 cm

Figure 2. Range of test data.

The major principal stress vs density data were plotted in various ways, with the rate of deformation and temperature as the parameters. It soon became evident that the initial density of the samples also had to be considered as a controlling parameter. In fact, the effect of the initial density was more pronounced than the temperature effect, while the effect of the rate of deformation was obscured.

Figure 3 shows the σ_1 vs ρ relationship with temperature as a parameter for two groups of densities: 0.10 to 0.12 and 0.20 to 0.27 g cm^{-3}. The influence of temperature does not become prominent until a stress level above 10 bars is reached, the stress at any density increasing with a decrease in temperature. At temperatures very near 0°C, the density of ice is approached at stress levels below 30 bars, while at -40°C the same stress results in a density of less than 0.7 g cm^{-3} (Fig. 3b).

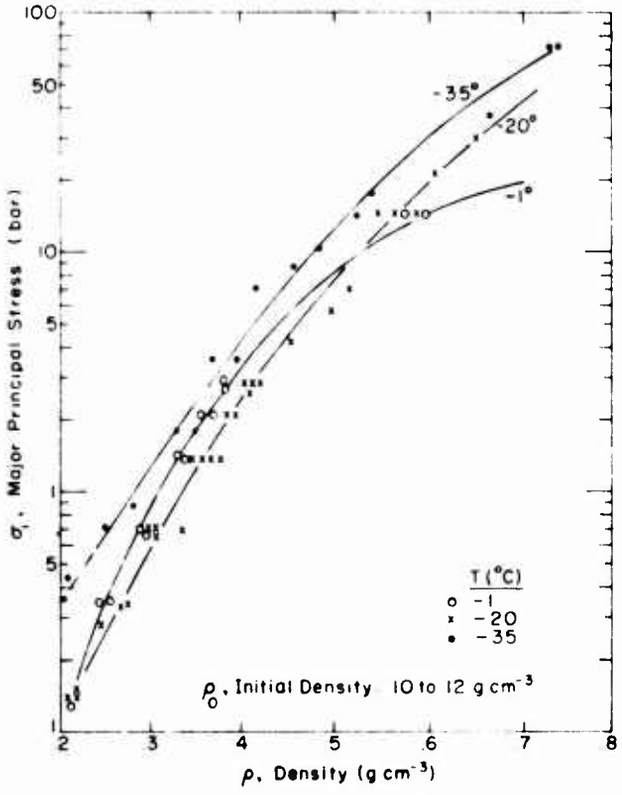

a. Initial density 0.10 to 0.12 g cm^{-3}

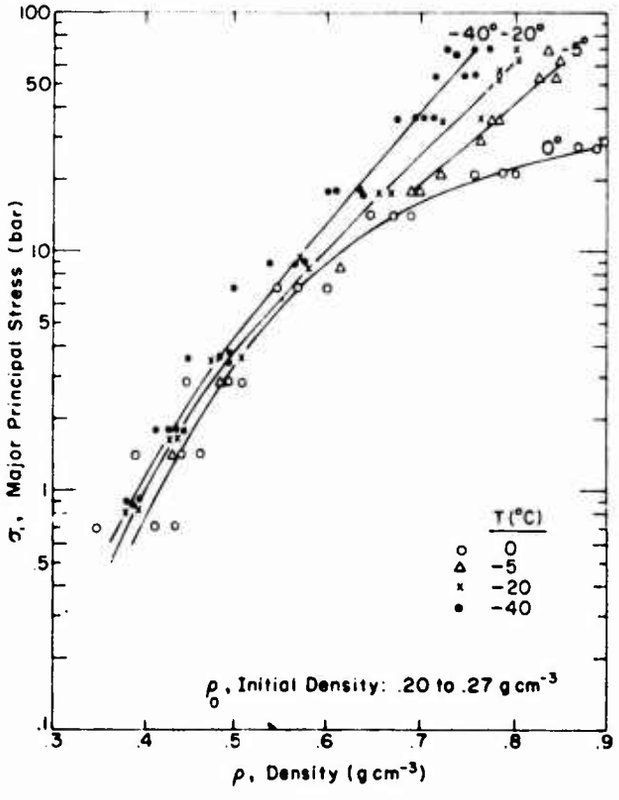

b. Initial density 0.20 to 0.27 g cm^{-3}.

Figure 3. Major principal stress vs density with temperature as a parameter.

Figure 4 shows the σ_1 vs ρ relationship for various temperatures with initial density as a parameter. The influence of the initial density is particularly strong at temperatures near 0°C (Fig. 4a), the stress at any density increasing with a decrease in the initial density. At a density of 0.4 g cm^{-3}, for example, a change in the initial density from 0.2 to 0.1 represents an order of magnitude increase in the stress value.

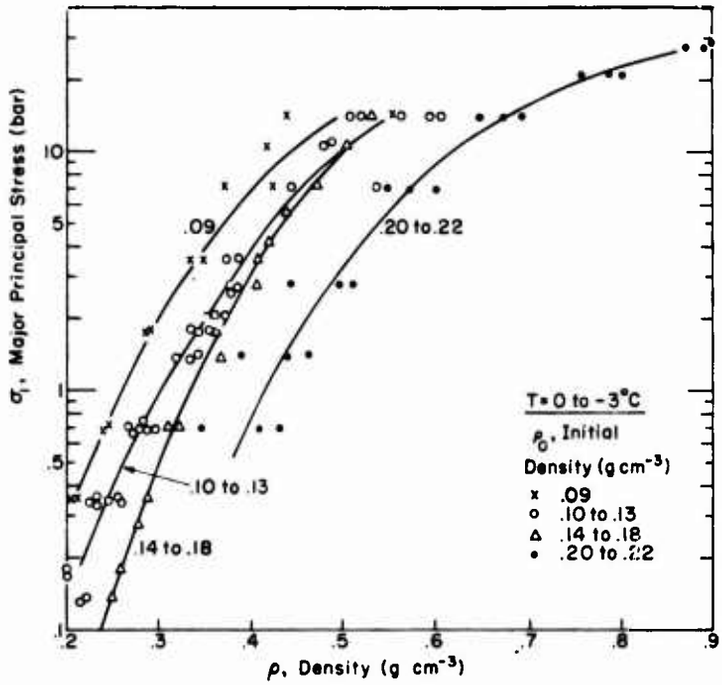

a. Temperature 0 to -3°C.

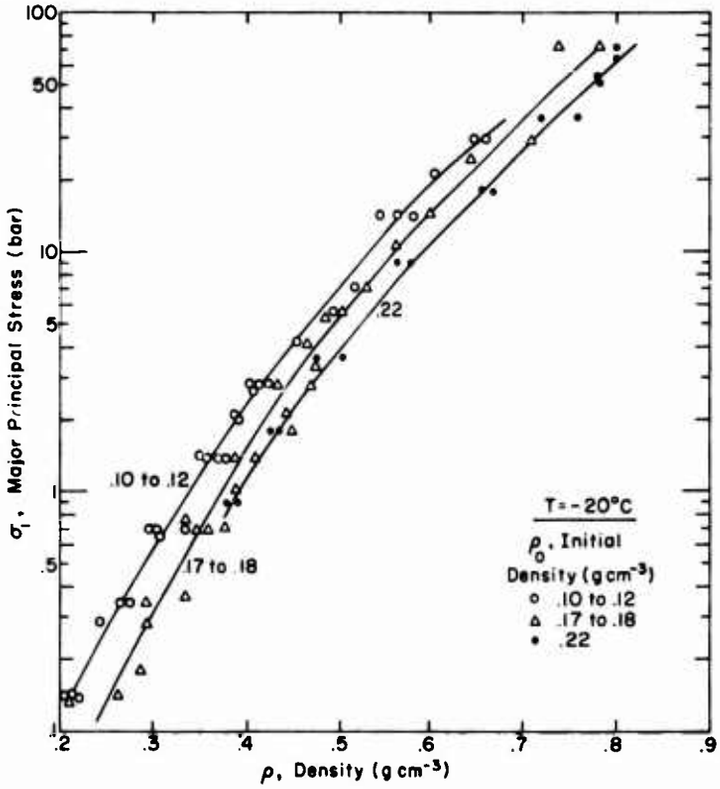

b. Temperature -20°C.

Figure 4. Major principal stress vs density with initial density as a parameter.

At higher temperatures, the plot of log σ_1 vs ρ results in a curve (Fig. 4a); as the temperature decreases, the log σ_1 vs ρ relationship approaches a straight line (Fig. 4d) in the stress range of 0.1 to 75 bars.

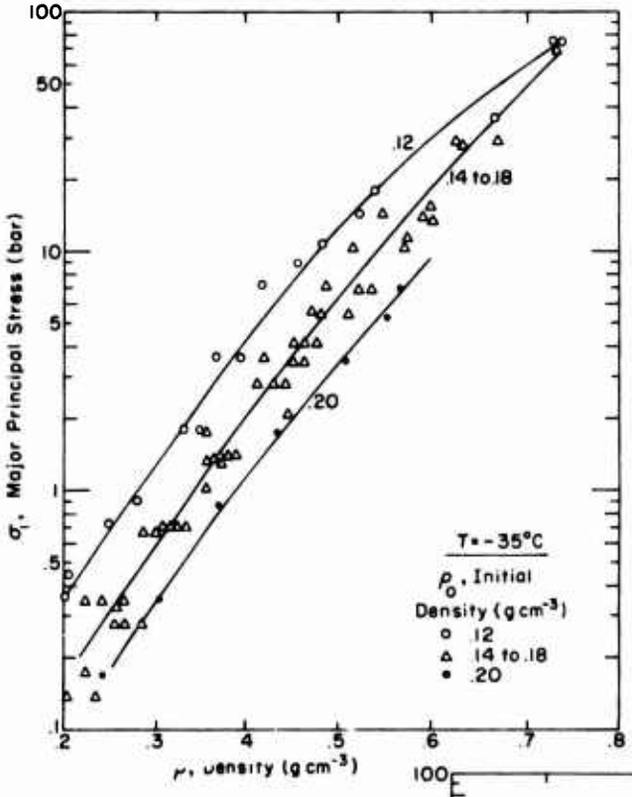

c. Temperature -35°C.

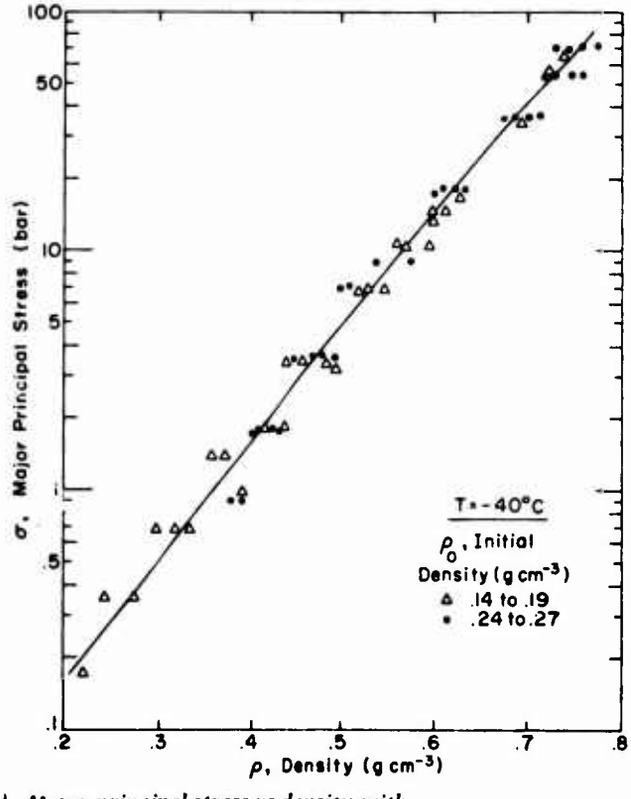

d. Temperature -40°C.

Figure 4 (cont'd). Major principal stress vs density with initial density as a parameter.

Although the strain rates in these tests were 1 to 4 orders of magnitude higher than those of Kinosita (1967), shown as region J in Figure 2, data at -20°C (Fig. 4b) show excellent agreement with his values at -7° to -18°C.

The significant findings from these tests are:

1. The great sensitivity of the σ_1 vs ρ relationship to the initial density of snow.
2. The lack of any significant sensitivity of the σ_1 vs ρ relationship to the loading or strain rate.

These effects are discussed and shown in more detail later.

Effect of rate of deformation

The major principal stress vs rate of deformation data with density as a parameter are shown for various temperatures in Figure 5. At near 0°C (Fig. 5a, b), the rate of deformation has no effect on the stress for densities above 0.6 g cm^{-3}. At densities below 0.6 an increase in the deformation rate results in a slight decrease in stress; this was evident for both the 0.1 and 0.2 (initial density) snow.

At temperatures of -20°C and below, an increase in the deformation rate results in a low rate increase in stress at all densities (Fig.5c, d). An increase of 1 order of magnitude in the rate of deformation corresponds to a stress increase of approximately 5% at 0.7 density and 10% to 15% at 0.3 density.

The apparent lack of any definite effect due to a change in the sinkage rate of plates in snow has also been reported by Harrison (1957).

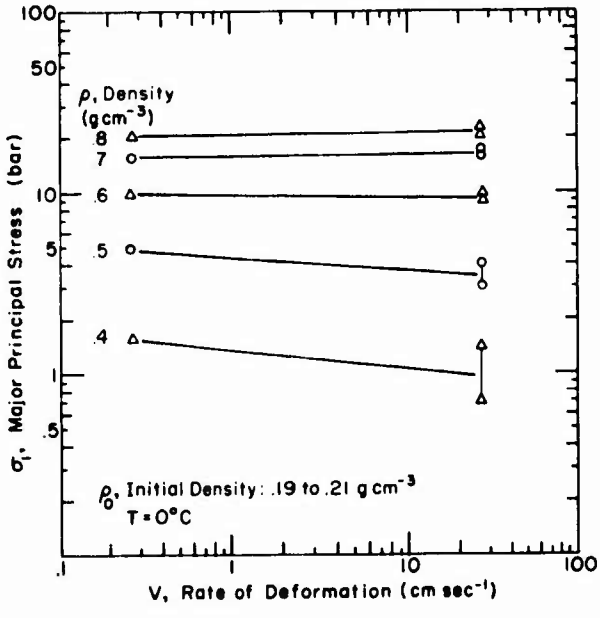

a. Temperature 0°C, initial density 0.19 to 0.21 g cm^{-3}.

Figure 5. Major principal stress vs rate of deformation with density as a parameter.

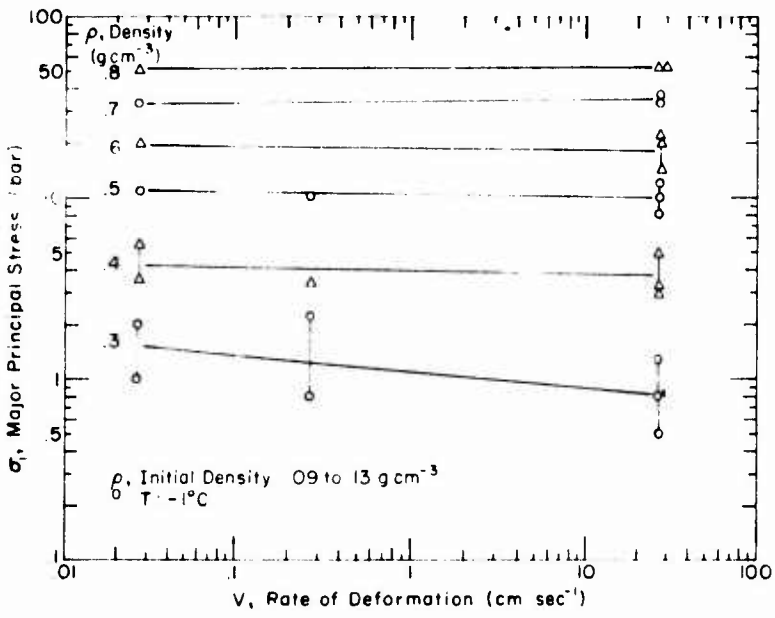

b. Temperature -1°C, initial density 0.09 to 0.13 g cm⁻³

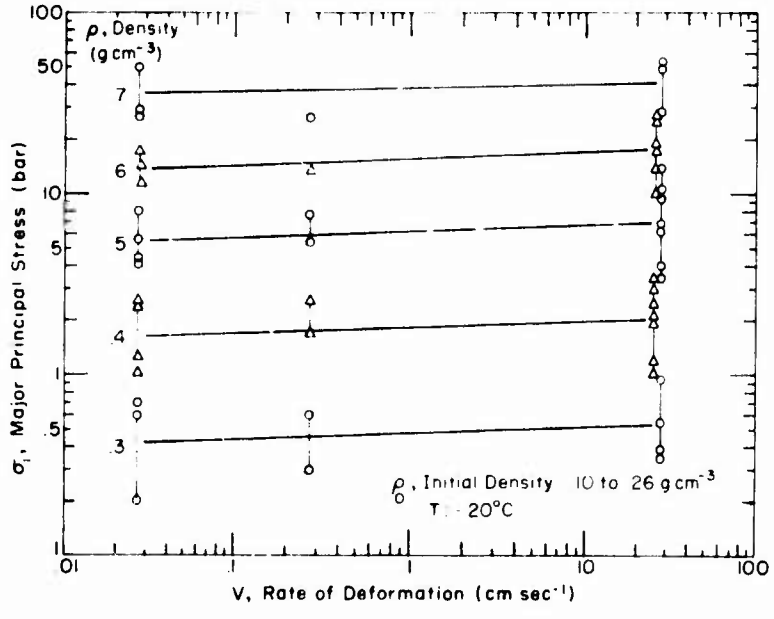

c. Temperature -20°C, initial density 0.10 to 0.26 g cm⁻³

Figure 5 (cont'd). Major principal stress vs rate of deformation with density as a parameter.

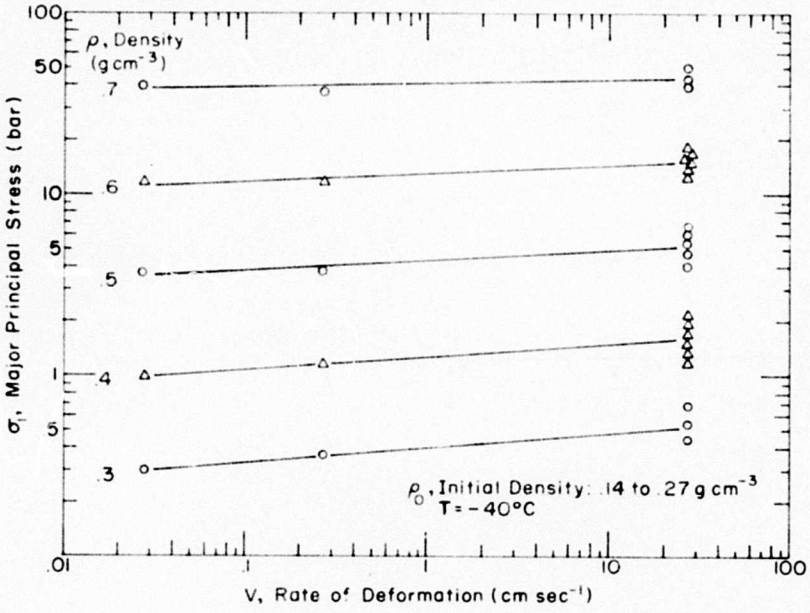

d. Temperature -40°C, initial density 0.14 to 0.27 g cm^{-3}.

Figure 5 (cont'd).

Extrapolation of the 0.3 density line in Figure 5d to Mellor's (1974) plane wave impact rates of 20 to 40 m sec^{-1} (roughly 2 orders of magnitude higher) yields a stress value of approximately 0.9 bar. Mellor's values at the 0.3 density point are between 2.5 and 9 bars (Fig. 2). However, as shown previously in Figure 4a, the two snow samples with a very low initial density (0.09 g cm^{-3}) gave a stress value of 2 bars at the 0.3 density point, at a temperature near 0°C. The data here suggest that snow of a low initial density ($\approx$ 0.1 g cm^{-3}) compressed at a high rate and at a low temperature may result in stress values comparable to those calculated by Mellor for plane wave impact. The data are in agreement with Mellor's calculated values for avalanche impact pressures at 10 m sec^{-1}.

Effect of temperature

Figure 6 shows the stress vs temperature relationship with density as a parameter. For snow with a low initial density (0.10 to 0.14 g cm^{-3}) the stress is not sensitive to temperature at densities below 0.5 (Fig. 6a); an increase in stress values does occur with a decrease in temperature at densities above 0.5. Snow with a higher initial density (0.20 to 0.27) shows an increase in stress with decreasing temperature at all densities, the effect of temperature becoming more pronounced with an increase in density (Fig. 6b).

The same data are shown in Figure 7 as a density vs temperature relationship with stress as a parameter for the two groups of initial snow densities.

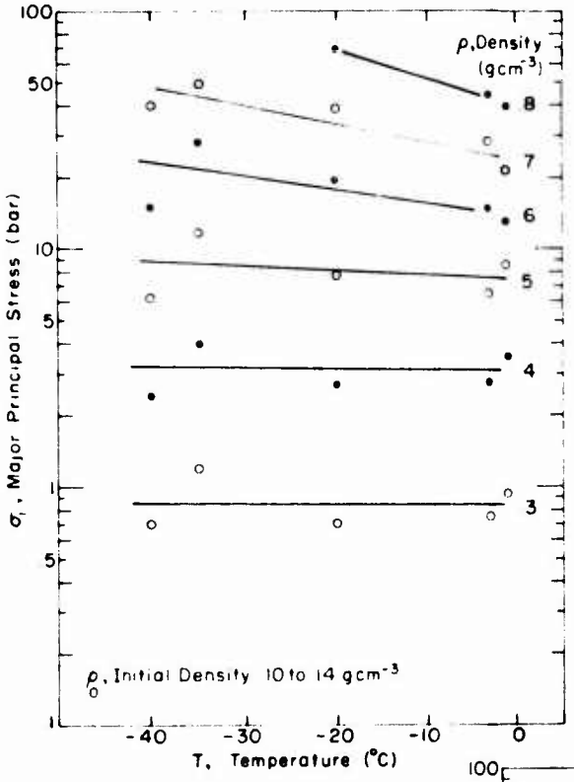

a. Initial density 0.10 to 0.14 g cm^{-3}.

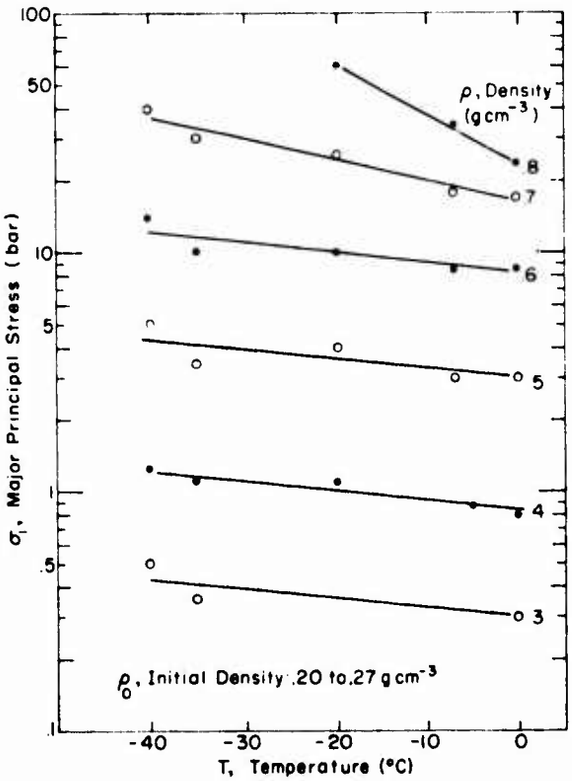

b. Initial density 0.20 to 0.27 g cm^{-3}.

Figure 6. Major principal stress vs temperature with density as a parameter.

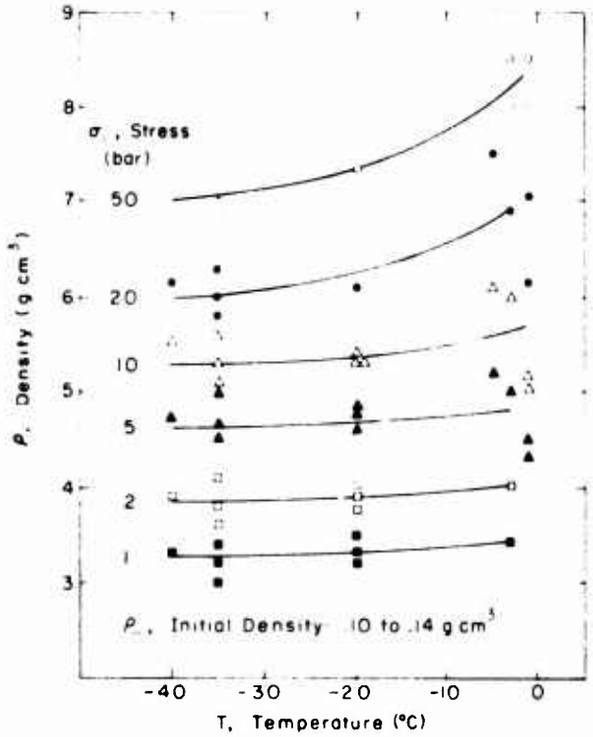

a. Initial density 0.10 to 0.14 g cm^{-3}.

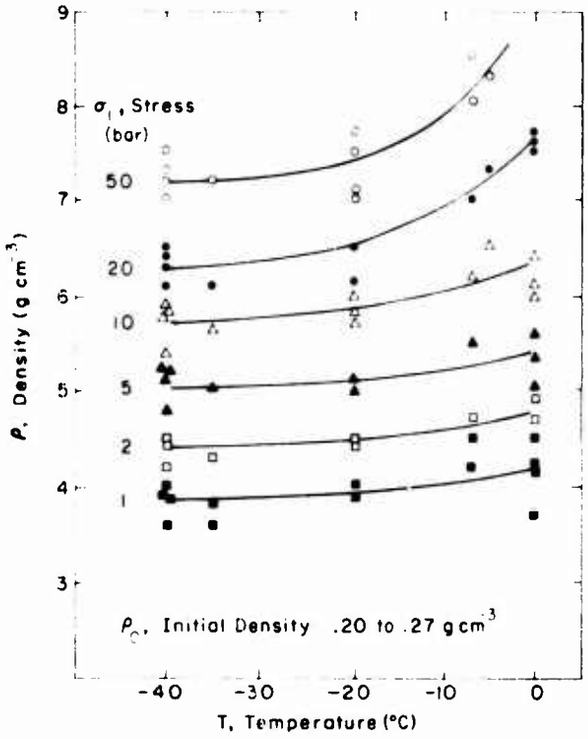

b. Initial density 0.20 to 0.27 g cm^{-3}.

Figure 7. Density vs temperature with stress as a parameter.

Effect of initial snow density

The influence of the initial snow density on the stress-density relationship has been very evident throughout the previously shown graphs. Prior to these tests, it had been intuitively assumed that a specific pressure applied to a snow surface would result in a specific snow density. That is, at a particular temperature and rate of loading, fresh, undisturbed snow would have to be compressed to a particular density to resist the particular pressure, regardless of the density of the snow prior to the load application, the initial density determining only the extent of deformation (sinkage), not the resulting density. It was expected that a pressure of 1 bar (or approximately 1 kg cm^{-2}), for example, applied to snow with an initial density of 0.1 g cm^{-3}, would compact the snow to the same density as if the same pressure had been applied to snow with an initial density of 0.2 g cm^{-3}. That this assumption was incorrect is evident in Figures 8a, b.

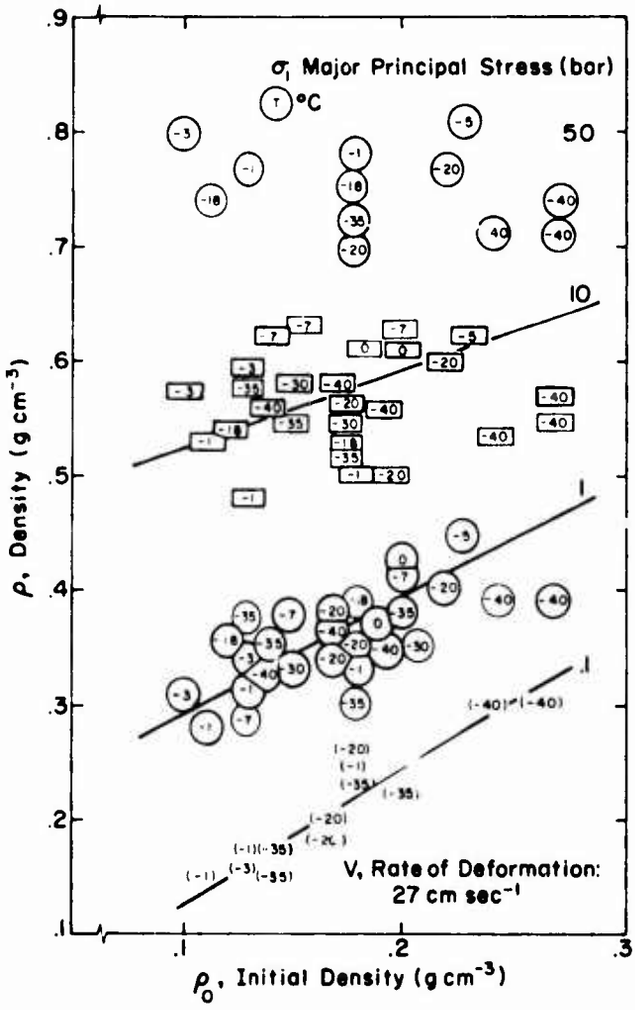

a. Rate of deformation 27 cm sec^{-1}.

Figure 8. Density vs initial density with stress as a parameter.

For example, a pressure of 1 bar applied at a rate of 27 cm sec^{-1} to 0.1 density snow yielded a resulting density of approximately 0.3 (Fig. 8a). The same pressure applied to a 0.2 density snow yielded a resulting density of 0.4. The temperature, shown for each data point in Figure 8a, was not a controlling parameter, at least not for pressures up to 10 bars.

This phenomenon could not be attributed to any lag in the readout mechanism (in this case, the ram travel readout lagging behind the load readout on the oscilloscope screen at high ram travel rates), since the same effect of initial density was observed also at deformation rates (ram travel) 1000 times slower (Fig. 8b).

The data from Figures 8a and b are replotted in a more convenient and meaningful manner in Figures 8c and d, respectively. The effect of the initial snow density is particularly significant at low stress levels for both the fast (27 cm sec^{-1}) and slow (0.027 cm sec^{-1}) deformation rates, the lines converging, by necessity, toward the upper boundary condition*: $\rho = \rho_0 = \rho_{ice}$.

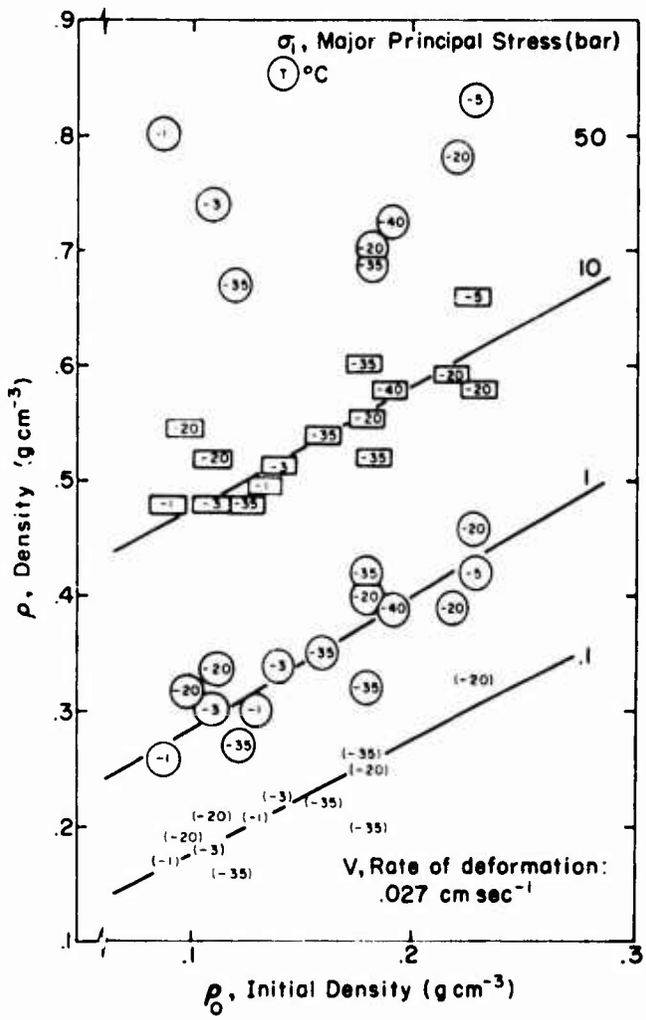

b. Rate of deformation 0.027 cm sec^{-1}.

*It should be noted that no data are yet available for snow with initial densities above 0.3 g cm^{-3}. Consequently, the convergence toward the upper boundary condition may not necessarily follow straight lines as shown in Figures 8c and d. For low stress levels and high initial densities, the lines will very likely move and approach the envelope $\rho = \rho_0$ and then continue toward ρ_{ice}.

The reason for the influence of the initial density on the stress-density relationship is not clear. To compact snow, which has an initial density of 0.1 g cm^{-3}, to a density of 0.5 g cm^{-3} requires a pressure of 10 bars, while to compact 0.3 density snow to a density of 0.5 requires a pressure of only 1 bar (Fig. 8c and d). That same pressure of 1 bar, applied to the 0.1 density snow, would result in a density of only 0.3 g cm^{-3}.

Looking from another perspective: to resist a pressure of 10 bars, a 0.1 density snow has to be compacted to a density of 0.5, while a 0.2 density snow would have to be compacted to a density of 0.6 g cm^{-3} (Fig. 8c and d).

One explanation is possible under the following hypothesis: the particle shape of fresh, low density snow (0.1 g cm^{-3}) is very irregular, consisting of needles, plates, etc. in a structurally random orientation. When the snow is subjected to stress, densification is achieved primarily by breaking these irregular particles; the original structure is destroyed through actual crushing or breaking of the structural components. In a higher density snow (0.3 g cm^{-3}, for example) the particle size is more regular, more nearly spherical, due to settlement and metamorphism. When this snow is subjected to stress, densification is achieved primarily through reorientation of the particles; breaking of the bonds between the particles occurs, combined with the subsequent frictional resistance during particle reorientation. If the total cross-sectional area of the broken bonds for the 0.3 density snow is less than the total cross-sectional area of the broken particles in the 0.1 density snow, the latter will produce a higher resistance to stress. Temperature being the same, the cross-sectional area of the material to be broken becomes the controlling stress resistance parameter.

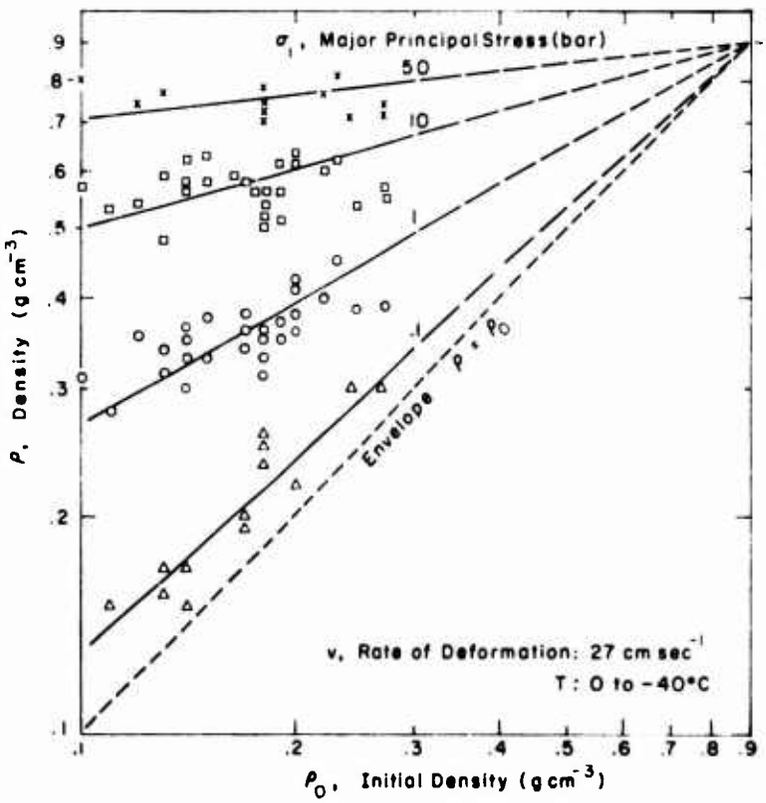

c. Rate of deformation 27 cm sec^{-1} (log-log plot).

Figure 8 (cont'd). Density vs initial density with stress as a parameter.

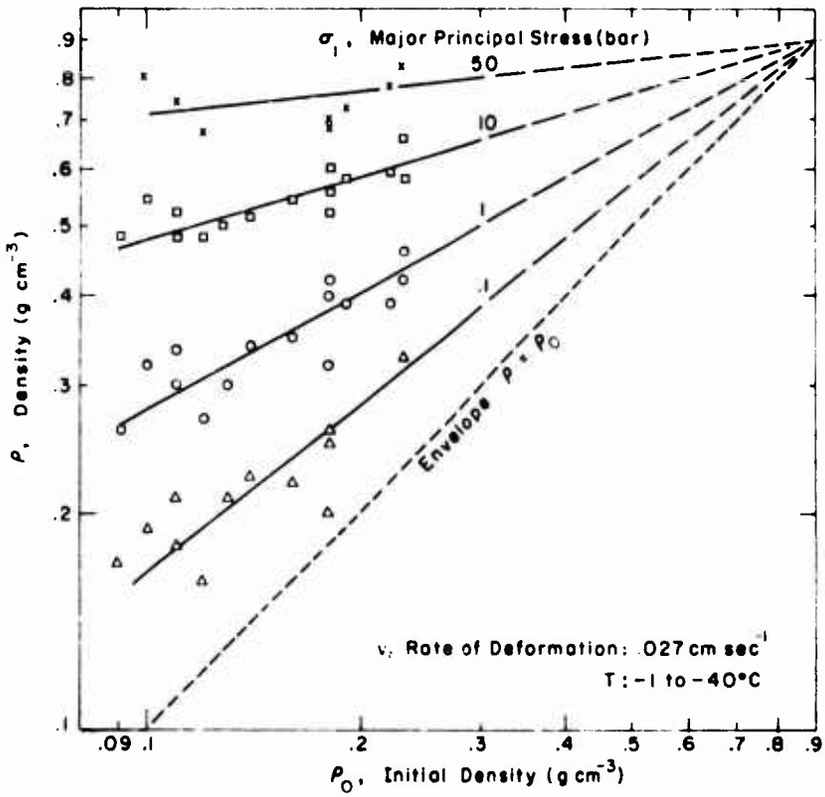

d. Rate of deformation 0.027 cm sec^{-1} (log-log plot).

Frictional resistance during the subsequent reorientation of the particles would be present in both cases. But reorientation of the irregular particles in the first case (0.1 density snow) would not be possible without breaking of the particles themselves, while in the second case (0.3 density snow) reorientation of the more spherical particles would be possible only by breaking of the intergranular bonds. (In an analogy, it is not difficult to visualize that at relatively low stress a mass of sticks and irregular plates in a random orientation may produce a higher resistance to densification than a mass of balls arranged in a loose, highly porous structure. In the first case, densification could be achieved primarily by breaking the structural elements of the mass, while in the second case, densification could be achieved by mere rearrangement of the balls under vertical pressure.)

This hypothesis may explain the behavior of the snow at low stress levels. As stress is increased the mechanism of further densification becomes more similar for both snows, since their structures are becoming more similar, and the effect of initial density, therefore, becomes less pronounced.

The rate of deformation has some influences at the low stress levels (below 1 bar), the resistance to stress being slightly higher at the high rate of deformation. Snow with an initial density of 0.15 g cm^{-3} produced a resistance to stress below 0.1 bar at 0.2 density when compressed at the rate of 0.027 cm sec^{-1} (Fig. 8d), while at the 27 cm sec^{-1} rate, the resistance to stress at 0.2 density was above 0.1 bar (Fig. 8c). The effect of deformation rate was no longer evident at 1 bar and above.

Stress-deformation relationship

For application in snow trafficability analyses, the stress-deformation (pressure-sinkage) behavior of snow is of a more practical significance than the stress-density relationship.

The deformation data are plotted as function of initial density, with stress as a parameter, in Figure 9. Initial plotting of deformation vs initial density for the various sample heights did not show the sample height (2.5 to 12.7 cm) to be a controlling parameter; it was therefore possible to collapse the data into nondimensional (deformation/sample height) values.

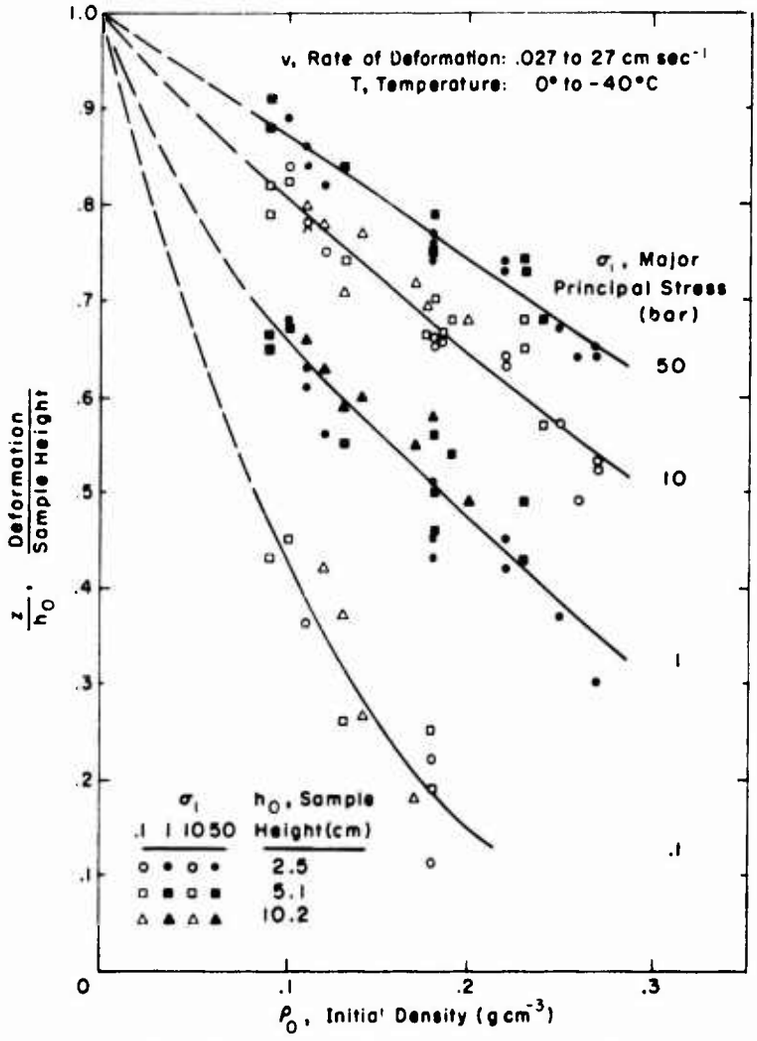

Figure 9. Deformation/sample height vs initial density with stress as a parameter.

The stress-deformation relationships for the 2.5-, 5.1-, and 10.2-cm-high samples are shown in Figure 10, with initial density as a parameter. Figure 11 summarizes the stress vs sinkage data (collapsed into a nondimensional z/h_0 form and interpolated from the three previous figures) with initial density as a parameter.

Since the snow samples were of a finite depth on a rigid base, the stress-deformation relationship is not linear on a log-log plot (the standard method for plotting pressure-sinkage data). Also, in these tests lateral restraint was provided. For clarity, the z/h_0 values are plotted here on an arithmetic scale; a log-log plot results in an even more pronounced curvature. This "bottom effect"

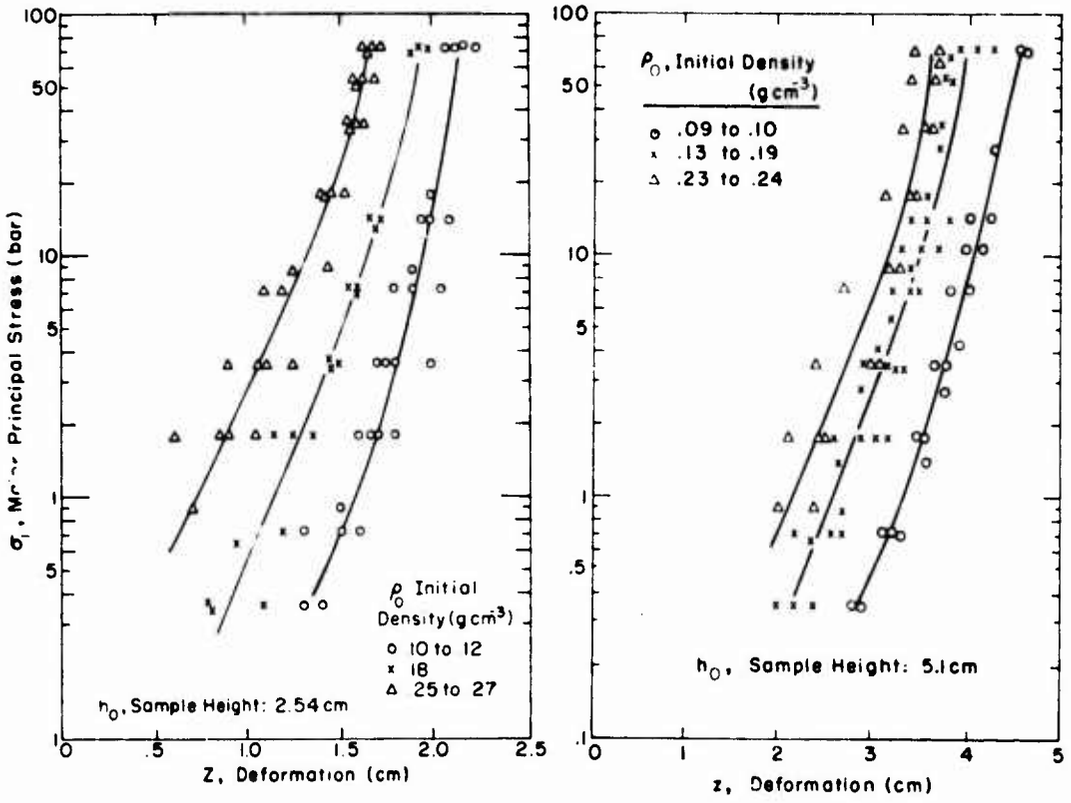

a. Sample height 2.5 cm. *b. Sample height 5.1 cm*

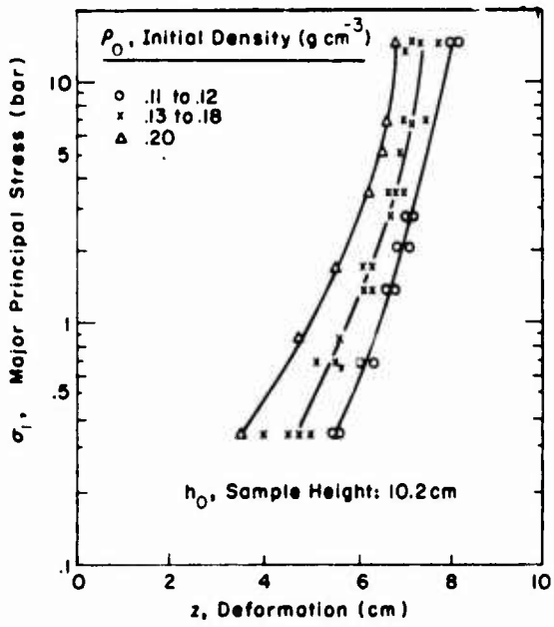

c. Sample height 10.2 cm.

Figure 10. Major principal stress vs deformation with initial density as a parameter.

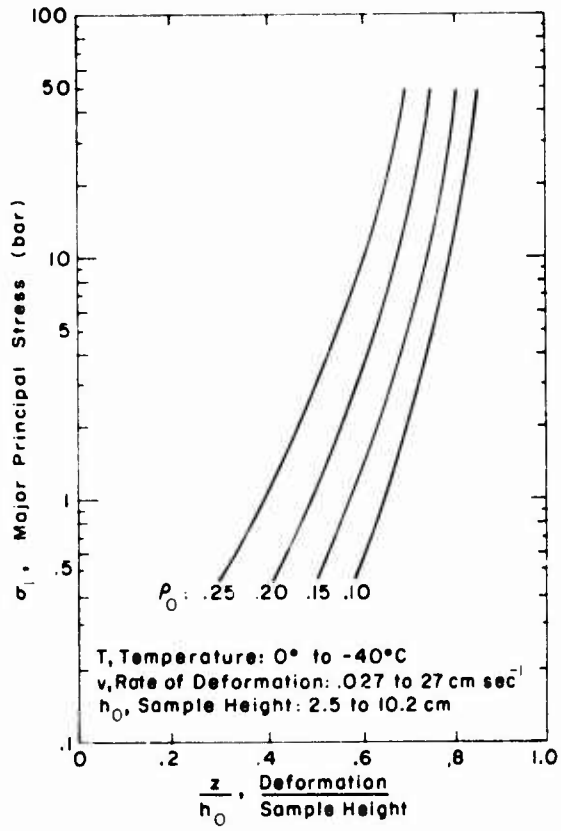

Figure 11. Major principal stress vs deformation/ sample height with initial density as a parameter.

and its treatment for determining the moduli of deformation for trafficability evaluation have been discussed by Bekker (1969). Because of the "bottom effect," characteristic for any compressible, relatively shallow material on a rigid base, the data fit neither Assur's (1964) pressure-sinkage nor Liston's (1964) dimensional similitude theories. Previous tests on deep snow have, however, shown good agreement with Assur's theory (Abele 1970).

SUMMARY AND CONCLUSIONS

Laboratory tests, using a modern 10,000-kg load capacity MTS machine equipped with an oscilloscope with load-deformation and time trace storage were conducted on shallow, undisturbed snow samples on a rigid base under uniaxial load to determine the stress vs density and stress vs deformation (pressure-sinkage) relationships as influenced by the rate of deformation (0.027 to 27 cm sec^{-1}), temperature (0° to -40°C) and initial density (0.09 to 0.27 g cm^{-3}) in the pressure range of 0.1 to 75 bars.

The rate of deformation, over a range of 3 orders of magnitude, does not have a significant effect on the stress-density relationship. At near 0°C temperature, an increase in the rate of deformation v results in a slight decrease in the major principal stress σ_1 at densities ρ below 0.6 g cm^{-3}, and no change in σ_1 at densities above 0.6 g cm^{-3}. At -20° to -40°C, there is a slight increase in σ_1 for any ρ, with an increase in v.

A decrease in temperature increases the resistance to stress and deformation, the temperature effect increasing with applied pressure and initial density. For snow with an initial density ρ_0 of approximately 0.1 g cm^{-3}, the temperature effect becomes apparent only at stress levels above 10 bars (corresponding resulting density $\geqq 0.5$ g cm^{-3}). For snow with $\rho_0 \geqq 0.2$, increase in stress with a decrease in temperature is evident at all densities and stress levels.

The effect on the initial density of the snow samples is significant. For any stress, an increase in the initial density results in an increase in the resulting density, this effect being particularly evident at low stress levels (< 10 bars) and at temperatures near 0°C. Expressed in another way, for any density ρ the resistance to stress σ_1 increases with a decrease in the initial density ρ_0, this effect decreasing with a decrease in temperature.

While some influence of the initial density on the stress-density or stress-deformation relationships could have been expected, the high degree of this influence is somewhat surprising. The reason for this effect is not entirely clear, the difference in particle shape and structure with a change in density being one possible explanation. For example (refer to Fig. 8c and d):

	To compact snow with an initial density ρ_0 of:	to a density ρ of:	requires a stress σ_1 of:
	0.1 g cm^{-3}	0.3 g cm^{-3}	1 bar
	0.2 g cm^{-3}	0.3 g cm^{-3}	$<$ 1 bar
	0.3 g cm^{-3}	0.5 g cm^{-3}	1 bar
but	0.1 g cm^{-3}	0.5 g cm^{-3}	10 bars
	0.2 g cm^{-3}	0.5 g cm^{-3}	$<$ 10 bars

From the above it is apparent that snows of different initial densities react quite differently to a given stress, at least up to about 10 bars. Snow whose density of 0.3 g cm^{-3} is the result of natural consolidation through some period of time (in the context of this study considered "initial" density) does not have the same resistance to stress as snow whose density of 0.3 g cm^{-3} has been achieved by rapid mechanical compaction ("resulting" density). This behavior can only be attributed to differences in the textural or structural arrangement of the grains. Therefore, in addition to temperature and strain or stress rate, the initial density, being an indicator of structure, also has to be considered as a controlling parameter in snow compressibility relationships.

Because of the typical "bottom effect" of a shallow compressible material on a rigid base, the pressure-sinkage data do not conform with established or proposed methods for convenient determination of deformation moduli.

MICROSTRUCTURAL ANALYSIS

Introduction

As noted at the outset of this report, the high compressibility of snow is the most prominent mechanical characteristic that distinguishes it from most other engineering materials. Even the application of small loads can produce very substantial changes in such properties as density (porosity) and permeability. Crushing of individual snow particles (grains and crystals) must certainly occur at the higher compressive stresses, and such crushing may also be accompanied by recrystallization, involving significant changes in the size, shape and orientation of constitutent grains and/or crystals. The extent of this recrystallization could be expected to depend on both

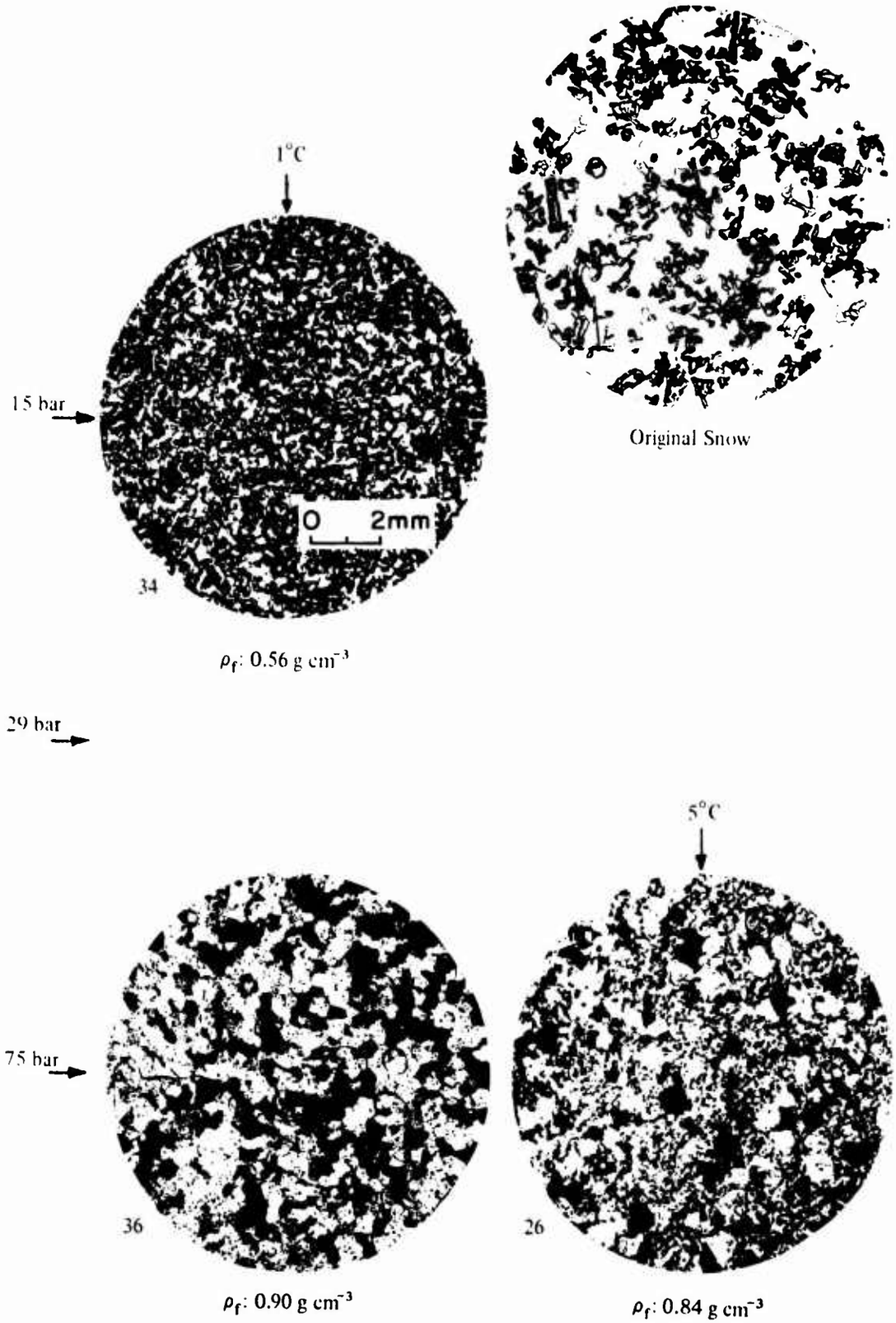

Figure 12. Thin section photographs of the crystal structure of artificially compacted snow samples.

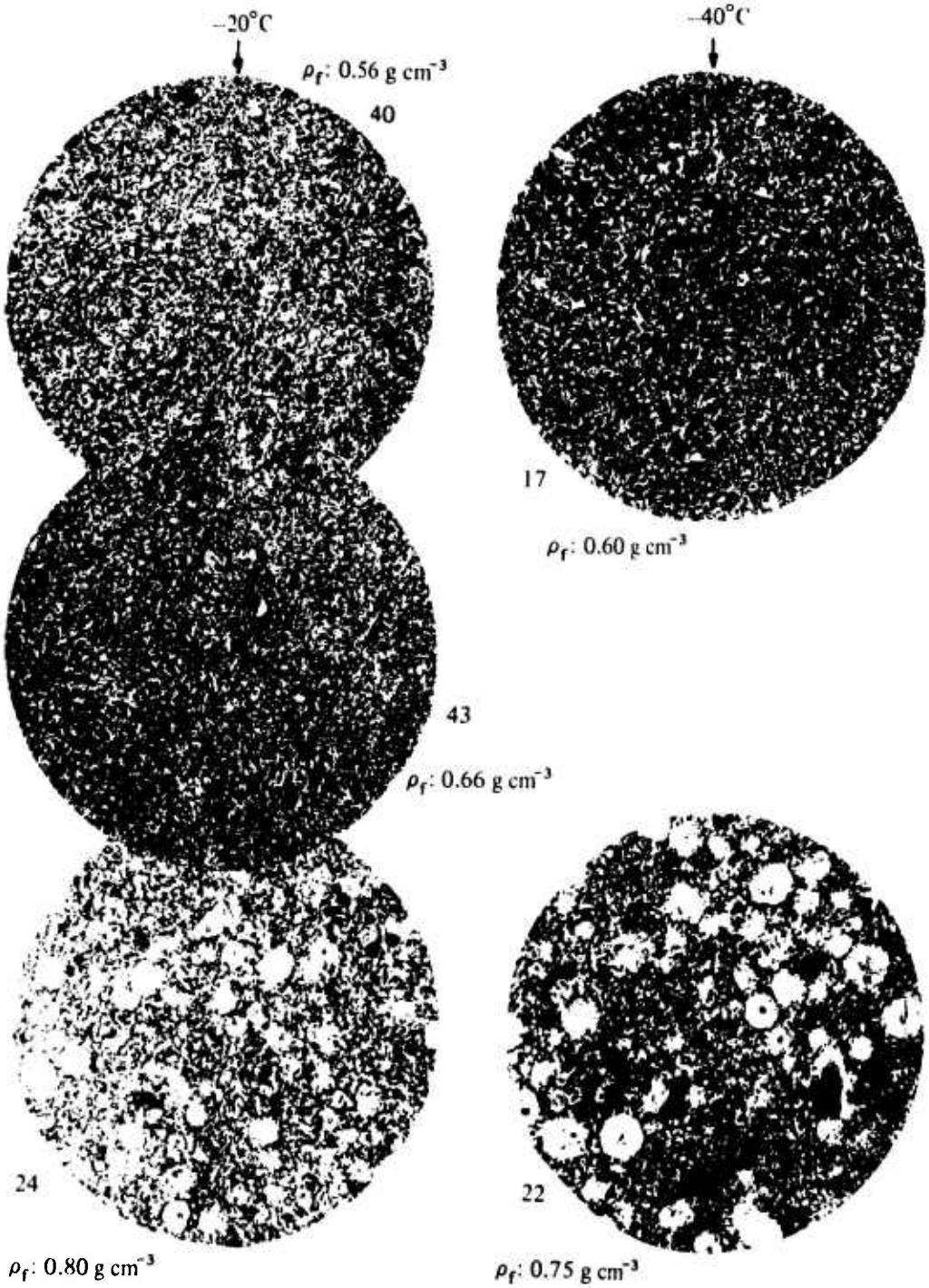

Figure 12 (cont'd).

the magnitude of the stress and the temperature at which compression occurs. It is the purpose of this section of the report to describe and interpret the textures of compacted samples obtained in the previously discussed series of tests.

Analytical methods

The simplest method of investigating the crystalline and granular texture of compacted snow is to prepare thin sections of representative samples. Since most of the compacts obtained in the present series of tests are permeable, the samples must first be impregnated with a filler to facilitate mounting them on glass slides and to prevent disruption of the grain structure during sectioning. Aniline was used as a filler in this study; it has a low solubility for ice, freezes at -11°C, does not noticeably deform the grain structure during freezing and melts out to a transparent isotropic liquid.

The samples were sectioned with a microtome of the type used to prepare histological slices. Full details of the technique are given by Gow (1969). Photomicrographs of finished sections were obtained with a Bausch and Lomb bellows camera fitter with polarizers. The use of polarizers permits the direct observation of all crystals in the section. Photographic detail is further enhanced if the temperature of the section is raised to about -7°C to allow all intergranular aniline to melt.

Results and discussion

Structural characteristics of some representative compacts are illustrated in Figure 12. These structures can generally be related, in a systematic fashion, to the test temperatures and levels of applied stress. Also, changes in structure can generally be shown to correlate reasonably well with other changes in the physical properties of compressed specimens, e.g. density.

In only one of the samples tested at the low end of the stress range (nominal stress 12 to 15 bars) did the density exceed 0.61 g cm^{-3}, and this particular sample (no. 51, tested at -3°C) seems a little exceptional in that none of the samples tested at -1° exceeded 0.60 g cm^{-3}. Temperature seems to exert little, if any, systematic effect on the densities of these low-stressed compacts. This behavior is compatible with the formation of a close-packed, loosely bonded structure such as that exhibited by samples 34, 40 and 17. However, there is just enough of a hint of grain rounding in sample 34, tested at -1°C, to suggest that this particular sample may have undergone incipient melting. A typical example of original snow structure is also shown in Figure 12. This snow is composed mainly of angular composites, but it also contains numerous needle-like crystals, columns and plates. By comparison, structural changes in samples 40 and 17 appear to be limited to some crushing of original grains to permit more economical packing under the applied stress.

Conversion to ice* occurred only in the most highly compressed samples at temperatures above -5°C. Sample 36, tested at -1°C, has recrystallized completely into a mosaic texture devoid of all trace of original snow structure. The texture is composed substantially of equidimensional crystals that tend to exhibit undulose extinction, indicative perhaps of residual intracrystalline strain induced during compression. This ice contains abundant small air bubbles despite the fact that its porosity is less than 3%. Although the shapes of bubbles are variable, a large proportion are well rounded; individual bubbles rarely exceed 0.1 mm in diameter. In this particular sample, densification and recrystallization may have been intensified by pressure melting, as evidenced by the occurrence of traces of liquid water observed on top of the sample immediately after it was removed from the press. Sample 26 (tested at -5°C) is less completely recrystallized, being composed of large crystals embedded in a fine-grained but thoroughly crystalline matrix. The large crystals, averaging 0.6 mm in diameter, are comparable in size to those in sample 36.

* Ice may contain bubbles but it is not permeable; this fact distinguishes it from compressed snow.

The structure of sample 43, compressed at an intermediate level of stress (29 bars), differs little from that of sample 40 of the same temperature series (-20°C). However, sample 24 of the same series and sample 22, tested at -40°C, both show very definite signs of recrystallization that has yielded textures which, to use the terminology of metamorphic rocks, e.g. recrystallized sandstone, would be called porphyroblastic. The matrix possesses limited permeability, as evidenced by the slow but definite uptake of aniline, so that both compacts are still technically compressed snow, albeit very dense. The larger crystals (porphyroblasts) in samples 24 and 22, which appear as hard, ice-like pellets to the unaided eye, were certainly not present in the snow prior to testing. These particles are typically polycrystalline in nature and usually exhibit radiate structure and, not infrequently, a central bubble or bubbles. Since they cannot have originated by freezing of pockets of water (ambient test temperatures being much too low), it is concluded that these larger crystals must have nucleated in regions of localized stress concentration. Some of this recrystallization may have occurred during the period of time when compressed samples were removed to the -8°C cold-room for density measurements prior to storage at -35°C.

The extent to which recrystallization increases with increasing temperatures in the most highly compressed samples clearly reflects the importance of the temperature factor at the higher stress levels. The highly recrystallized texture exhibited by sample 36 (compacted at 75 bars at -1°C) is very similar to that observed when metallic powders are transformed into dense compacts by hot pressing (sintering under load).

The intracrystalline nature of the pores in sample 36 is also very similar to that observed in hot-pressed compacts. These pores constitute the residual air that was not eliminated through holes drilled in the load plate (see Fig. 1).

As noted previously, it would be very difficult to evaluate the extent of post-deformational recrystallization in the present series of samples because microstructural examinations were not made until some time after the compression tests were completed. At the higher compressive stresses, preexisting particles would undergo appreciable crushing and granulation which could be conducive to extensive post-deformational recrystallization because of the increased thermodynamic instability associated with a highly compacted and finely crushed aggregate.

The importance of this kind of recrystallization in ice subjected to compactive pressures appreciably higher than those obtained in the present test is vividly demonstrated in the sequence of time lapse photographs (Fig. 13) obtained of a single thin section cut from a pellet of very fine-grained ice produced by the crushing and compression of fragments of single crystal ice in a pelletizer. The ice fragments were compressed incrementally to a nominal pressure of 235 bars at -8°C in a cylinder equipped with a vacuum device to remove air from the sample. The final pressure was maintained for 2 hours before depressurizing. The pellet of compressed ice was then removed and sectioned in readiness for time lapse photography between crossed polaroids at -3°C. Photograph A illustrates the structural condition of the sample approximately 15 minutes after depressurization. Photograph D shows the extent of recrystallization approximately 5 days later. Photographs B and C, taken at intermediate stages, show the process by which a sample of deformed, fine-grained crystallites recrystallizes into a coarse-grained mosaic of substantially strain-free, equidimensional and randomly oriented crystals. The driving force for this recrystallization can probably be attributed to stored energy induced during deformation (compression). Observation of the progress of recrystallization in this particular instance seems to indicate: 1) that as soon as a new grain is nucleated, it does not change its orientation throughout the entire recrystallization process, 2) that new grains continue to grow until mutual impingement with neighboring grains prevents further enlargement, 3) that the recrystallization process continues until all the original fine-grained matrix is consumed entirely by the growth of new crystals.

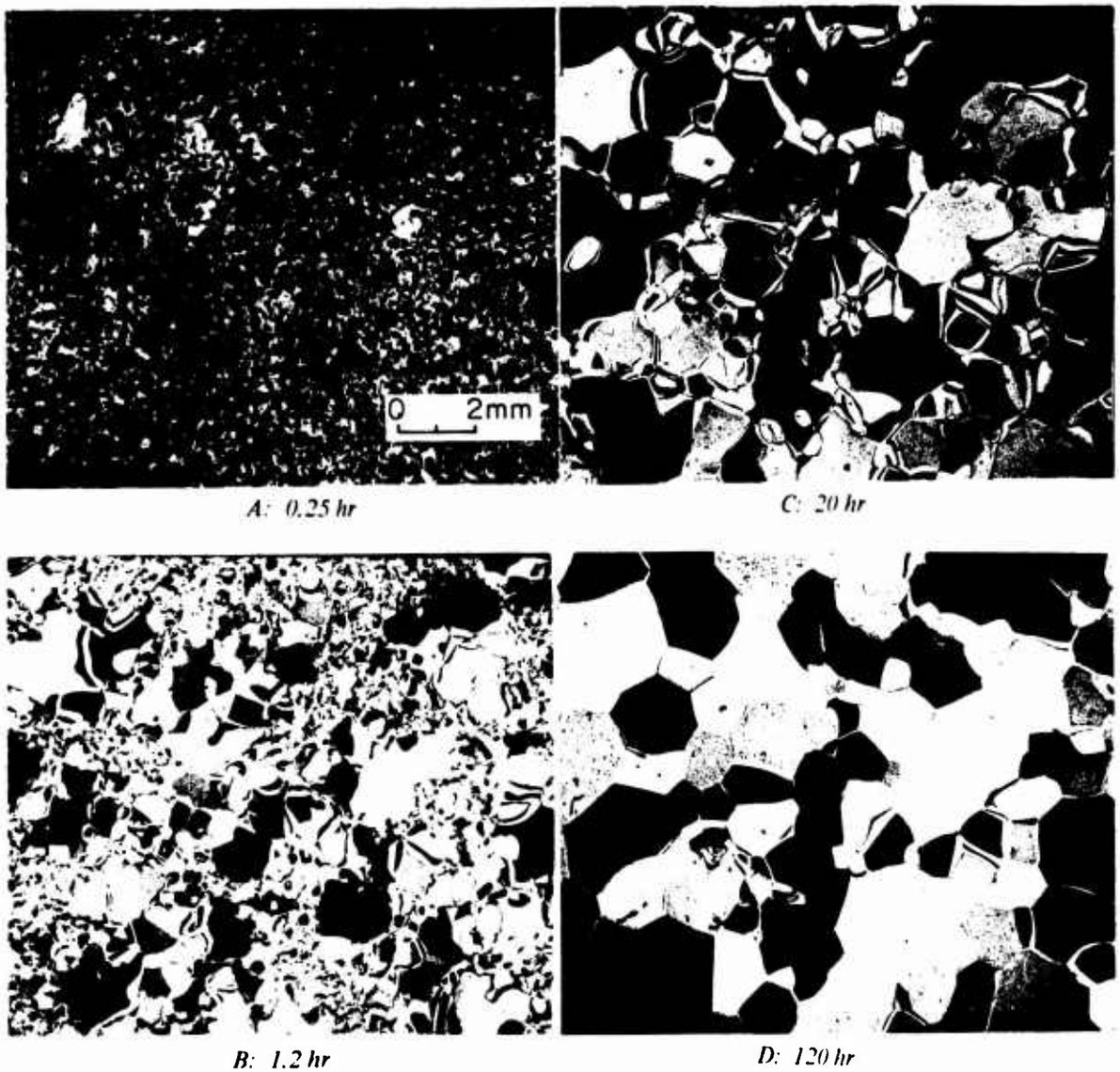

Figure 13. Time-lapse photographs of the recrystallization of a highly compressed ice pellet.

The final stage of recrystallization is concerned primarily with the elimination of residual "pockets of strain," particularly at locations where several small crystals intersect. Photograph D represents the virtual end point of this recrystallization. Only a few "strain-fringed" grain boundaries remain to be eliminated. Stability of structure is also indicated by the straightening out of grain boundaries and by the widespread occurrence of equiangular (120°) grain boundary intersections. A further interesting aspect of this particular sample is the virtual absence of air bubbles. This condition, in conjunction with the small size and randomly oriented nature of the component crystals, is very much desired in experimental test pieces, e.g. in tests of the deformation and fracture characteristics of polycrystalline ice.

At the other extreme, we have the example of the slow natural compression of polar snows where the total load needed to convert snow into ice rarely exceeds 10 bars, but where time is a very important factor. An example of this is illustrated in Figure 14 in the sequence of thin sections from Camp Century, Greenland. At this location the temperature of the snow remains essentially constant at -24°C, and the rate of loading is only about 0.035 kg cm^{-2} yr^{-1}, or of the order of 10^{-9} bar sec^{-1}.

0.3m
Density: 0.35 g cm^{-3}
Load: 0.01 bar
Age: 0.2 yr

9.0m
Density: 0.53 g cm^{-3}
Load: 0.40 bar
Age: 12 yr

100m
Density: 0.88 g cm^{-3}
Load: 7.10 bar
Age: 198 yr

Figure 14. Thin section structure photographs of naturally compacted snow and ice from Camp Century, Greenland.

Note that the grains and or crystals at the comparable densities at Camp Century are very much larger than in any of the current test series, though the size of particles in the parent snow is about the same for both.

Some incidental compression tests were run at temperatures between -5° and -20°C, but none of these samples were retained for microstructural analysis. This was unfortunate since, judging from the gross differences in texture between sample 26 (-5°C) and sample 24 (-20°C), at some temperature between these two extremes the response of snow to the higher compactive pressures changes quite drastically.

Time did not permit any really systematic study of the effects of rate of compression on the structure of the compacts. Since the density data do not show any significant effect, it is suspected that changing the rate of deformation (in the type of test conducted here) would exercise little if any significant control on structure.

Conclusion

The densification of artificially compacted snow may be accompanied by recrystallization of the deformed aggregate. The extent of this recrystallization increases with both an increase in the compactive pressure and increasing temperatures, especially at temperatures close to the melting point. Only in the sample compressed to 75 bars at -1°C did the texture of the snow become completely recrystallized. This recrystallized texture, including the widespread intracrystalline entrapment of pores, conforms very closely to the textures obtained with the sustained hot pressing of metallic powders. Generally, the texture of artificially compacted snow bears little resemblance to that of naturally compacted snow of the same density. This difference can be attributed largely to the short term nature of the loading of artificially compacted samples, which effectively eliminates the time factor that is so important in the densification and recrystallization of perennial snow covers. We might sum up by saying that for pressure in excess of that needed to pack snow to a density of 0.55-0.60 g cm^{-3}:

1. Increasing the pressure further will tend to increase both the end point density and degree of recrystallization that can be reached at any given temperature.

2. The end point density and the degree of recrystallization for any given pressure will also tend to increase with increasing temperature.

LITERATURE CITED

Abele, G. (1970) Deformation of snow under rigid plates at a constant rate of penetration. U.S. Army Cold Regions Research and Engineering Laboratory (USA CRREL) Research Report 273.

Assur, A. (1964) Locomotion over soft soil and snow. Paper presented at the Automotive Engineering Congress, Detroit, Mich.

Bekker, M.G. (1969) *Introduction to terrain-vehicle systems*. Ann Arbor: University of Michigan Press, p. 6, 60-65.

Gow, A.J. (1969) On the rates of growth of grains and crystals in south polar firn. *Journal of Glaciology*, vol. 8, no. 53, p. 241-252.

Harrison, W.L. (1957) Study of snow values related to vehicle performance. U.S. Army Land Locomotion Laboratory Report 23, OTAC.

Kinosita, S. (1967) Compression of snow at constant speed. International Conference on Physics of Snow and Ice, Hokkaido University, Japan.

Liston, R.A. and Hegedus, E. (1964) Dimensional analysis of load-sinkage relationships in soils and snow. U.S. Army Land Locomotion Laboratory Report 100, ATAC.

Mellor, M. (1974) A review of basic snow mechanics. International Symposium on Snow Mechanics, International Commission of Snow and Ice, IUGG, Grindelwald, Switzerland.

Mellor, M. (in press) Dynamics of snow avalanches. In *Geology and mechanics of rock slides and avalanches*.

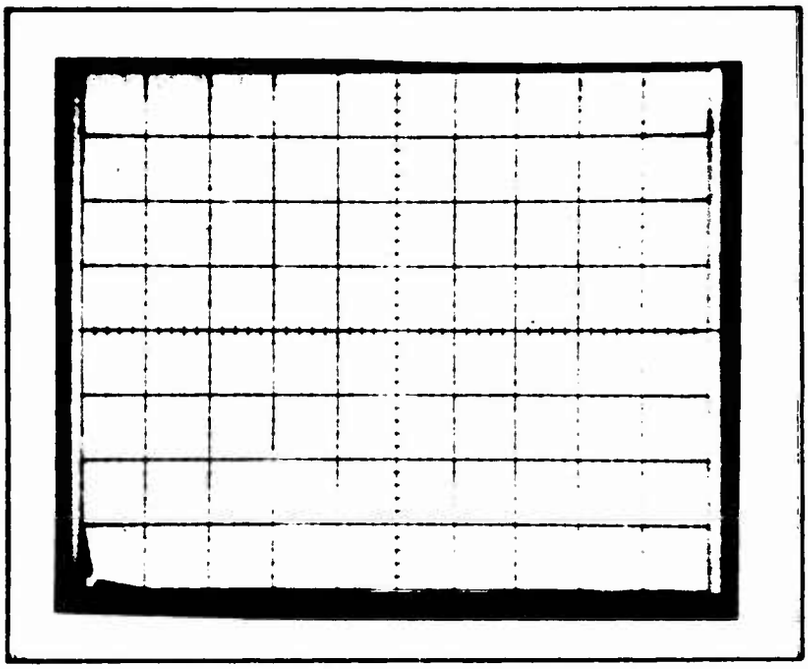

Date: 13 Feb 74

Sample

Snow type: Fresh

T (°C) = -7
d (cm) = 20.3
h_o (cm) = 7.5
A (cm^2) = 323.3
V_o (cm^3) = 2421
W (g) = 375/312
ρ_o (gcm^{-3}) = .155

h_1 (cm) = 1.1
V_1 (cm^3) = 355
ρ_1 (gcm^{-3}) = .878

Test No. 1 Rate of deform. ($cm\ sec^{-1}$) = 27

Load: Vert. scale: 1 div. = 4550 (kg)
Stroke: Horiz. scale: 1 div. = 0.85 (cm)

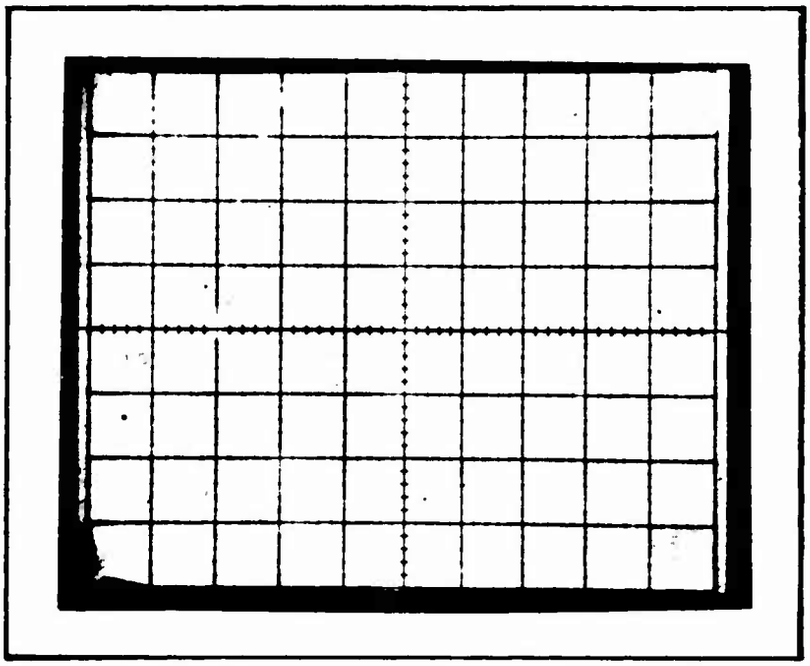

Date: 13 Feb 74

Sample

Snow type: Fresh

T (°C) = -7
d (cm) = 20.3
h_o (cm) = 7.5
A (cm^2) = 323.3
V_o (cm^3) = 2421
W (g) = 337/273
ρ_o (gcm^{-3}) = .139

h_1 (cm) = 1.02
V_1 (cm^3) = 329
ρ_1 (gcm^{-3}) = .834

Test No. 2 Rate of deform. ($cm\ sec^{-1}$) = 27

Load: Vert. scale: 1 div. = 2275 (kg)
Stroke: Horiz. scale: 1 div. = 0.85 (cm)

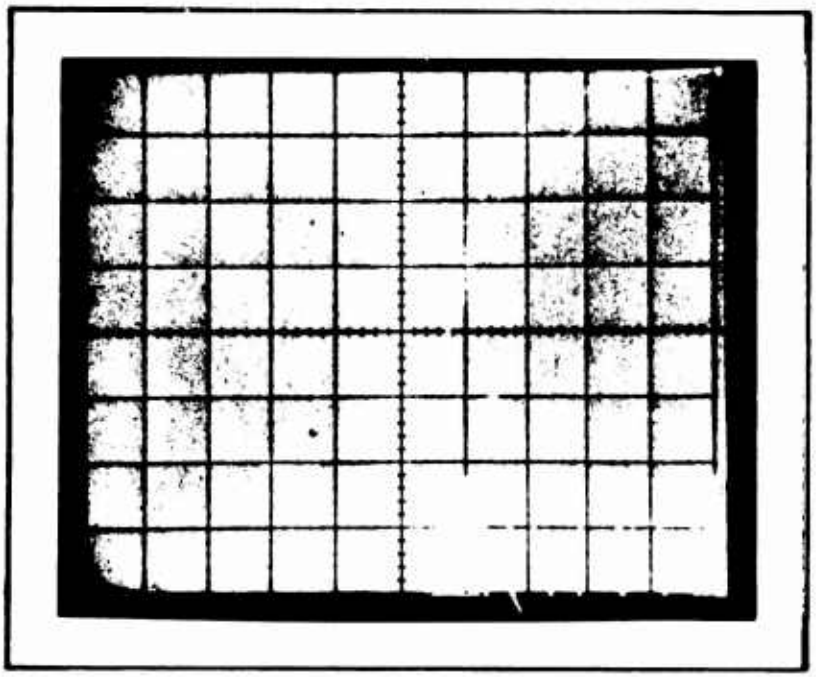

Date: 15 Feb 74

Sample

Snow type: Granular

T	(°C)	= -7
d	(cm)	= 20.3
h_o	(cm)	= 7.5
A	(cm^2)	= 323.3
V_o	(cm^3)	= 2421
W	(g)	= 942
ρ_o	(gcm^{-3})	= .388
h_1	(cm)	= 4.05
V_1	(cm^3)	= 1310
ρ_1	(gcm^{-3})	= .72

Test No. 3 Rate of deform. ($cm\ sec^{-1}$) = 27

Load: Vert. scale: 1 div. = 2275 (kg)
Stroke: Horiz. scale: 1 div. = 0.85 (cm)

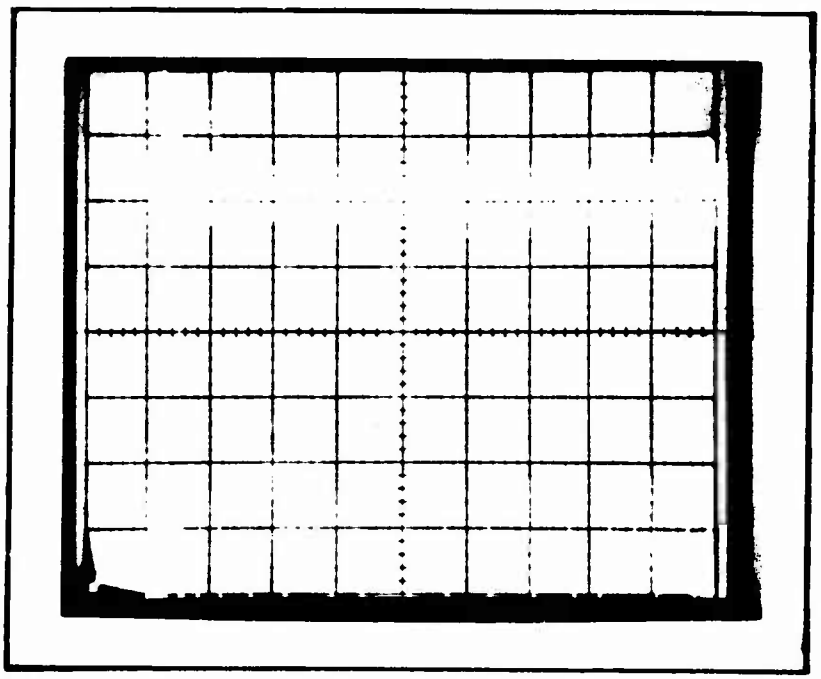

Date: 15 Feb 74

Sample Air resistance test
~~Snow type:~~
Perforated plate

T	(°C)	= -
d	(cm)	= 20.3
h_o	(cm)	= 7.5
A	(cm^2)	= 323.3
V_o	(cm^3)	= 2421
W	(g)	= -
ρ_o	(gcm^{-3})	= -
h_1	(cm)	= -
V_1	(cm^3)	= -
ρ_1	(gcm^{-3})	= -

Test No. 4 Rate of deform. ($cm\ sec^{-1}$) = 27

Load: Vert. scale: 1 div. = 22.7 (kg)
Stroke: Horiz. scale: 1 div. = 0.85 (cm)

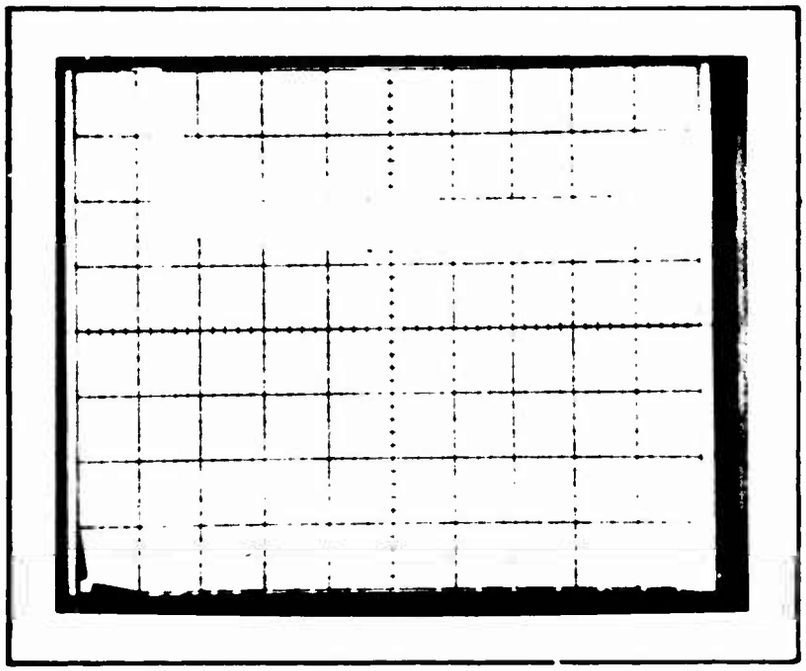

Date: 15 Feb 74

Sample Air resistance test
~~Snow type:~~ solid plate

T	(°C)	= -
d	(cm)	= 20.3
h_o	(cm)	= 7.5
A	(cm^2)	= 323.3
V_o	(cm^3)	= 2421
W	(g)	= -
ρ_o	(gcm^{-3})	= -
h_1	(cm)	= -
V_1	(cm^3)	= -
ρ_1	(gcm^{-3})	= -

Test No. 5 Rate of deform. ($cm\ sec^{-1}$) = 27

Load: Vert. scale: 1 div. = 22.7 (kg)
Stroke: Horiz. scale: 1 div. = 0.85 (cm)

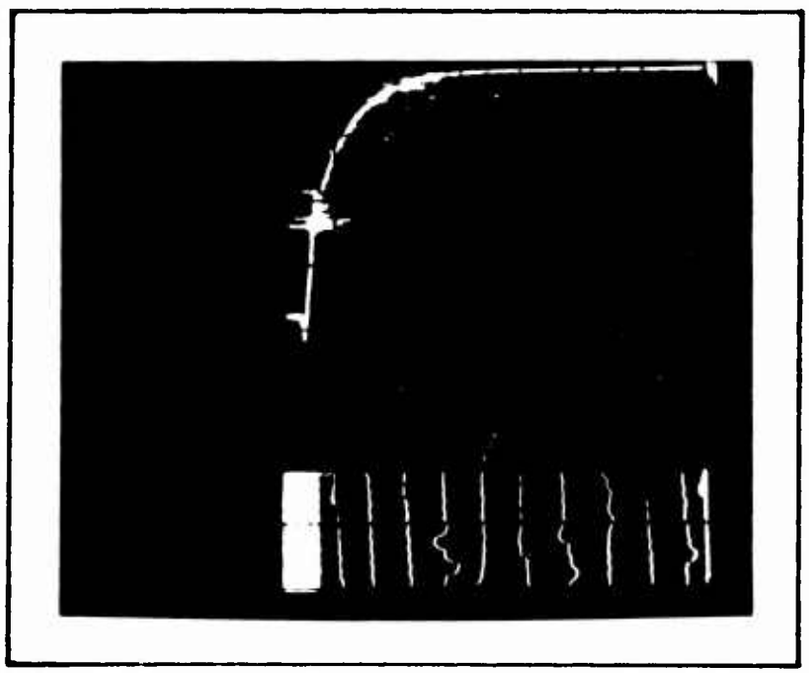

Date: 15 Feb 74

Sample

Snow type: Granular

T	(°C)	= -7
d	(cm)	= 20.3
h_o	(cm)	= 7.5
A	(cm^2)	= 323.3
V_o	(cm^3)	= 2421
W	(g)	= 478
ρ_o	(gcm^{-3})	= .198
h_1	(cm)	= 1.95
V_1	(cm^3)	= 630
ρ_1	(gcm^{-3})	= .76

Test No. 6 Rate of deform. ($cm\ sec^{-1}$) = 27

Load: Vert. scale: 1 div. = 2275 (kg)
Stroke: Horiz. scale: 1 div. = 0.85 (cm)

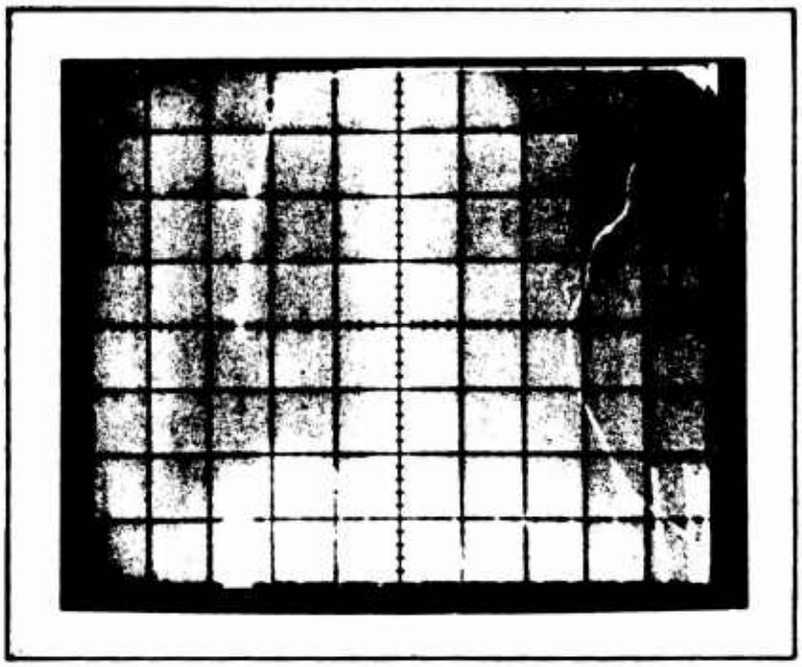

Date: 20 Feb 74

Sample

Snow type: Fresh

T	(^{o}C)	= -18
d	(cm)	= 20.3
h_o	(cm)	= 7.5
A	(cm^2)	= 323.3
V_o	(cm^3)	= 2421
W	(g)	= 293
ρ_o	(gcm^{-3})	= .12
h_1	(cm)	= 1.4
V_1	(cm^3)	= 452
ρ_1	(gcm^{-3})	= .65

Test No. 7 Rate of deform. ($cm\ sec^{-1}$) = 27

Load: Vert. scale: 1 div. = 2275 (kg)
Stroke: Horiz. scale: 1 div. = 0.85 (cm)

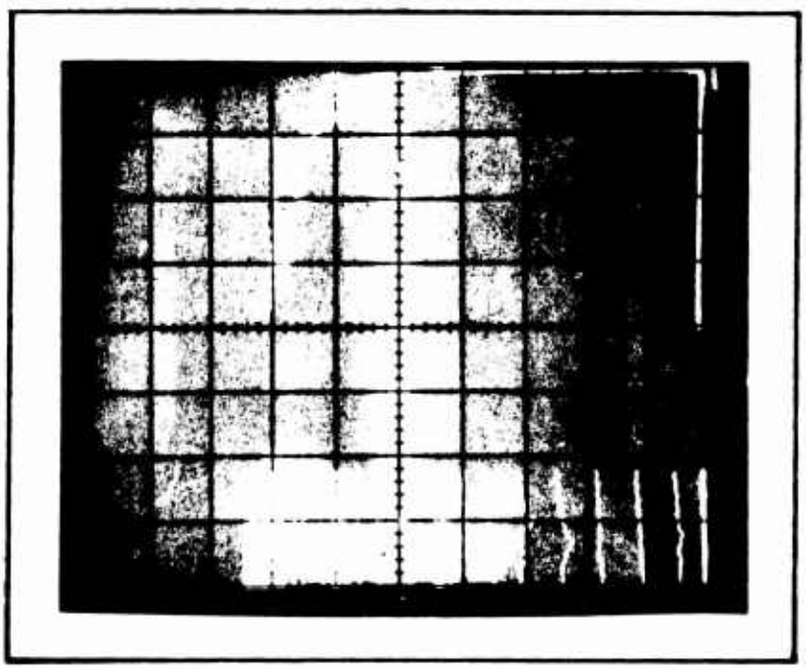

Date: 20 Feb 74

Sample

Snow type: Fresh

T	(^{o}C)	= -18
d	(cm)	= 20.3
h_o	(cm)	= 7.5
A	(cm^2)	= 323.3
V_o	(cm^3)	= 2421
W	(g)	= 436
ρ_o	(gcm^{-3})	= .18
h_1	(cm)	= 1.9
V_1	(cm^3)	= 614
ρ_1	(gcm^{-3})	= .71

Test No. 8 Rate of deform. ($cm\ sec^{-1}$) = 27 (incremental)

Load: Vert. scale: 1 div. = 2275 (kg)
Stroke: Horiz. scale: 1 div. = 0.85 (cm)

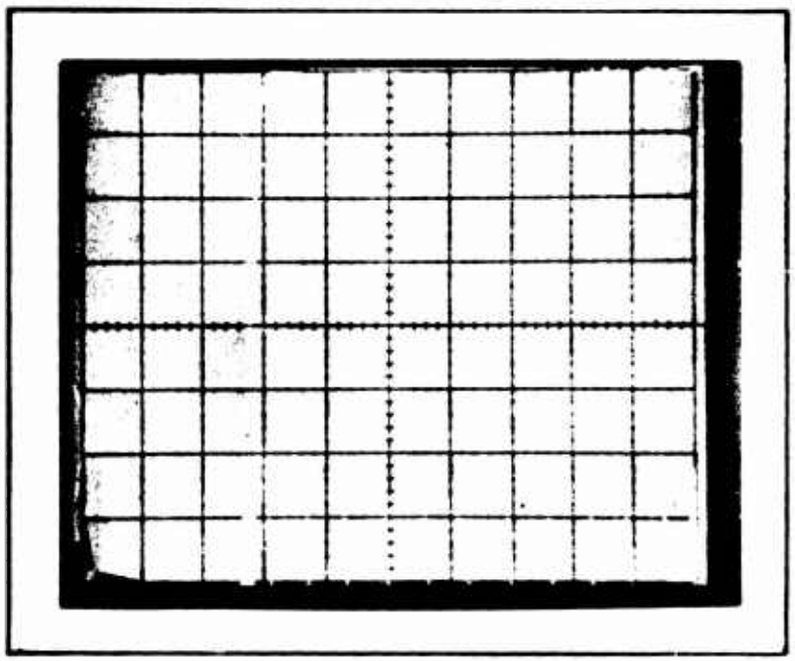

Date: 20Feb74

Sample

Snow type: Sample from Test No. 8

T	(^{o}C)	= -18
d	(cm)	= 20.3
h_o	(cm)	= 7.5
A	(cm^2)	= 323.3
V_o	(cm^3)	= 2421
W	(g)	= 436
ρ_o	(gcm^{-3})	= .18
h_1	(cm)	= 1.75
V_1	(cm^3)	= 565
ρ_1	(gcm^{-3})	= .77

Test No. 9 Rate of deform. ($cm\ sec^{-1}$) = 27

Load: Vert. scale: 1 div. = 2275 (kg)
Stroke: Horiz. scale: 1 div. = 0.85 (cm)

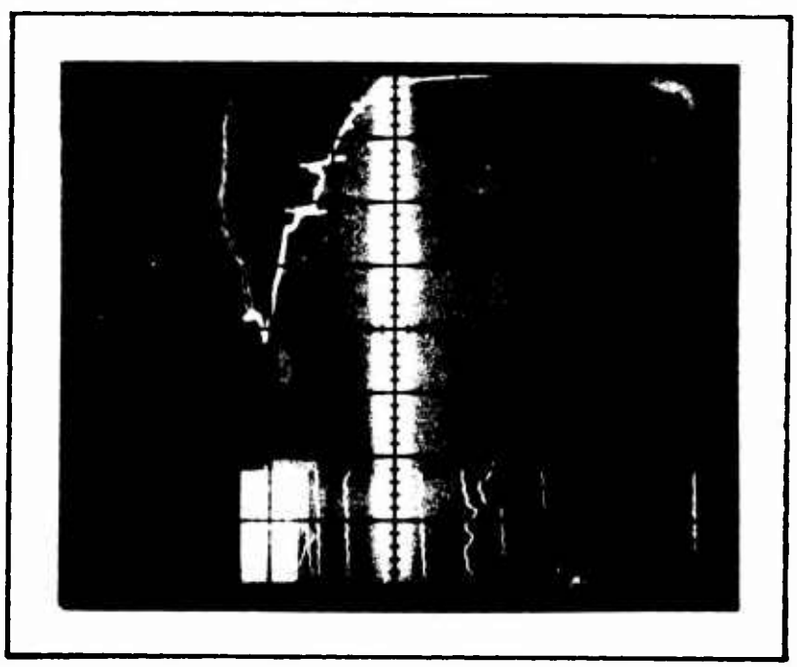

Date: 20Feb74

Sample

Snow type: Fresh, wet

T	(^{o}C)	= 0
d	(cm)	= 20.3
h_o	(cm)	= 7.5
A	(cm^2)	= 323.3
V_o	(cm^3)	= 2421
W	(g)	= 480
ρ_o	(gcm^{-3})	= .20
h_1	(cm)	= 1.65
V_1	(cm^3)	= 532
ρ_1	(gcm^{-3})	= .90

Test No. 10 Rate of deform. ($cm\ sec^{-1}$) = 27

Load: Vert. scale: 1 div. = 2275 (kg)
Stroke: Horiz. scale: 1 div. = 0.85 (cm)

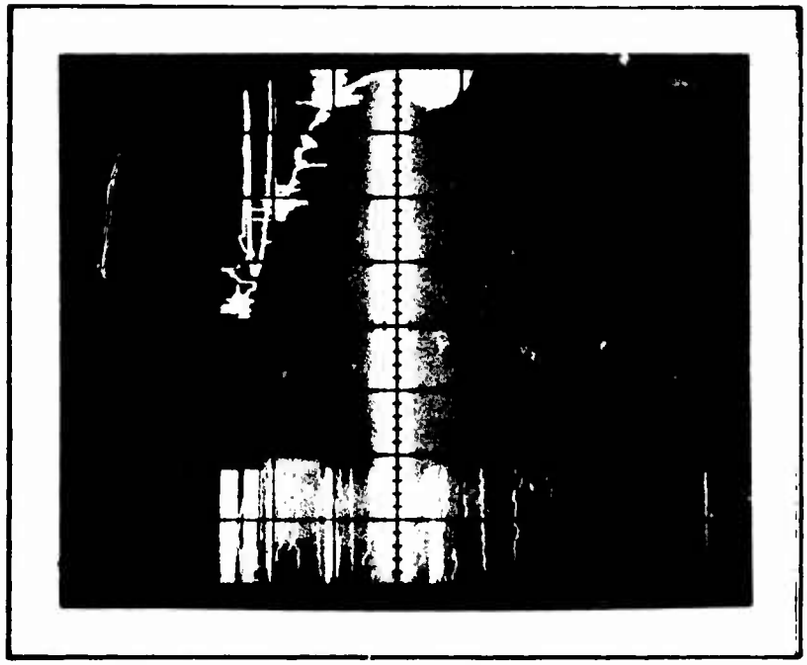

Date: 20 Feb 74

Sample

Snow type: Fresh, wet

T	(^{o}C)	= 0
d	(cm)	= 20.3
h_o	(cm)	= 7.5
A	(cm^2)	= 323.3
V_o	(cm^3)	= 2421
W	(g)	= 437
ρ_o	(gcm^{-3})	= .19
h_1	(cm)	= 1.5
V_1	(cm^3)	= 484
ρ_1	(gcm^{-3})	= .90

Test No. 11 Rate of deform. ($cm\ sec^{-1}$) = 27

Load: Vert. scale: 1 div. = 2275 (kg)
Stroke: Horiz. scale: 1 div. = 0.85 (cm)

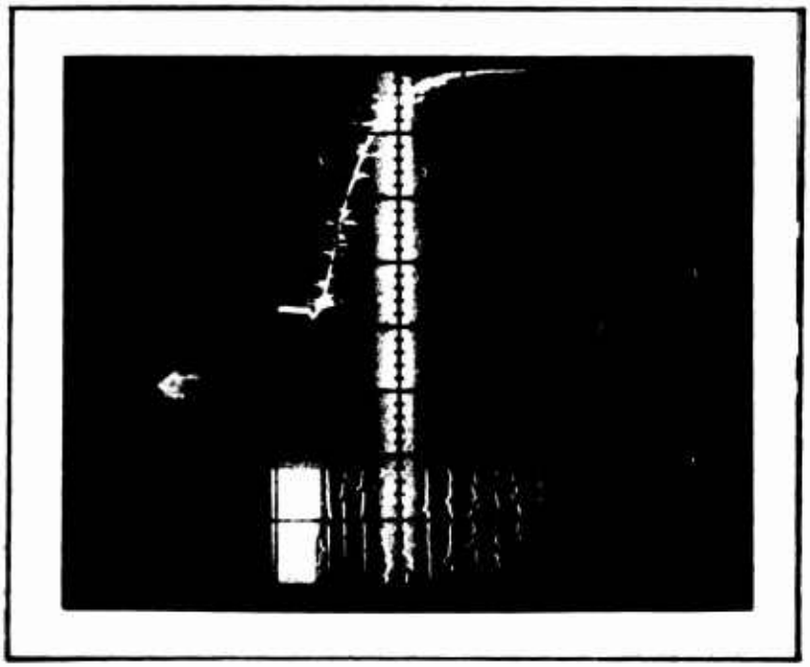

Date: 20 Feb 74

Sample

Snow type: Fresh, wet

T	(^{o}C)	= 0
d	(cm)	= 20.3
h_o	(cm)	= 7.5
A	(cm^2)	= 323.3
V_o	(cm^3)	= 2421
W	(g)	= 536
ρ_o	(gcm^{-3})	= .22
h_1	(cm)	= 1.9
V_1	(cm^3)	= 613
ρ_1	(gcm^{-3})	= .87

Test No. 12 Rate of deform. ($cm\ sec^{-1}$) = 2.7

Load: Vert. scale: 1 div. = 2275 (kg)
Stroke: Horiz. scale: 1 div. = 0.85 (cm)

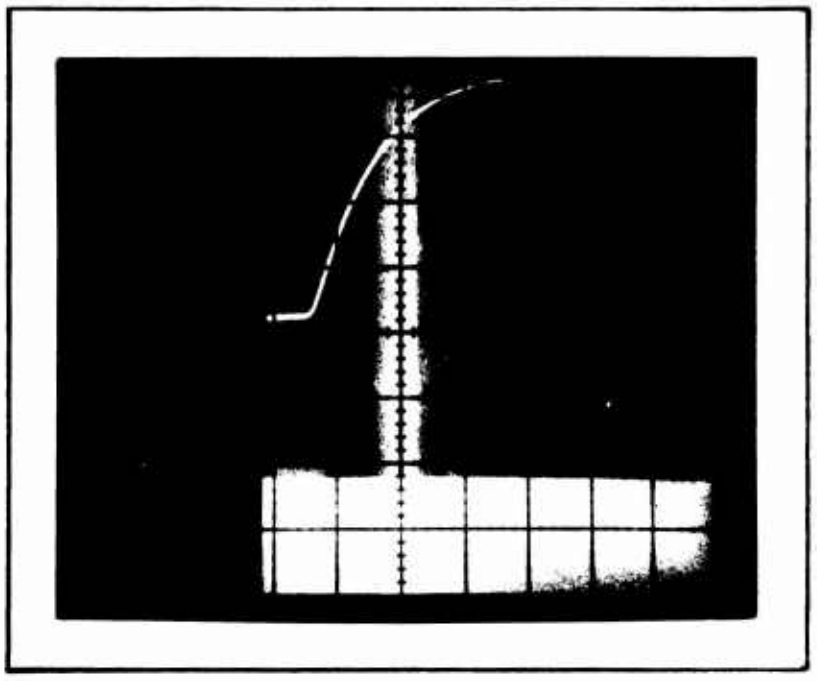

Date: 20 Feb 74

Sample

Snow type: Fresh, wet

T	(^{o}C)	= 0
d	(cm)	= 20.3
h_o	(cm)	= 7.5
A	(cm^2)	= 323.3
V_o	(cm^3)	= 2421
W	(g)	= 520
ρ_o	(gcm^{-3})	= .21
h_1	(cm)	= 1.8
V_1	(cm^3)	= 581
ρ_1	(gcm^{-3})	= .89

Test No. 13 Rate of deform. ($cm\ sec^{-1}$) = 0.27

Load: Vert. scale: 1 div. = 2275 (kg)
Stroke: Horiz. scale: 1 div. = 0.85 (cm)

Date: 22 Mar 74

Sample

Snow type: Fresh, cooled

T	(^{o}C)	= -30
d	(cm)	= 20.0
h_o	(cm)	= 7.6
A	(cm^2)	= 658
V_o	(cm^3)	= 5010
W	(g)	= 916
ρ_o	(gcm^{-3})	= .183
h_1	(cm)	= 2.3
V_1	(cm^3)	= 1512
ρ_1	(gcm^{-3})	= .61

Test No. 14 Rate of deform. ($cm\ sec^{-1}$) = 27

Load: Vert. scale: 1 div. = 2275 (kg)
Stroke: Horiz. scale: 1 div. = 1.27 (cm)

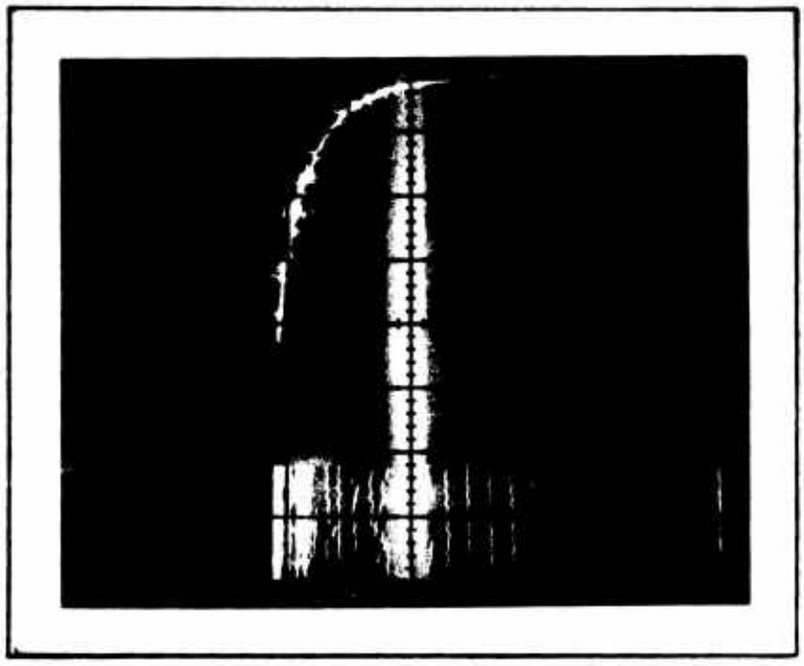

Date: 22 Mar 74

Sample

Snow type: Fresh, cooled

T	(^{o}C)	= -30
d	(cm)	= 29.0
h_o	(cm)	= 12.7
A	(cm^2)	= 658
V_o	(cm^3)	= 8350
W	(g)	= 1337
ρ_o	(gcm^{-3})	= .16
h_1	(cm)	= 3.4
V_1	(cm^3)	= 2235
ρ_1	(gcm^{-3})	= .60

Test No. 15 Rate of deform. ($cm\ sec^{-1}$) = 27

Load: Vert. scale: 1 div. = 2275 (kg)
Stroke: Horiz. scale: 1 div. = 1.27 (cm)

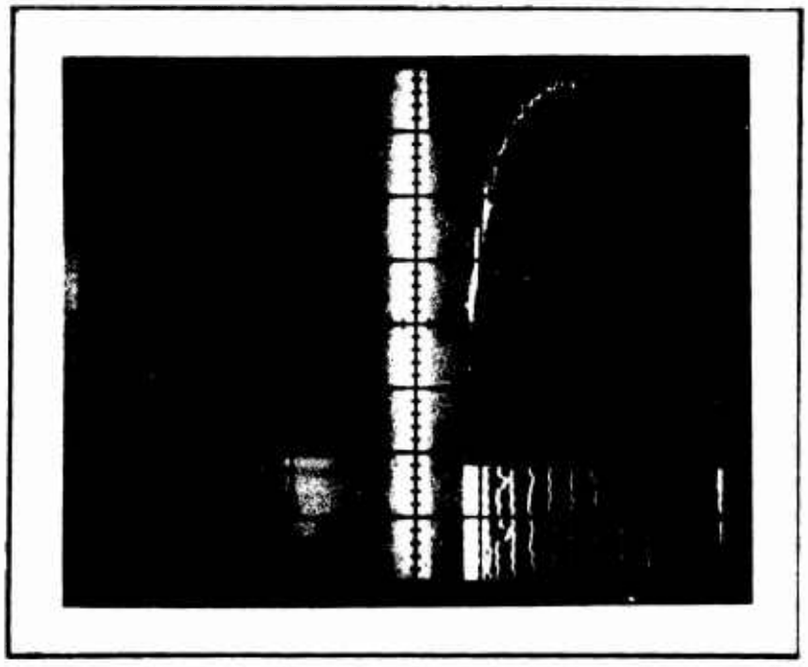

Date: 22 Mar 74

Sample

Snow type: Fresh, cooled

T	(^{o}C)	= -40
d	(cm)	= 29.0
h_o	(cm)	= 7.6
A	(cm^2)	= 656
V_o	(cm^3)	= 5010
W	(g)	= 942
ρ_o	(gcm^{-3})	= .188
h_1	(cm)	= 2.4
V_1	(cm^3)	= 1580
ρ_1	(gcm^{-3})	= .596

Test No. 17 Rate of deform. ($cm\ sec^{-1}$) = 27

Load: Vert. scale: 1 div. = 2275 (kg)
Stroke: Horiz. scale: 1 div. = 1.27 (cm)

(Trace lost on Test No. 16)

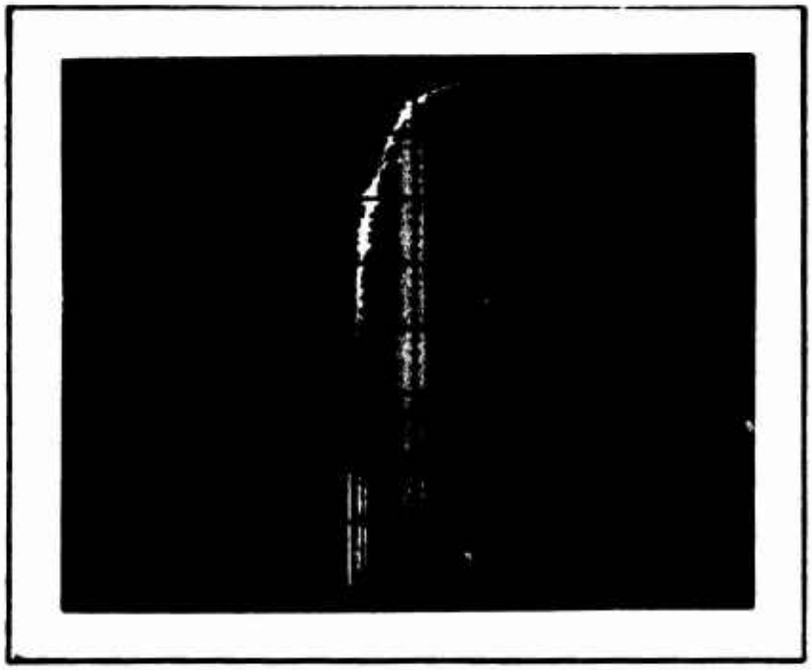

Date: 22 Mar 74

Sample

Snow type: fresh, cooled

T	(°C)	= -4.0
d	(cm)	= 29.0
h_o	(cm)	= 10.2
A	(cm^2)	= 658
V_o	(cm^3)	= 6675
W	(g)	= 910
ρ_o	(gcm^{-3})	= .136
h_1	(cm)	= 2.3
V_1	(cm^3)	= 1510
ρ_1	(gcm^{-3})	= .603

Test No. 18 Rate of deform. ($cm\ sec^{-1}$) = 27

Load: Vert. scale: 1 div. = 2275 (kg)
Stroke: Horiz. scale: 1 div. = 1.27 (cm)

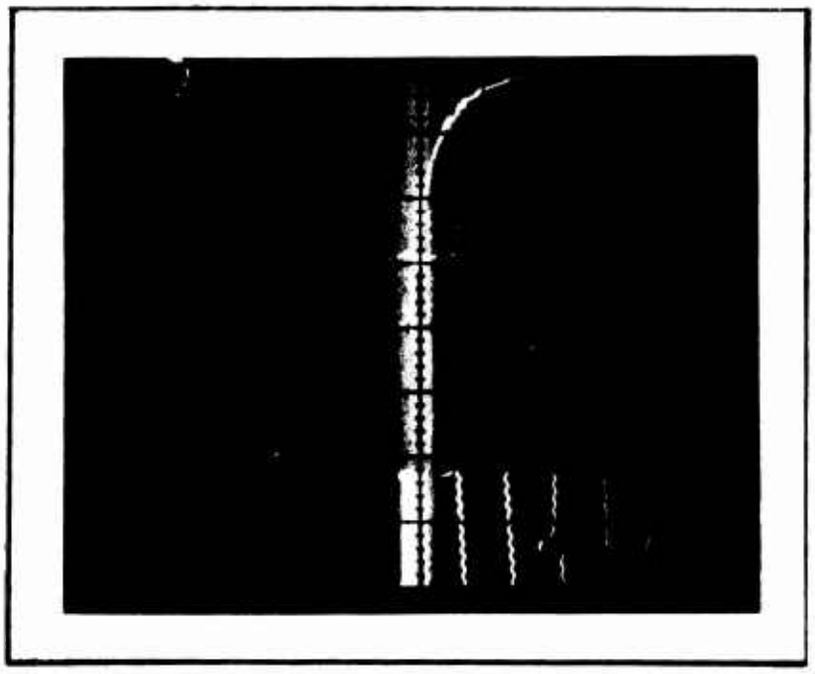

Date: 22 Mar 74

Sample

Snow type: fresh, cooled

T	(°C)	= -4.0
d	(cm)	= 12.7
h_o	(cm)	= 5.1
A	(cm^2)	= 126.6
V_o	(cm^3)	= 643
W	(g)	= 152
ρ_o	(gcm^{-3})	= .237
h_1	(cm)	= 1.65
V_1	(cm^3)	= 209
ρ_1	(gcm^{-3})	= .728

Test No. 19 Rate of deform. ($cm\ sec^{-1}$) = 27

Load: Vert. scale: 1 div. = 2275 (kg)
Stroke: Horiz. scale: 1 div. = 0.635 (cm)

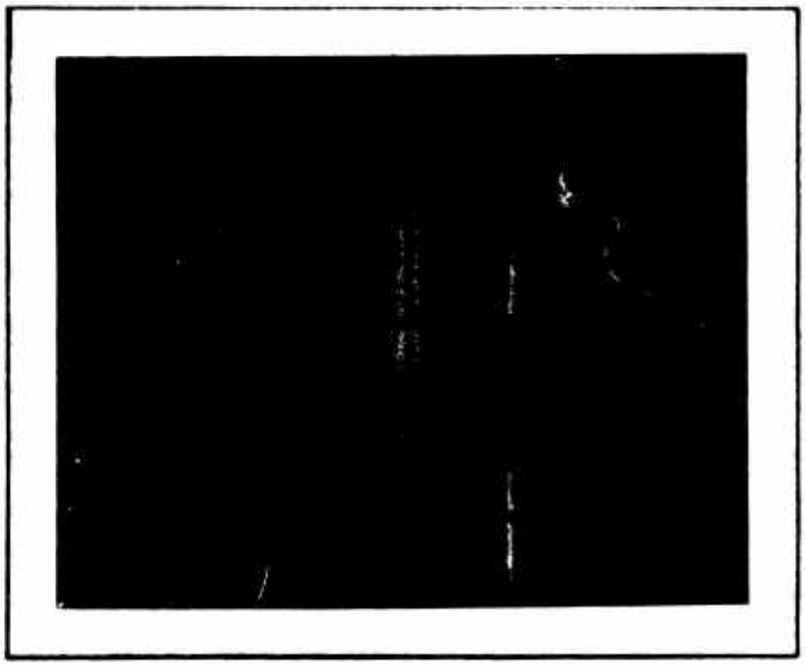

Date: 22 Mar 74

Sample

Snow type: Fresh, cooled

T	(^{o}C)	= -10
d	(cm)	= 12.7
h_o	(cm)	= 2.5
A	(cm^2)	= 126.6
V_o	(cm^3)	= 321.5
W	(g)	= 86
ρ_o	(gcm^{-3})	= .268
h_1	(cm)	= 0.92
V_1	(cm^3)	= 116.3
ρ_1	(gcm^{-3})	= .74

Test No. 20 Rate of deform. (cm sec^{-1}) = 27

Load: Vert. scale: 1 div. = 2275 (kg)
Stroke: Horiz. scale: 1 div. = 0.635 (cm)

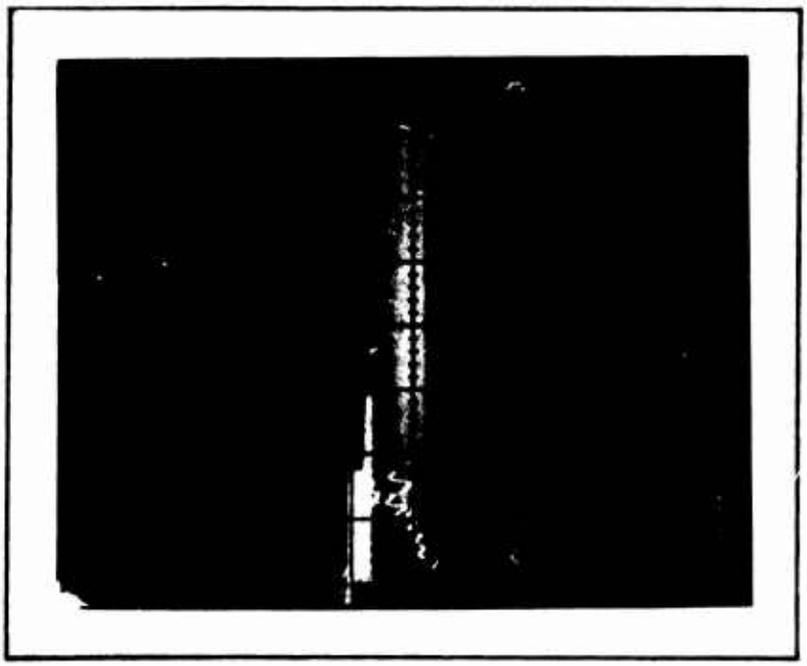

Date: 28 Mar 74

Sample

Snow type: Fresh, cooled

T	(^{o}C)	= -10
d	(cm)	= 12.7
h_o	(cm)	= 2.5
A	(cm^2)	= 126.6
V_o	(cm^3)	= 321.5
W	(g)	= 88
ρ_o	(gcm^{-3})	= .274
h_1	(cm)	= 0.9
V_1	(cm^3)	= 114
ρ_1	(gcm^{-3})	= .772

Test No. 21 Rate of deform. (cm sec^{-1}) = 27

Load: Vert. scale: 1 div. = 1125 (kg)
Stroke: Horiz. scale: 1 div. = .254 (cm)

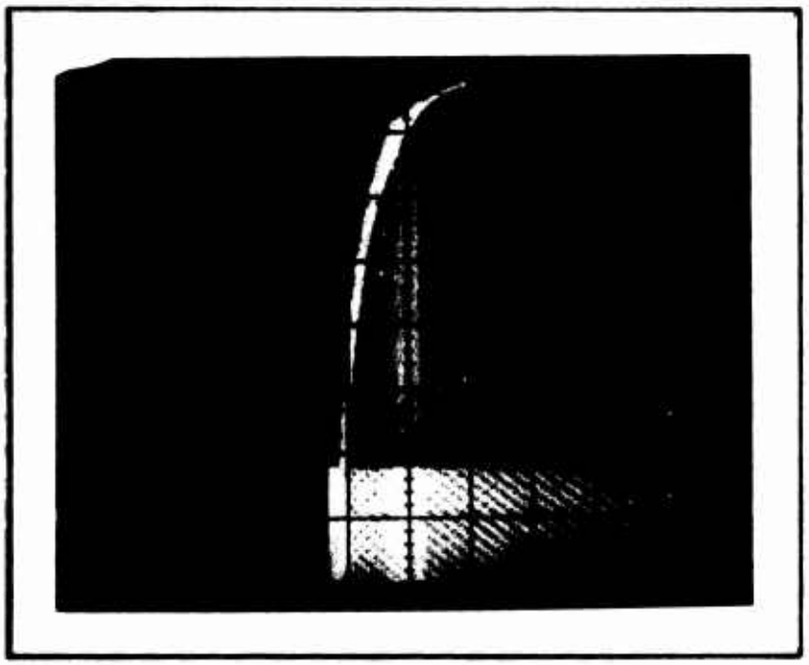

Date: 28 Mar 74

Sample

Snow type: Fresh, cooled

T	(^{o}C)	= -40
d	(cm)	= 12.7
h_o	(cm)	= 2.5
A	(cm^2)	= 126.6
V_o	(cm^3)	= 321.5
W	(g)	= 81
ρ_o	(gcm^{-3})	= .252
h_1	(cm)	= .85
V_1	(cm^3)	= 107.5
ρ_1	(gcm^{-3})	= .754

Test No. 22 Rate of deform. ($cm\ sec^{-1}$) = .27

Load: Vert. scale: 1 div. = 1138 (kg)
Stroke: Horiz. scale: 1 div. = .254 (cm)

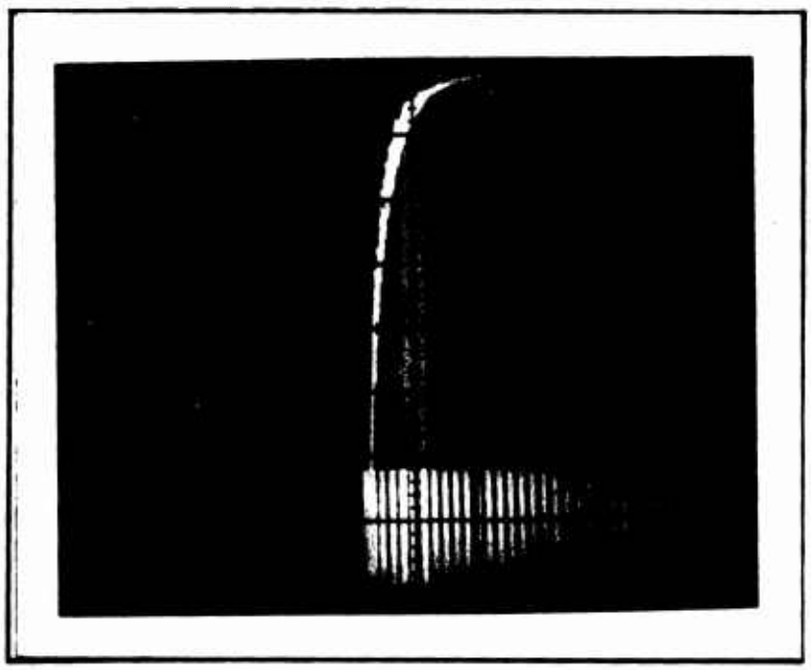

Date: 28 Mar 74

Sample

Snow type: Fresh, cooled

T	(^{o}C)	= -40
d	(cm)	= 12.7
h_o	(cm)	= 5.1
A	(cm^2)	= 126.6
V_o	(cm^3)	= 643
W	(g)	= 121
ρ_o	(gcm^{-3})	= .188
h_1	(cm)	= 1.3
V_1	(cm^3)	= 164.5
ρ_1	(gcm^{-3})	= .736

Test No. 23 Rate of deform. ($cm\ sec^{-1}$) = .027

Load: Vert. scale: 1 div. = 1138 (kg)
Stroke: Horiz. scale: 1 div. = .635 (cm)

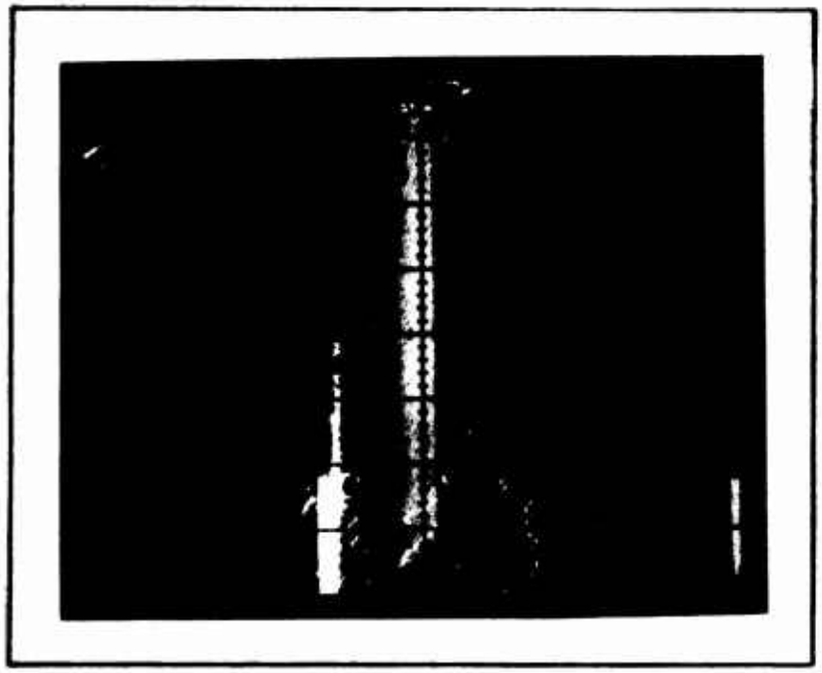

Date: 28 Mar 74

Sample

Snow type: Fresh, cooled

T	(^{o}C)	= -20
d	(cm)	= 12.7
h_o	(cm)	= 2.5
A	(cm^2)	= 126.6
V_o	(cm^3)	= 321.5
W	(g)	= 71
ρ_o	(gcm^{-3})	= .221
h_1	(cm)	= .70
V_1	(cm^3)	= 88.6
ρ_1	(gcm^{-3})	= .801

Test No. 24 Rate of deform. ($cm\ sec^{-1}$) = 27

Load: Vert. scale: 1 div. = 1138 (kg)
Stroke: Horiz. scale: 1 div. = .254 (cm)

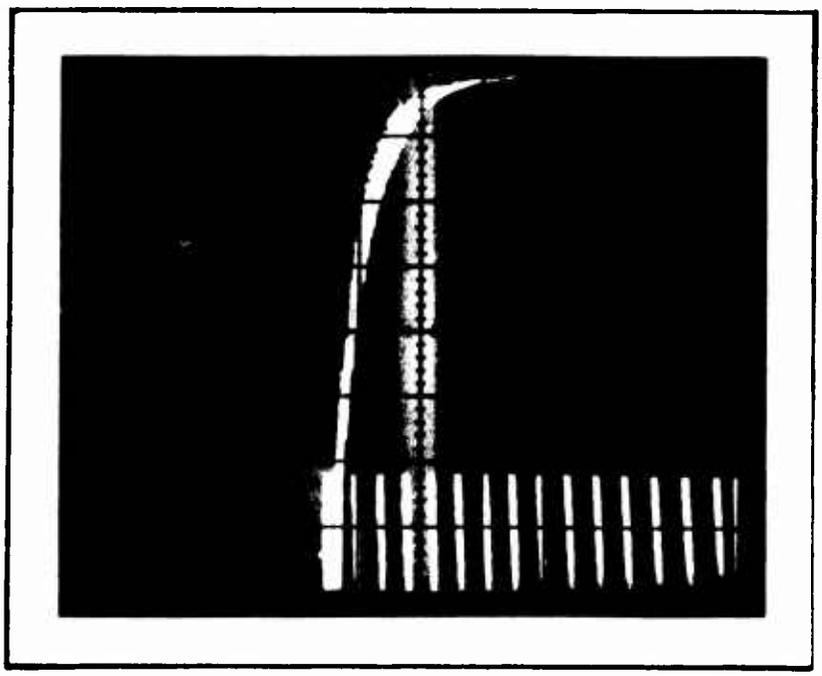

Date: 28 Mar 74

Sample

Snow type: Fresh, cooled

T	(^{o}C)	= -20
d	(cm)	= 12.7
h_o	(cm)	= 2.5
A	(cm^2)	= 126.6
V_o	(cm^3)	= 321.5
W	(g)	= 71
ρ_o	(gcm^{-3})	= .221
h_1	(cm)	= .70
V_1	(cm^3)	= 71
ρ_1	(gcm^{-3})	= .801

Test No. 25 Rate of deform. ($cm\ sec^{-1}$) = .027

Load: Vert. scale: 1 div. = 1138 (kg)
Stroke: Horiz. scale: 1 div. = .254 (cm)

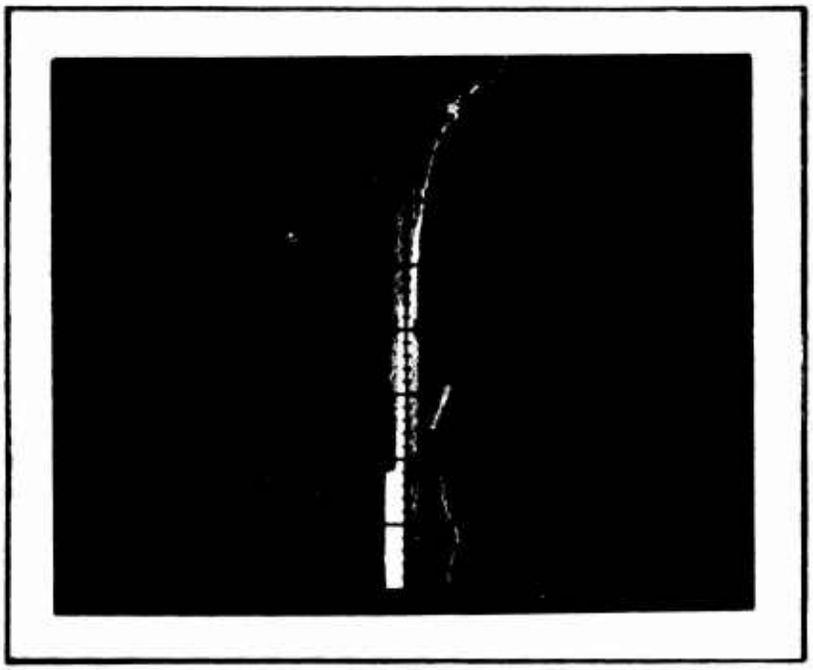

Date: 28 Mar 74

Sample

Snow type: Fresh, settled

T	(^{o}C)	= -5
d	(cm)	= 12.7
h_o	(cm)	= 5.1
A	(cm^2)	= 126.6
V_o	(cm^3)	= 643
W	(g)	= 146
ρ_o	(gcm^{-3})	= .227
h_1	(cm)	= 1.38
V_1	(cm^3)	= 175
ρ_1	(gcm^{-3})	= .835

Test No. 26 Rate of deform. (cm sec^{-1}) = 27

Load: Vert. scale: 1 div. = 1138 (kg)
Stroke: Horiz. scale: 1 div. = .635 (cm)

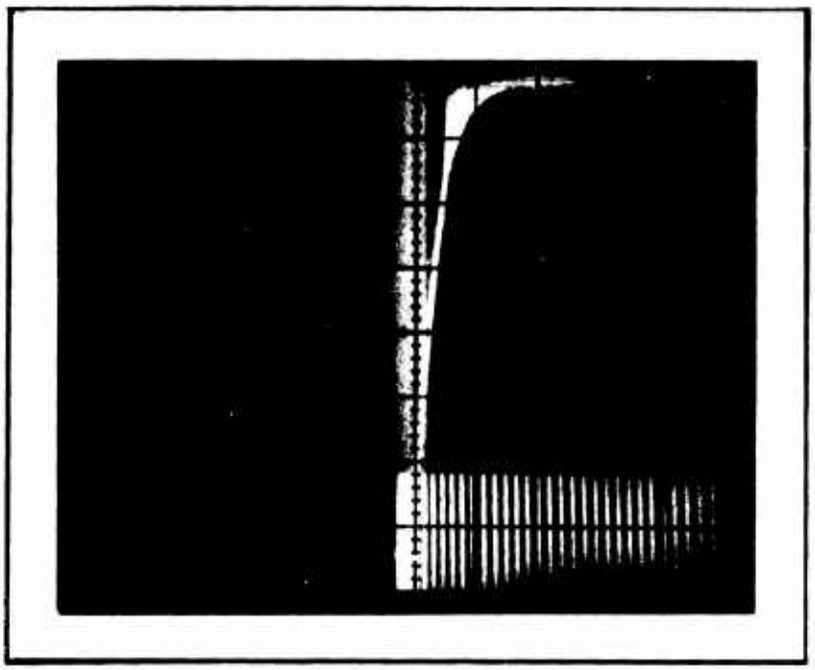

Date: 28 Mar 74

Sample

Snow type: Fresh, settled

T	(^{o}C)	= -5
d	(cm)	= 12.7
h_o	(cm)	= 5.1
A	(cm^2)	= 126.6
V_o	(cm^3)	= 643
W	(g)	= 147
ρ_o	(gcm^{-3})	= .229
h_1	(cm)	= 1.37
V_1	(cm^3)	= 173
ρ_1	(gcm^{-3})	= .850

Test No. 27 Rate of deform. (cm sec^{-1}) = .027

Load: Vert. scale: 1 div. = 1138 (kg)
Stroke: Horiz. scale: 1 div. = .635 (cm)

CRREL Form 42 (OT)
15 May 74

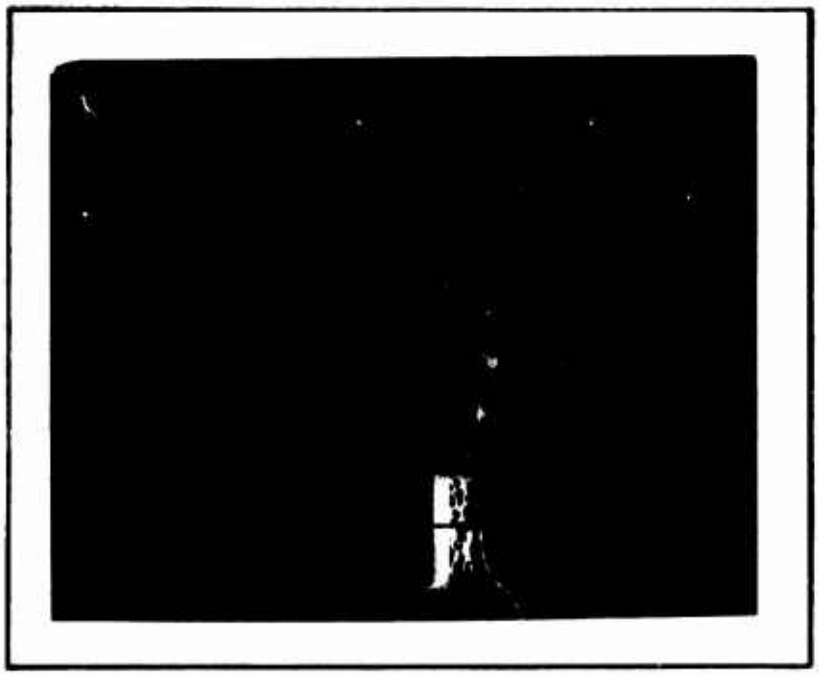

Date: 5 Apr 74

Sample

Snow type: Fresh

T	(°C)	= -35
d	(cm)	= 29.0
h_o	(cm)	= 7.6
A	(cm^2)	= 658
V_o	(cm^3)	= 5010
W	(g)	= 681
ρ_o	(gcm^{-3})	= .136
h_1	(cm)	= 1.75
V_1	(cm^3)	= 1150
ρ_1	(gcm^{-3})	= .592

Test No. 28 Rate of deform. ($cm\ sec^{-1}$) = 27

Load: Vert. scale: 1 div. = 227.5 (kg)
Stroke: Horiz. scale: 1 div. = 1.27 (cm)

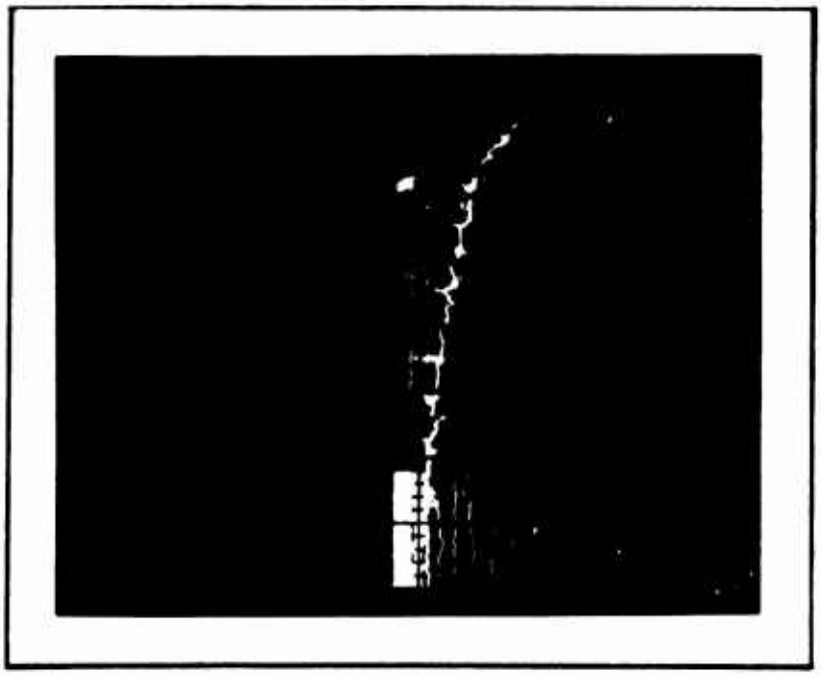

Date: 5 Apr 74

Sample

Snow type: Fresh, settled

T	(°C)	= -35
d	(cm)	= 29.0
h_o	(cm)	= 10.2
A	(cm^2)	= 658
V_o	(cm^3)	= 6675
W	(g)	= 1321
ρ_o	(gcm^{-3})	= .198
h_1	(cm)	= 3.35
V_1	(cm^3)	= 2200
ρ_1	(gcm^{-3})	= .601

Test No. 29 Rate of deform. ($cm\ sec^{-1}$) = 27

Load: Vert. scale: 1 div. = 569 (kg)
Stroke: Horiz. scale: 1 div. = 1.27 (cm)

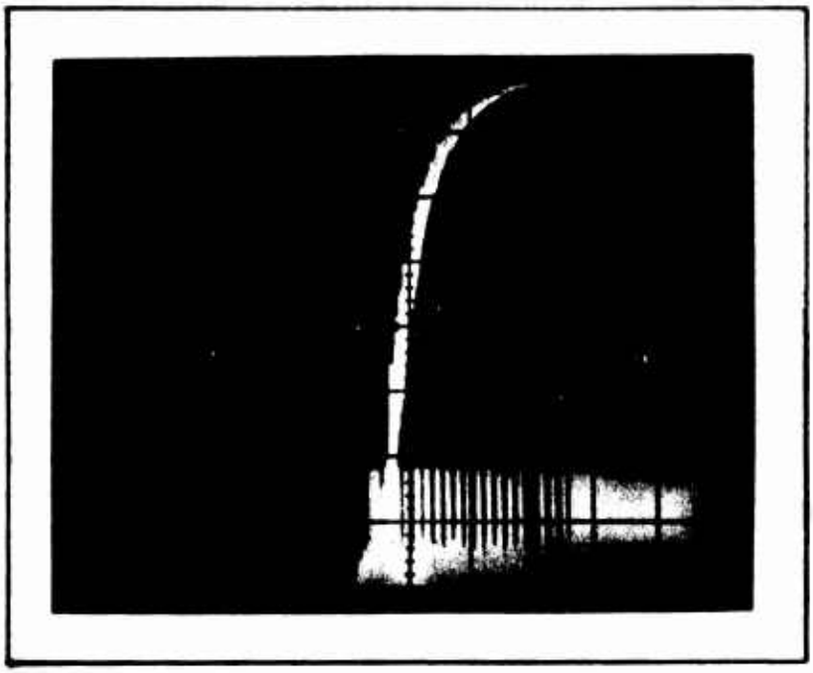

Date: 5 Apr 74

Sample

Snow type: fresh, settled

T	(^{o}C)	= -35
d	(cm)	= 29.0
h_o	(cm)	= 10.2
A	(cm^2)	= 658
V_o	(cm^3)	= 6675
W	(g)	= 1205
ρ_o	(gcm^{-3})	= .180
h_1	(cm)	= 3.15
V_1	(cm^3)	= 2070
ρ_1	(gcm^{-3})	= .581

Test No. 30 Rate of deform. ($cm\ sec^{-1}$) = .027

Load: Vert. scale: 1 div. = 569 (kg)
Stroke: Horiz. scale: 1 div. = 1.27 (cm)

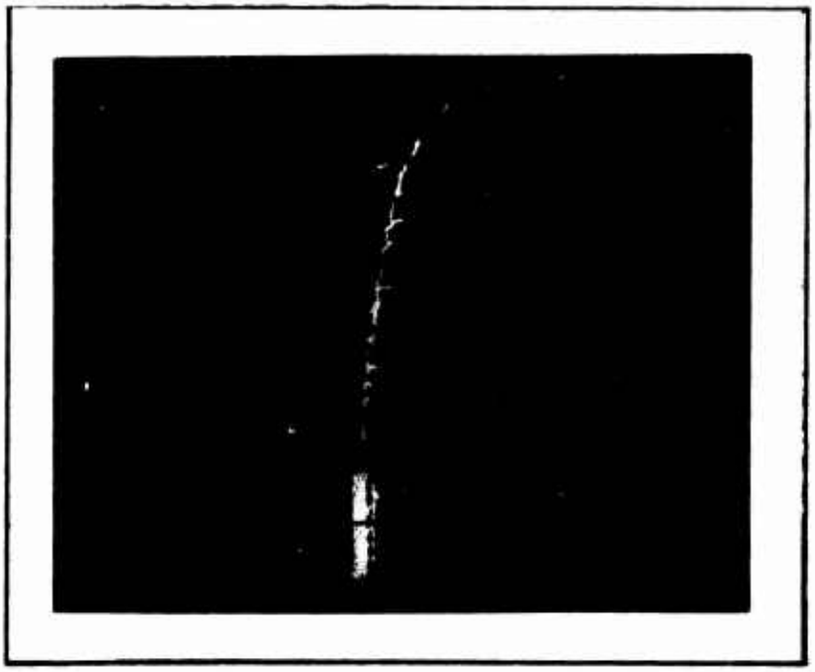

Date: 5 Apr 74

Sample

Snow type: fresh, settled

T	(^{o}C)	= -40
d	(cm)	= 29.0
h_o	(cm)	= 10.2
A	(cm^2)	= 658
V_o	(cm^3)	= 6675
W	(g)	= 1117
ρ_o	(gcm^{-3})	= .167
h_1	(cm)	= 2.80
V_1	(cm^3)	= 1840
ρ_1	(gcm^{-3})	= .607

Test No. 31 Rate of deform. ($cm\ sec^{-1}$) = 27

Load: Vert. scale: 1 div. = 1138 (kg)
Stroke: Horiz. scale: 1 div. = 1.27 (cm)

CRREL Form 42 (OT)
15 May 74

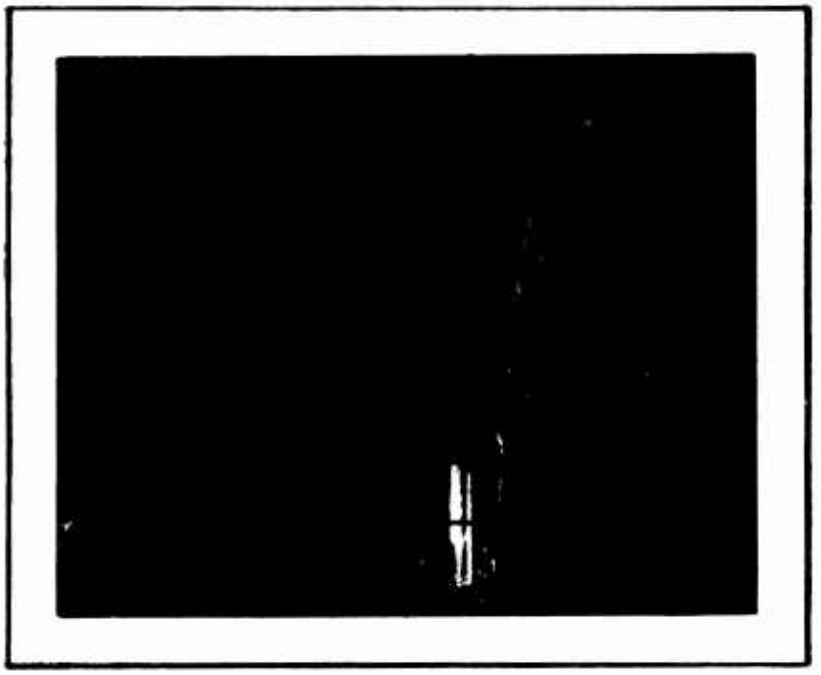

Date: 5 Apr 74

Sample

Snow type: Fresh, sublled

T	(°C)	= -20
d	(cm)	= 29.0
h_o	(cm)	= 7.6
A	(cm^2)	= 658
V_o	(cm^3)	= 5010
W	(g)	= 836
ρ_o	(gcm^{-3})	= .167
h_1	(cm)	= 2.13
V_1	(cm^3)	= 1400
ρ_1	(gcm^{-3})	= .597

Test No. 32 Rate of deform. ($cm\ sec^{-1}$) = 27

Load: Vert. scale: 1 div. = 227.5 (kg)
Stroke: Horiz. scale: 1 div. = 1.27 (cm)

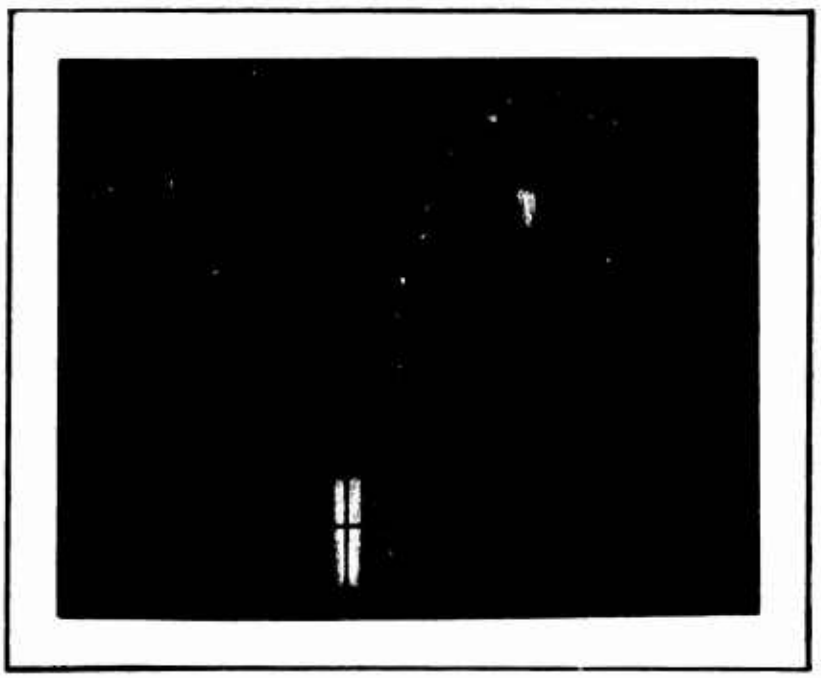

Date: 9 Apr 74

Sample

Snow type: Fresh

T	(°C)	= -1
d	(cm)	= 29.0
h_o	(cm)	= 10.2
A	(cm^2)	= 658
V_o	(cm^3)	= 6675
W	(g)	= 743
ρ_o	(gcm^{-3})	= .111
h_1	(cm)	= 1.9
V_1	(cm^3)	= 1249
ρ_1	(gcm^{-3})	= .595

Test No. 33 Rate of deform. ($cm\ sec^{-1}$) = 27

Load: Vert. scale: 1 div. = 227.5 (kg)
Stroke: Horiz. scale: 1 div. = 1.27 (cm)

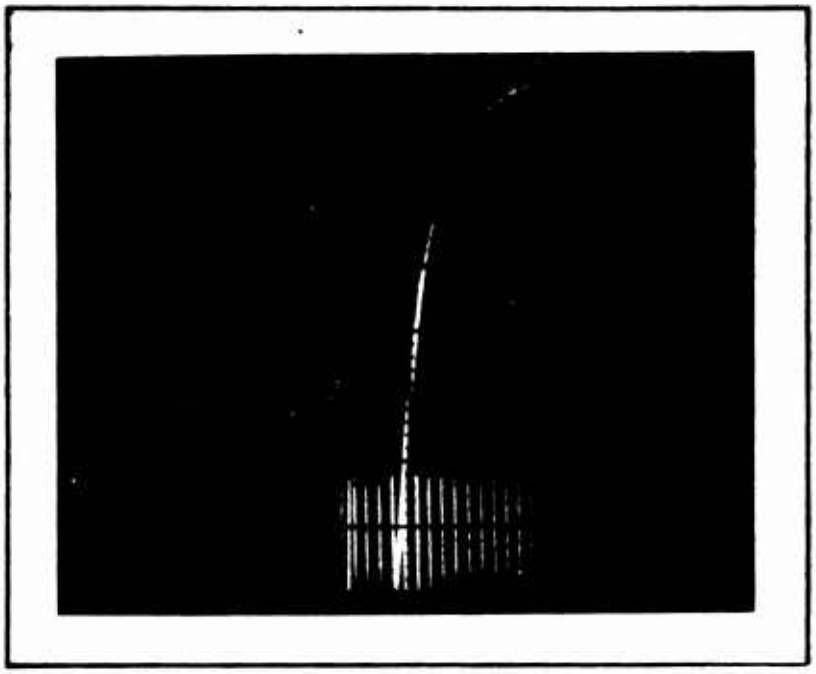

Date: 9 Apr 74

Sample

Snow type: Fresh

T	(^{o}C)	= -1
d	(cm)	= 29.0
h_o	(cm)	= 10.2
A	(cm^2)	= 658
V_o	(cm^3)	= 6675
W	(g)	= 788
ρ_o	(gcm^{-3})	= .118
h_1	(cm)	= 2.13
V_1	(cm^3)	= 1400
ρ_1	(gcm^{-3})	= .563

Test No. 34 Rate of deform. ($cm\ sec^{-1}$) = .27

Load: Vert. scale: 1 div. = 227.5 (kg)
Stroke: Horiz. scale: 1 div. = 1.27 (cm)

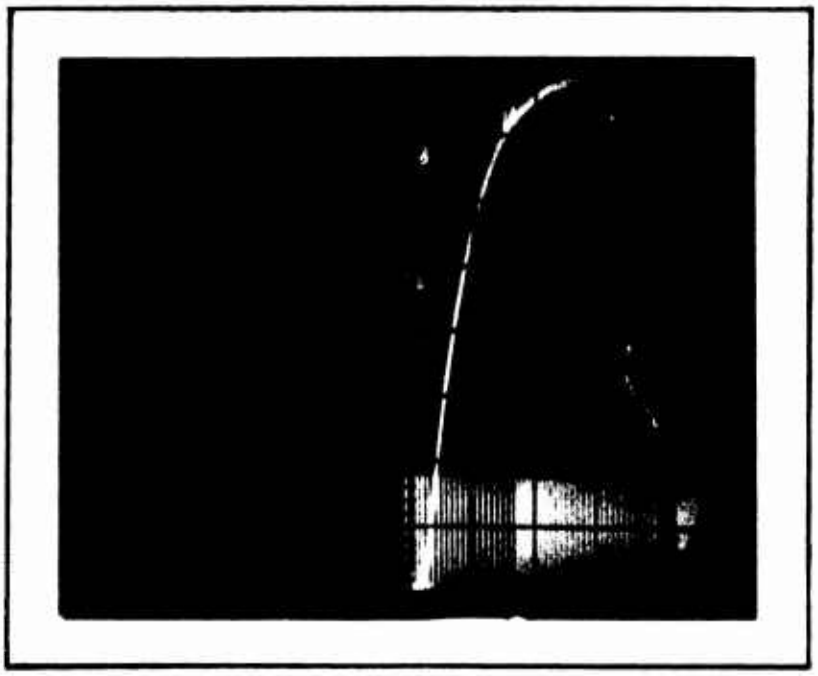

Date: 9 Apr 74

Sample

Snow type: Fresh

T	(^{o}C)	= -1
d	(cm)	= 29.0
h_o	(cm)	= 10.2
A	(cm^2)	= 658
V_o	(cm^3)	= 6675
W	(g)	= 850
ρ_o	(gcm^{-3})	= .127
h_1	(cm)	= 2.27
V_1	(cm^3)	= 1490
ρ_1	(gcm^{-3})	= .57

Test No. 35 Rate of deform. ($cm\ sec^{-1}$) = .027

Load: Vert. scale: 1 div. = 227.5 (kg)
Stroke: Horiz. scale: 1 div. = 1.27 (cm)

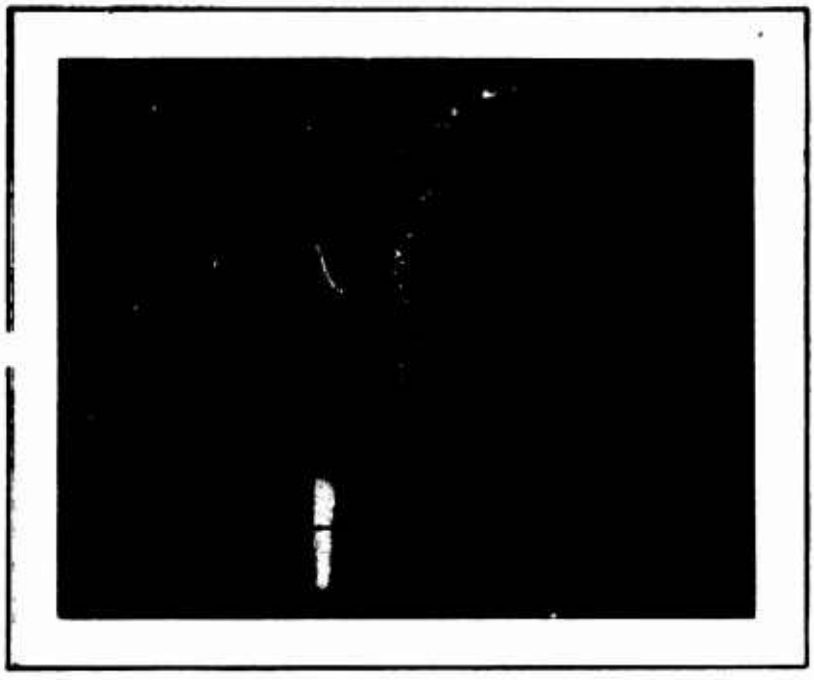

Date: 9 Apr 74

Sample

Snow type: Fresh

T	(°C)	= -1
d	(cm)	= 12.7
h_o	(cm)	= 5.1
A	(cm^2)	= 126.6
V_o	(cm^3)	= 643
W	(g)	= 84
ρ_o	(gcm^{-3})	= .131
h_1	(cm)	= .74
V_1	(cm^3)	= 93.6
ρ_1	(gcm^{-3})	= .896

Test No. 36 Rate of deform. ($cm\ sec^{-1}$) = 27

Load: Vert. scale: 1 div. = 227.5 (kg)
Stroke: Horiz. scale: 1 div. = .635 (cm)

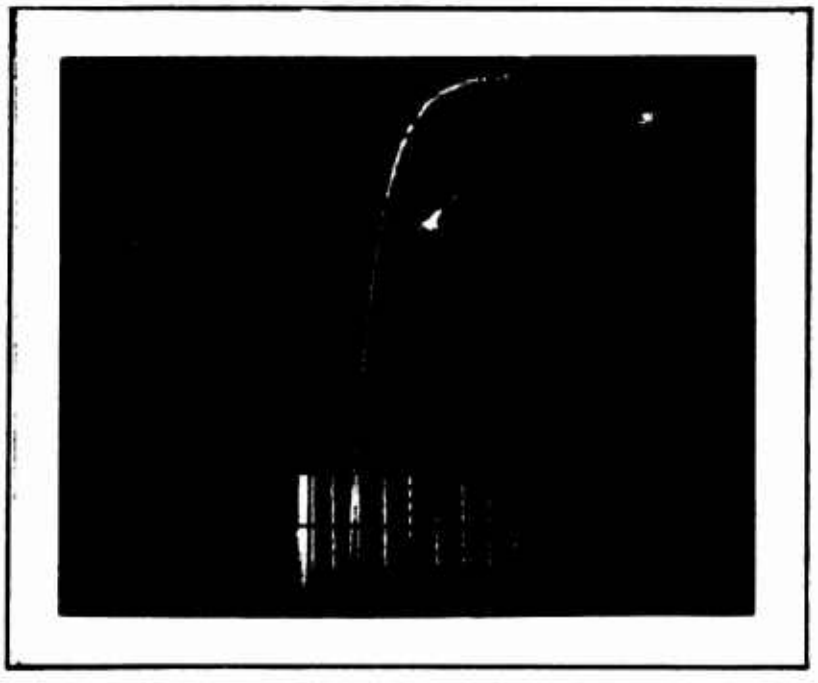

Date: 9 Apr 74

Sample

Snow type: Fresh

T	(°C)	= -1
d	(cm)	= 12.7
h_o	(cm)	= 5.1
A	(cm^2)	= 126.6
V_o	(cm^3)	= 643
W	(g)	= 60
ρ_o	(gcm^{-3})	= .093
h_1	(cm)	= .53
V_1	(cm^3)	= 67.1
ρ_1	(gcm^{-3})	= .894

Test No. 37 Rate of deform. ($cm\ sec^{-1}$) = .27

Load: Vert. scale: 1 div. = 227.5 (kg)
Stroke: Horiz. scale: 1 div. = .635 (cm)

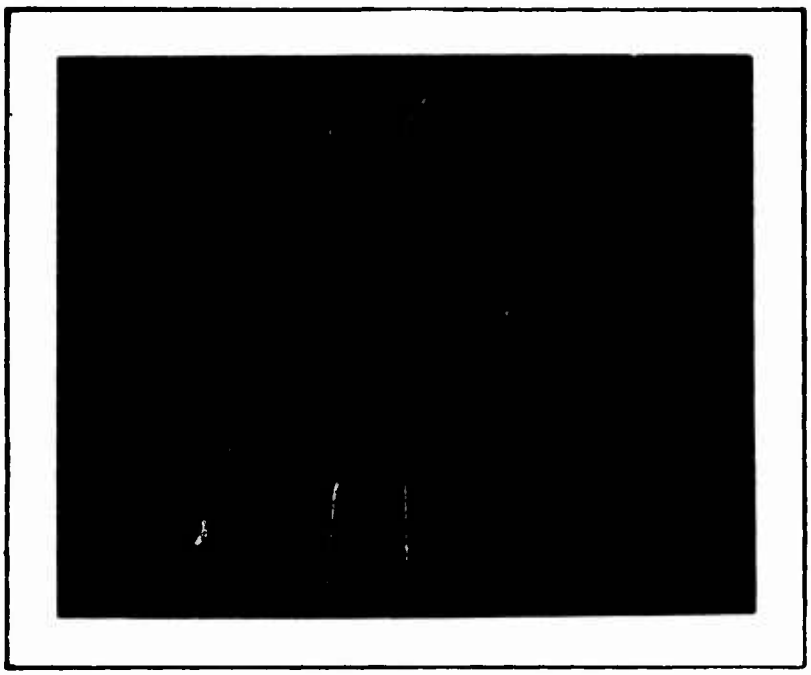

Date: 9 Apr 74

Sample

Snow type: Fresh

T	(^{o}C)	= -1
d	(cm)	= 12.7
h_o	(cm)	= 5.1
A	(cm^2)	= 126.6
V_o	(cm^3)	= 643
W	(g)	= 58
ρ_o	(gcm^{-3})	= .090
h_1	(cm)	= .52
V_1	(cm^3)	= 65.8
ρ_1	(gcm^{-3})	= .882

Test No. 38 Rate of deform. ($cm\ sec^{-1}$) = .027

Load: Vert. scale: 1 div. = 227.5 (kg)
Stroke: Horiz. scale: 1 div. = .635 (cm)

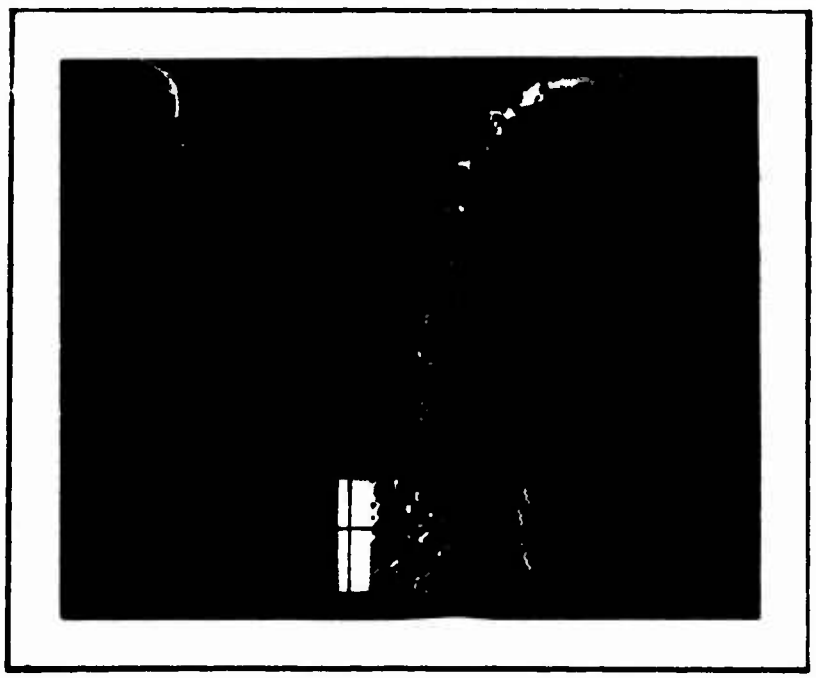

Date: 9 Apr 74

Sample

Snow type: Fresh, settled

T	(^{o}C)	= -1
d	(cm)	= 12.7
h_o	(cm)	= 5.1
A	(cm^2)	= 126.6
V_o	(cm^3)	= 643
W	(g)	= 113
ρ_o	(gcm^{-3})	= .176
h_1	(cm)	= .99
V_1	(cm^3)	= 125
ρ_1	(gcm^{-3})	= .904

Test No. 39 Rate of deform. ($cm\ sec^{-1}$) = 27

Load: Vert. scale: 1 div. = 227.5 (kg)
Stroke: Horiz. scale: 1 div. = .635 (cm)

CRREL Form 42 (OT)
15 May 74

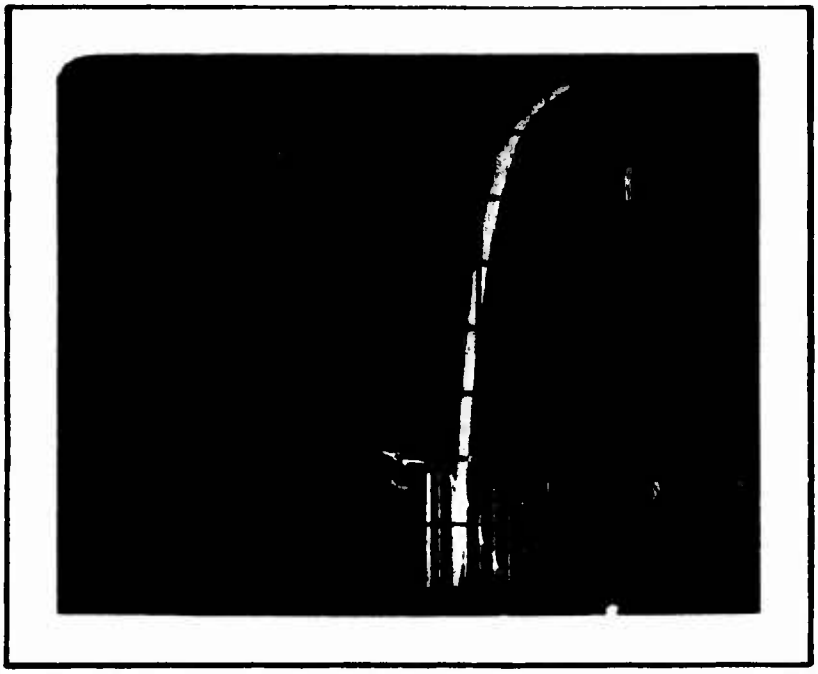

Date: 10 Apr 74

Sample

Snow type: fresh

T	(°C)	= -20
d	(cm)	= 29.0
h_o	(cm)	= 7.6
A	(cm^2)	= 658
V_o	(cm^3)	= 5010
W	(g)	= 562
ρ_o	(gcm^{-3})	= .112
h_1	(cm)	= 1.52
V_1	(cm^3)	= 1000
ρ_1	(gcm^{-3})	= .562

Test No. 40 Rate of deform. ($cm\ sec^{-1}$) = .27

Load: Vert. scale: 1 div. = 227.5 (kg)
Stroke: Horiz. scale: 1 div. = 1.27 (cm)

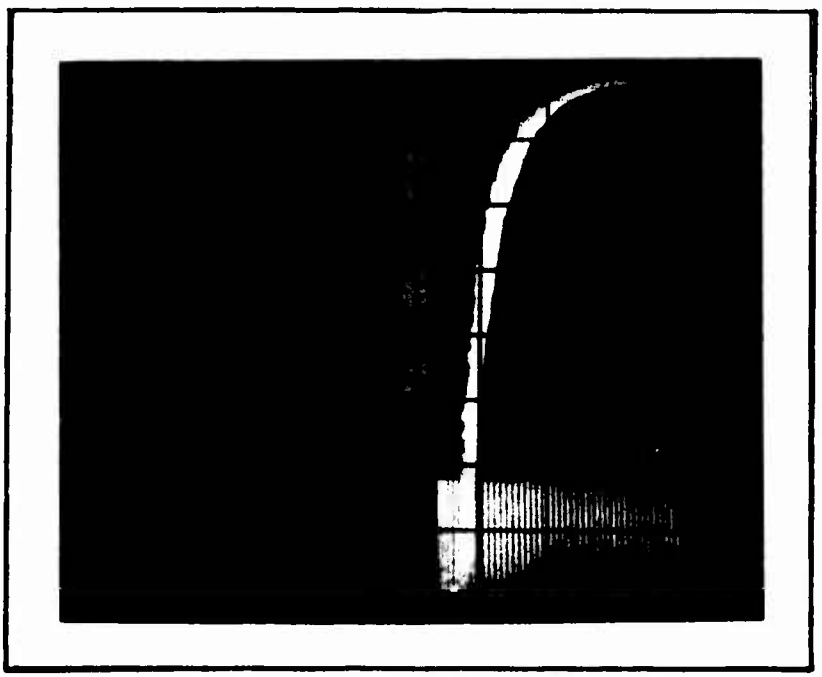

Date: 10 Apr 74

Sample

Snow type: fresh

T	(°C)	= -20
d	(cm)	= 29.0
h_o	(cm)	= 7.6
A	(cm^2)	= 658
V_o	(cm^3)	= 5010
W	(g)	= 569
ρ_o	(gcm^{-3})	= .113
h_1	(cm)	= 1.59
V_1	(cm^3)	= 1045
ρ_1	(gcm^{-3})	= .545

Test No. 41 Rate of deform. ($cm\ sec^{-1}$) = .027

Load: Vert. scale: 1 div. = 227.5 (kg)
Stroke: Horiz. scale: 1 div. = 1.27 (cm)

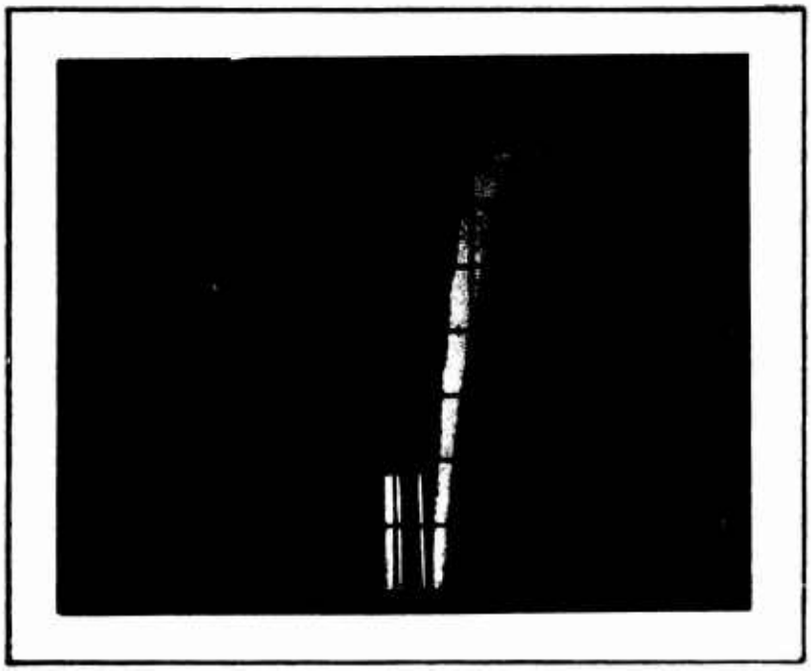

Date: 10 Apr 74

Sample

Snow type: Fresh, settled

T	(^{o}C)	= -20
d	(cm)	= 20.3
h_o	(cm)	= 5.1
A	(cm^2)	= 323.3
V_o	(cm^3)	= 1633
W	(g)	= 301
ρ_o	(gcm^{-3})	= .184
h_1	(cm)	= 1.31
V_1	(cm^3)	= 423
ρ_1	(gcm^{-3})	= .712

Test No. 42 Rate of deform. ($cm\ sec^{-1}$) = .27

Load: Vert. scale: 1 div. = 227.5 (kg)
Stroke: Horiz. scale: 1 div. = .635 (cm)

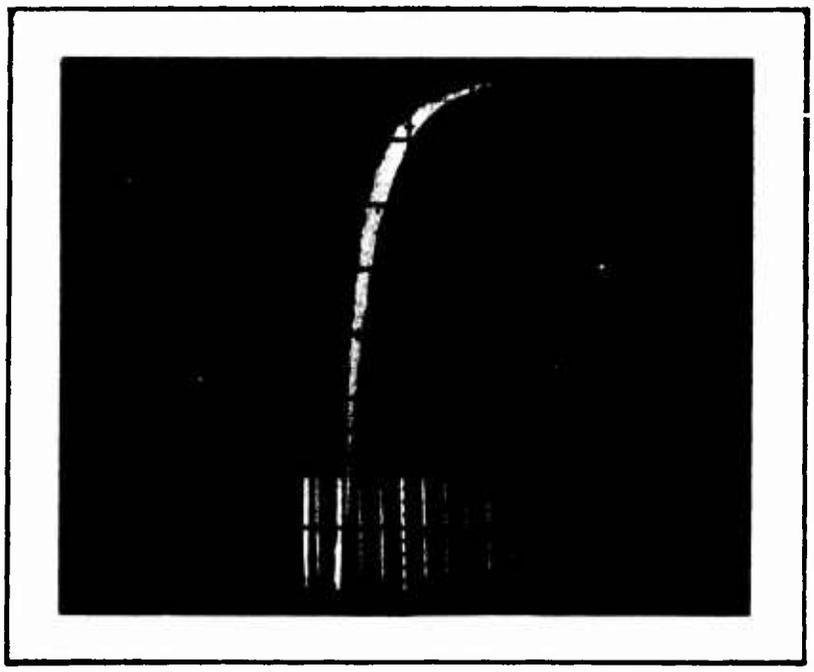

Date: 10 Apr 74

Sample

Snow type: Fresh

T	(^{o}C)	= -20
d	(cm)	= 20.3
h_o	(cm)	= 5.1
A	(cm^2)	= 323.3
V_o	(cm^3)	= 1633
W	(g)	= 170
ρ_o	(gcm^{-3})	= .104
h_1	(cm)	= .80
V_1	(cm^3)	= 258
ρ_1	(gcm^{-3})	= .660

Test No. 43 Rate of deform. ($cm\ sec^{-1}$) = .027

Load: Vert. scale: 1 div. = 227.5 (kg)
Stroke: Horiz. scale: 1 div. = .635 (cm)

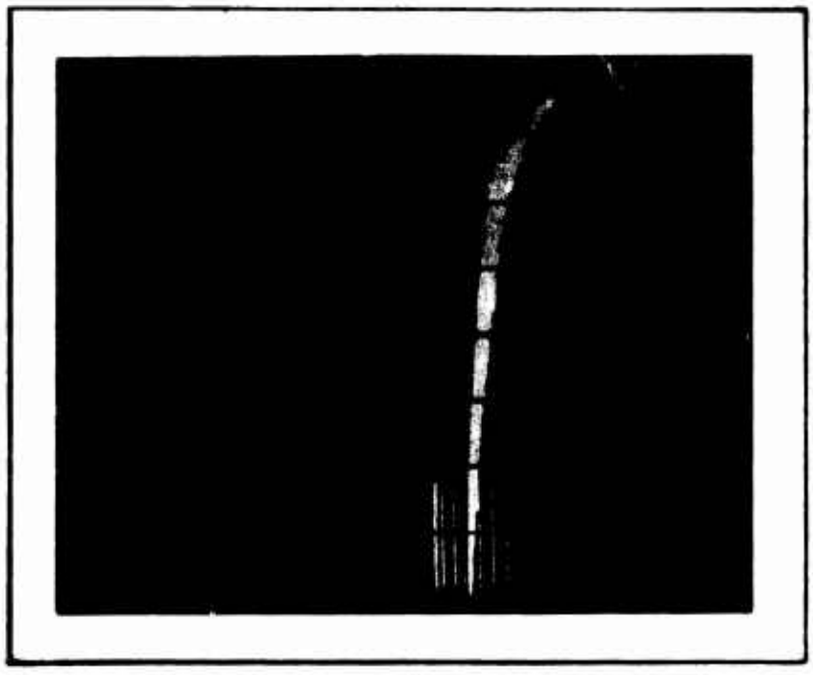

Date: 10 Apr 74

Sample

Snow type: Fresh, cooled

T	(^{o}C)	= -35
d	(cm)	= 20.3
h_o	(cm)	= 7.6
A	(cm^2)	= 323.3
V_o	(cm^3)	= 2460
W	(g)	= 400
ρ_o	(gcm^{-3})	= .162
h_1	(cm)	= 1.97
V_1	(cm^3)	= 637
ρ_1	(gcm^{-3})	= .628

Test No. 44 Rate of deform. ($cm\ sec^{-1}$) = .27

Load: Vert. scale: 1 div. = 227.5 (kg)
Stroke: Horiz. scale: 1 div. = 1.27 (cm)

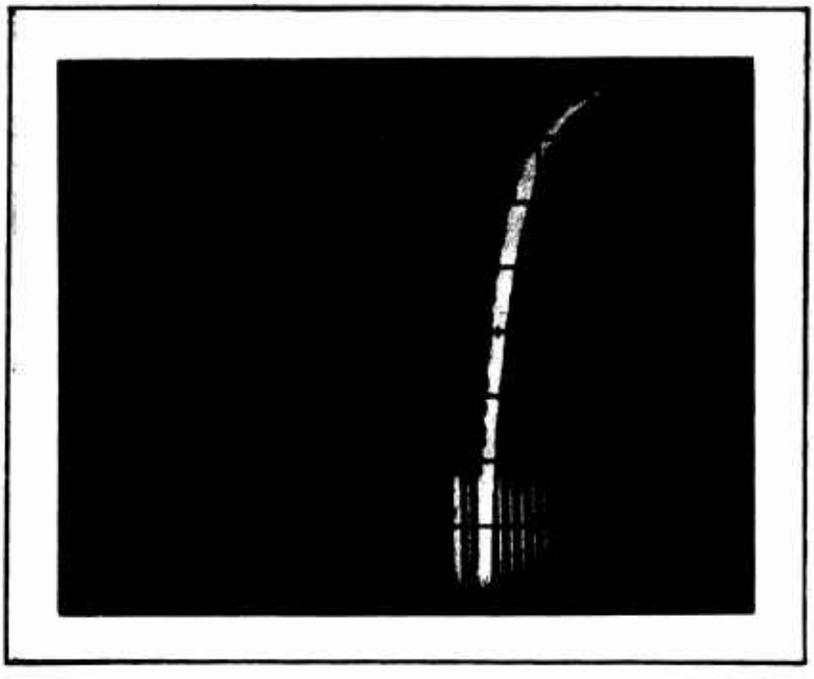

Date: 10 Apr 74

Sample

Snow type: Fresh, cooled

T	(^{o}C)	= -35
d	(cm)	= 20.3
h_o	(cm)	= 7.6
A	(cm^2)	= 323.3
V_o	(cm^3)	= 2460
W	(g)	= 407
ρ_o	(gcm^{-3})	= .165
h_1	(cm)	= 2.0
V_1	(cm^3)	= 647
ρ_1	(gcm^{-3})	= .629

Test No. 45 Rate of deform. ($cm\ sec^{-1}$) = .027

Load: Vert. scale: 1 div. = 227.5 (kg)
Stroke: Horiz. scale: 1 div. = 1.27 (cm)

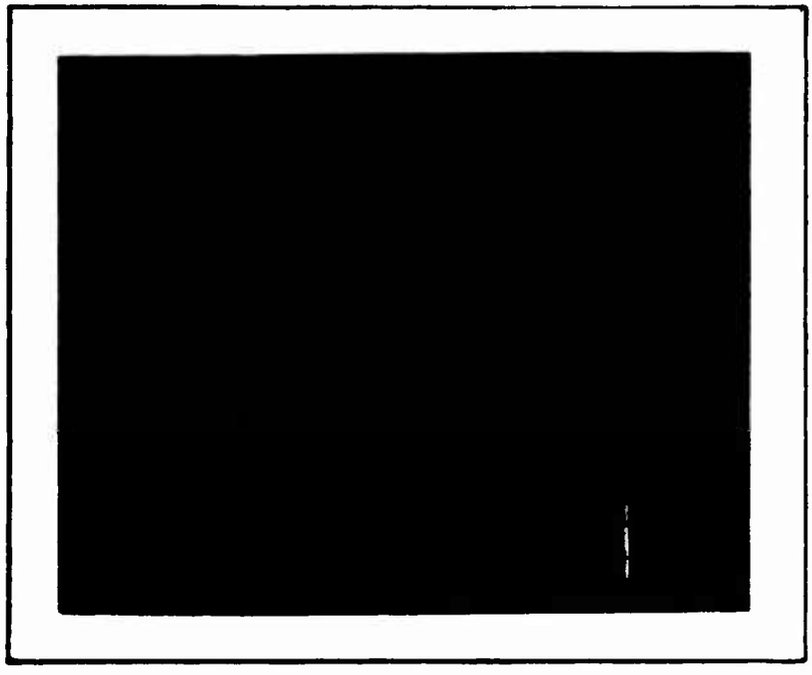

Date: 10 Apr 74

Sample

Snow type: Fresh, cooled

T	(^oC)	= -35.
d	(cm)	= 12.7
h_o	(cm)	= 2.5
A	(cm^2)	= 126.6
V_o	(cm^3)	= 321.5
W	(g)	= 37
ρ_o	(gcm^{-3})	= .115
h_1	(cm)	= .40
V_1	(cm^3)	= 50.6
ρ_1	(gcm^{-3})	= .731

Test No. 46 Rate of deform. ($cm\ sec^{-1}$) = .27

Load: Vert. scale: 1 div. = 569 (kg)
Stroke: Horiz. scale: 1 div. = 1.27 (cm)

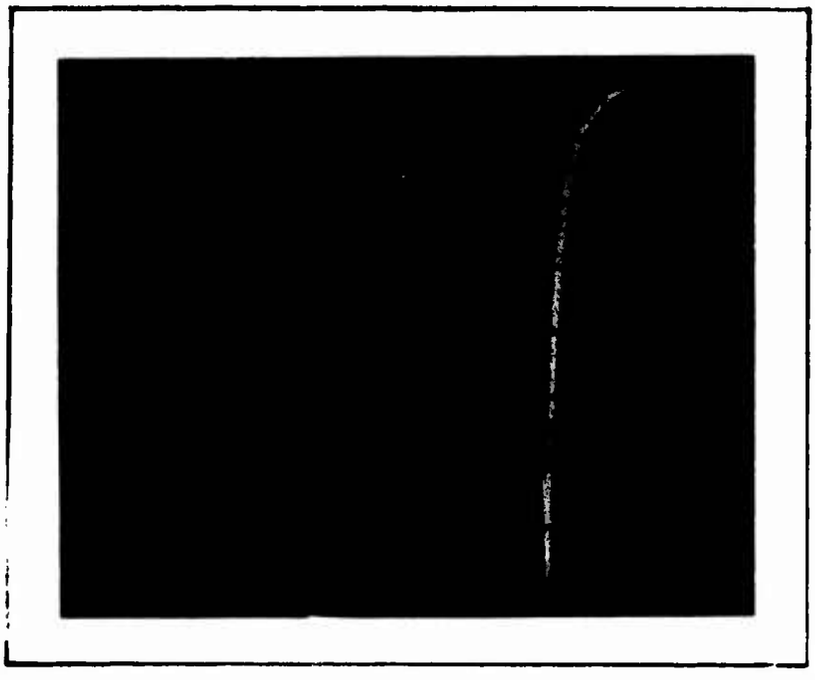

Date: 10 Apr 74

Sample

Snow type: Fresh, cooled

T	(^oC)	= -35
d	(cm)	= 12.7
h_o	(cm)	= 3.5
A	(cm^2)	= 126.6
V_o	(cm^3)	= 321.5
W	(g)	= 39
ρ_o	(gcm^{-3})	= .121
h_1	(cm)	= .42
V_1	(cm^3)	= 53
ρ_1	(gcm^{-3})	= .736

Test No. 47 Rate of deform. ($cm\ sec^{-1}$) = .027

Load: Vert. scale: 1 div. = 227.5 (kg)
Stroke: Horiz. scale: 1 div. = .635 (cm)

CRREL Form 42 (OT)
15 May 74

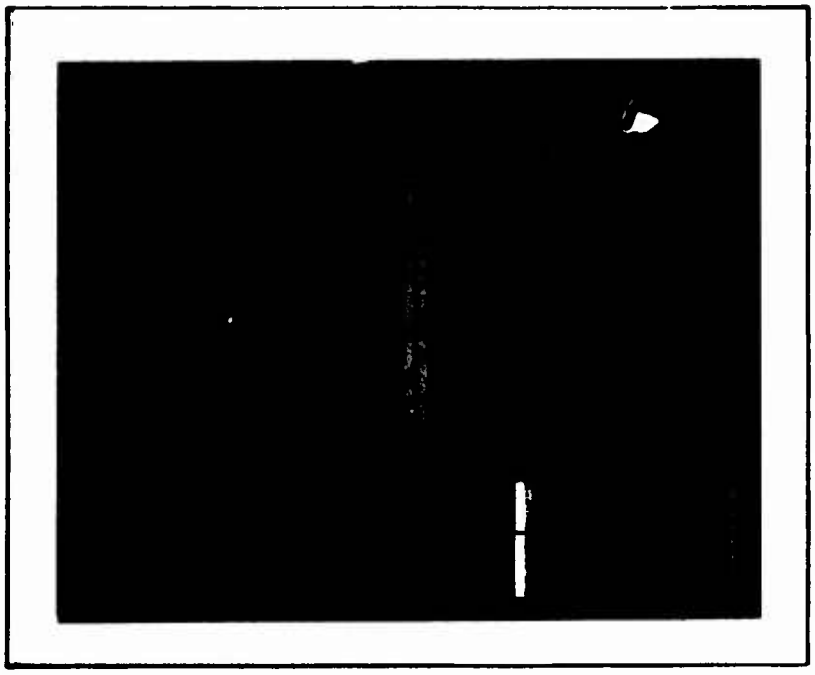

Date: 11 Apr 74

Sample

Snow type: fresh

T	(^{o}C)	= -3
d	(cm)	= 12.7
h_o	(cm)	= 2.5
A	(cm^2)	= 126.6
V_o	(cm^3)	= 321.5
W	(g)	= 33.5
ρ_o	(gcm^{-3})	= .104
h_1	(cm)	= .30
V_1	(cm^3)	= 38.0
ρ_1	(gcm^{-3})	= .884

Test No. 15 Rate of deform. ($cm\ sec^{-1}$) = 27

Load: Vert. scale: 1 div. = 227.5 (kg)
Stroke: Horiz. scale: 1 div. = .635 (cm)

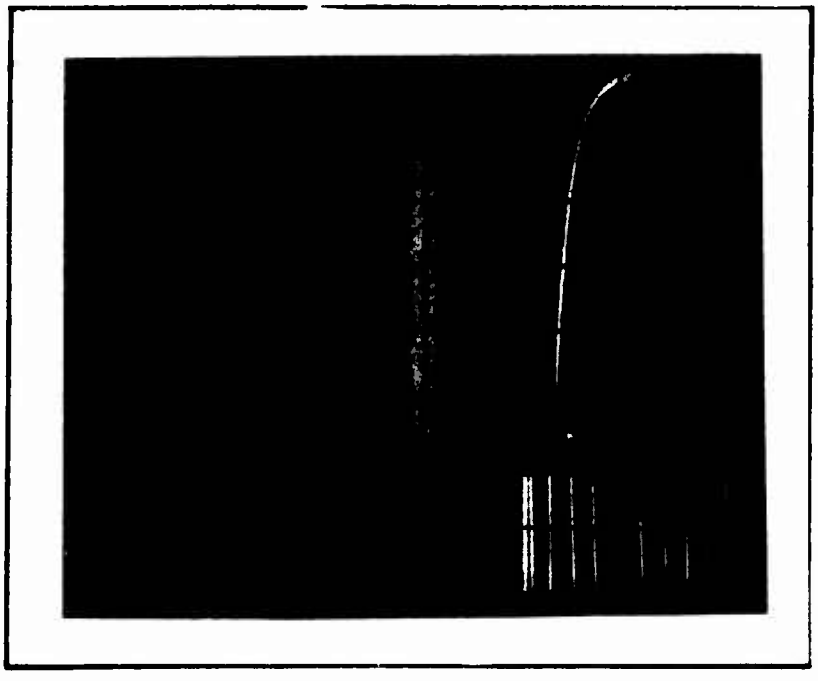

Date: 11 Apr 74

Sample

Snow type: fresh

T	(^{o}C)	= -3
d	(cm)	= 12.7
h_o	(cm)	= 2.5
A	(cm^2)	= 126.6
V_o	(cm^3)	= 321.5
W	(g)	= 36.0
ρ_o	(gcm^{-3})	= .112
h_1	(cm)	= .33
V_1	(cm^3)	= 41.8
ρ_1	(gcm^{-3})	= .862

Test No. 49 Rate of deform. ($cm\ sec^{-1}$) = .027

Load: Vert. scale: 1 div. = 227.5 (kg)
Stroke: Horiz. scale: 1 div. = .635 (cm)

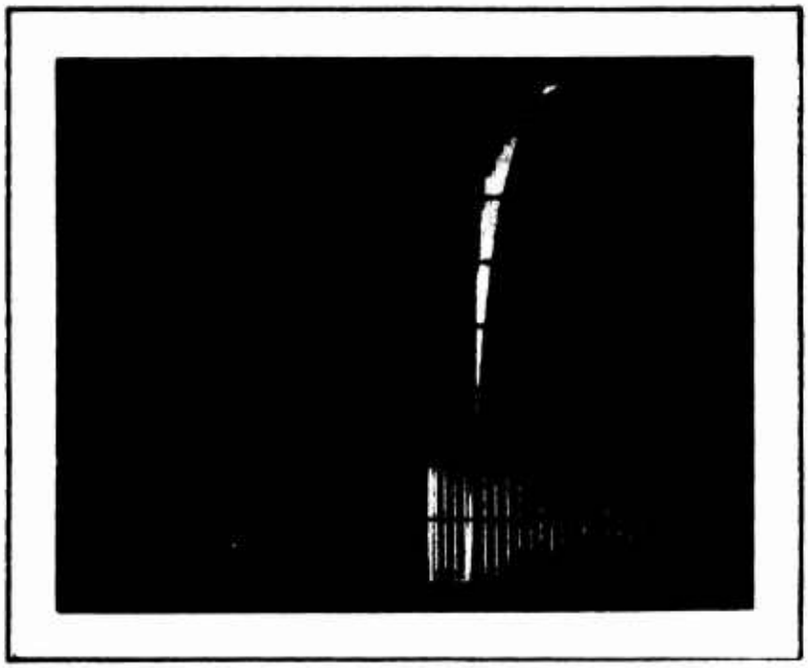

Date: 11 Apr 74

Sample

Snow type: Fresh

T	(^{o}C)	= -3
d	(cm)	= 20.3
h_o	(cm)	= 7.6
A	(cm^2)	= 323.3
V_o	(cm^3)	= 2460
W	(g)	= 343
ρ_o	(gcm^{-3})	= .139
h_1	(cm)	= 1.6
V_1	(cm^3)	= 517.5
ρ_1	(gcm^{-3})	= .663

Test No. 50 Rate of deform. ($cm\ sec^{-1}$) = .027

Load: Vert. scale: 1 div. = 227.5 (kg)
Stroke: Horiz. scale: 1 div. = 1.27 (cm)

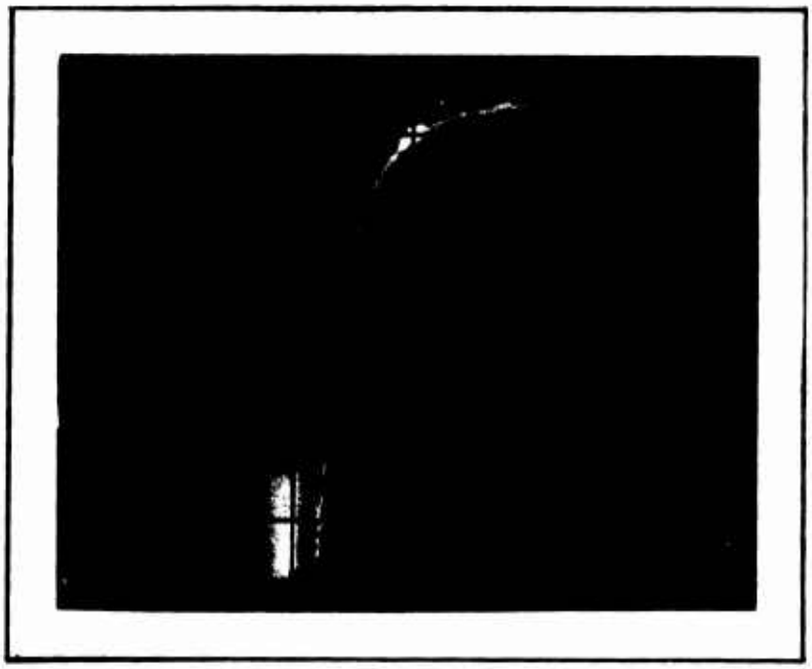

Date: 11 Apr 74

Sample

Snow type: Fresh

T	(^{o}C)	= -3
d	(cm)	= 20.0
h_o	(cm)	= 12.7
A	(cm^2)	= 658
V_o	(cm^3)	= 8350
W	(g)	= 1082
ρ_o	(gcm^{-3})	= .13
h_1	(cm)	= 2.6
V_1	(cm^3)	= 1710
ρ_1	(gcm^{-3})	= .634

Test No. 51 Rate of deform. ($cm\ sec^{-1}$) = 27

Load: Vert. scale: 1 div. = 227.5 (kg)
Stroke: Horiz. scale: 1 div. = 1.27 (cm)

CRREL Form 42 (OT)
15 May 74

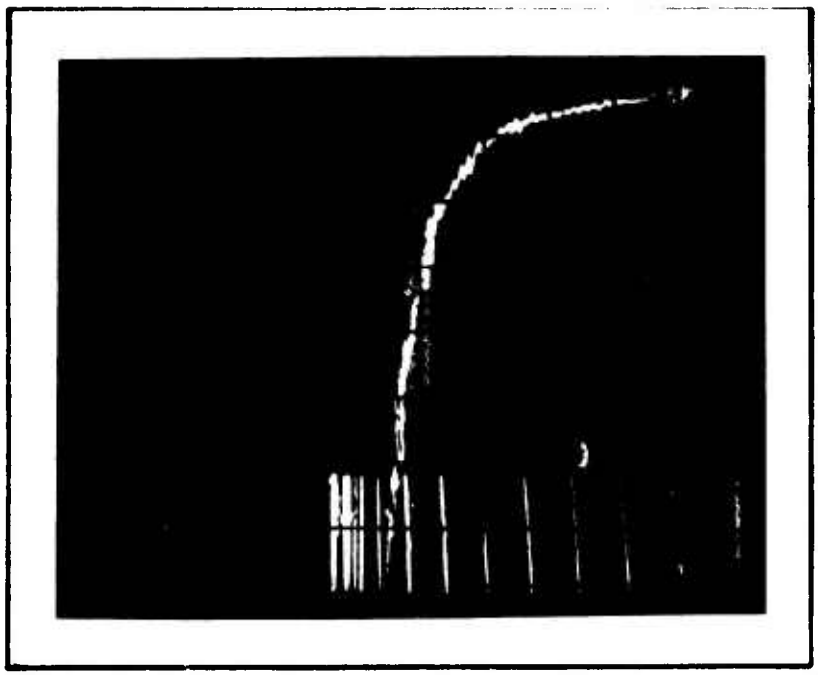

Date: 11 Apr 74

Sample

Snow type: Fresh, cooled

T	(°C)	= -20
d	(cm)	= 29.0
h_o	(cm)	= 12.7
A	(cm^2)	= 658
V_o	(cm^3)	= 8350
W	(g)	= 1300
ρ_o	(gcm^{-3})	= .166
h_1	(cm)	= 4.25
V_1	(cm^3)	= 2795
ρ_1	(gcm^{-3})	= .498

Test No. 52 Rate of deform. ($cm\ sec^{-1}$) = 27

Load: Vert. scale: 1 div. = 227.5 (kg)
Stroke: Horiz. scale: 1 div. = 1.27 (cm)

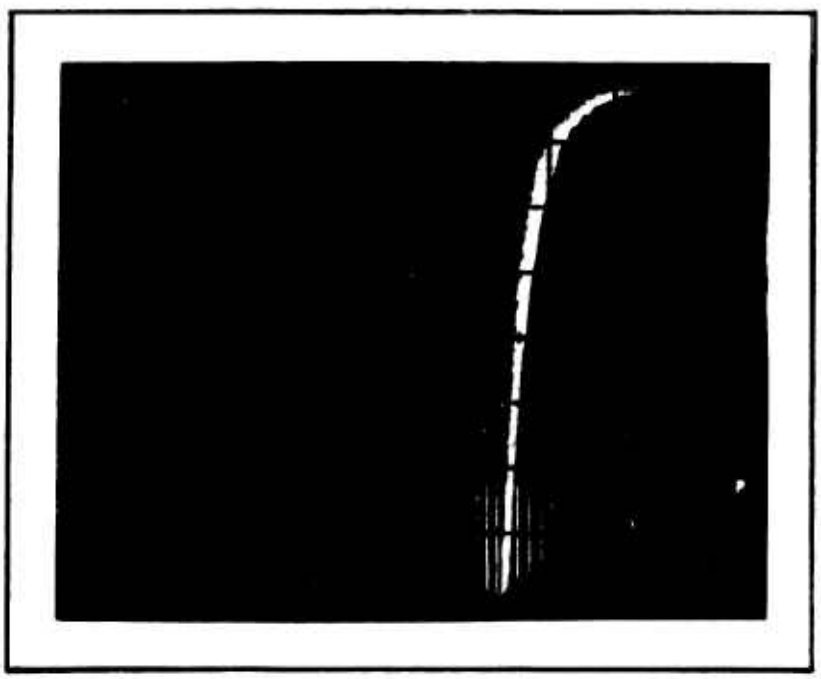

Date: 11 Apr 74

Sample

Snow type: Fresh, cooled

T	(°C)	= -20
d	(cm)	= 29.0
h_o	(cm)	= 7.6
A	(cm^2)	= 658
V_o	(cm^3)	= 5010
W	(g)	= 1139
ρ_o	(gcm^{-3})	= .227
h_1	(cm)	= 2.9
V_1	(cm^3)	= 1907
ρ_1	(gcm^{-3})	= .597

Test No. 53 Rate of deform. ($cm\ sec^{-1}$) = .027

Load: Vert. scale: 1 div. = 227.5 (kg)
Stroke: Horiz. scale: 1 div. = 1.27 (cm)

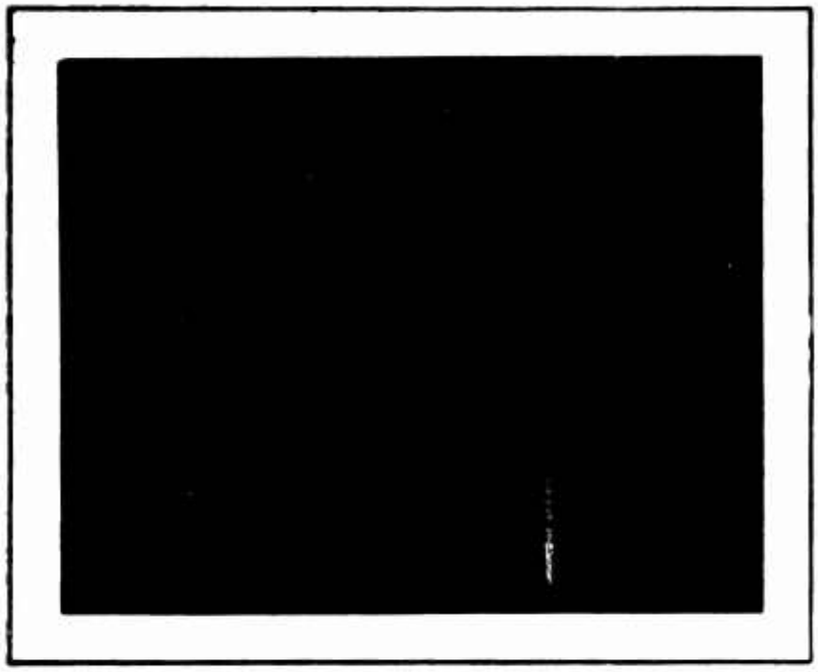

Date: 11 Apr 74

Sample

Snow type: Fresh, cooled

T	(°C)	= -20
d	(cm)	= 12.7
h_o	(cm)	= 2.5
A	(cm^2)	= 126.6
V_o	(cm^3)	= 321.5
W	(g)	= 56.5
ρ_o	(gcm^{-3})	= .176
h_1	(cm)	= .57
V_1	(cm^3)	= 72.1
ρ_1	(gcm^{-3})	= .784

Test No. 54 Rate of deform. ($cm\ sec^{-1}$) = 27

Load: Vert. scale: 1 div. = 227.5 (kg)
Stroke: Horiz. scale: 1 div. = .635 (cm)

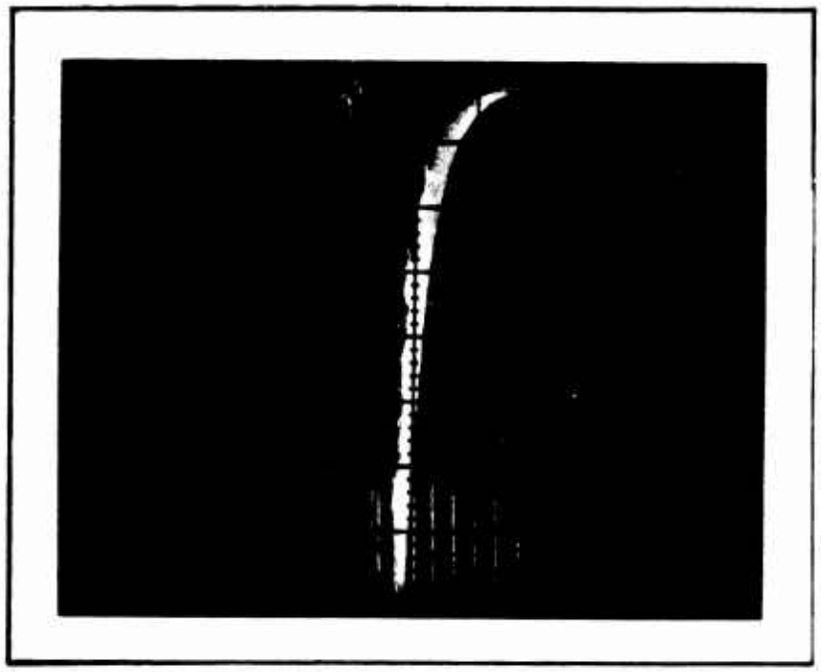

Date: 11 Apr 74

Sample

Snow type: Fresh, cooled

T	(°C)	= -20
d	(cm)	= 12.7
h_o	(cm)	= 5.1
A	(cm^2)	= 126.6
V_o	(cm^3)	= 643
W	(g)	= 112.5
ρ_o	(gcm^{-3})	= .175
h_1	(cm)	= 1.2
V_1	(cm^3)	= 152
ρ_1	(gcm^{-3})	= .740

Test No. 55 Rate of deform. ($cm\ sec^{-1}$) = .027

Load: Vert. scale: 1 div. = 227.5 (kg)
Stroke: Horiz. scale: 1 div. = .635 (cm)

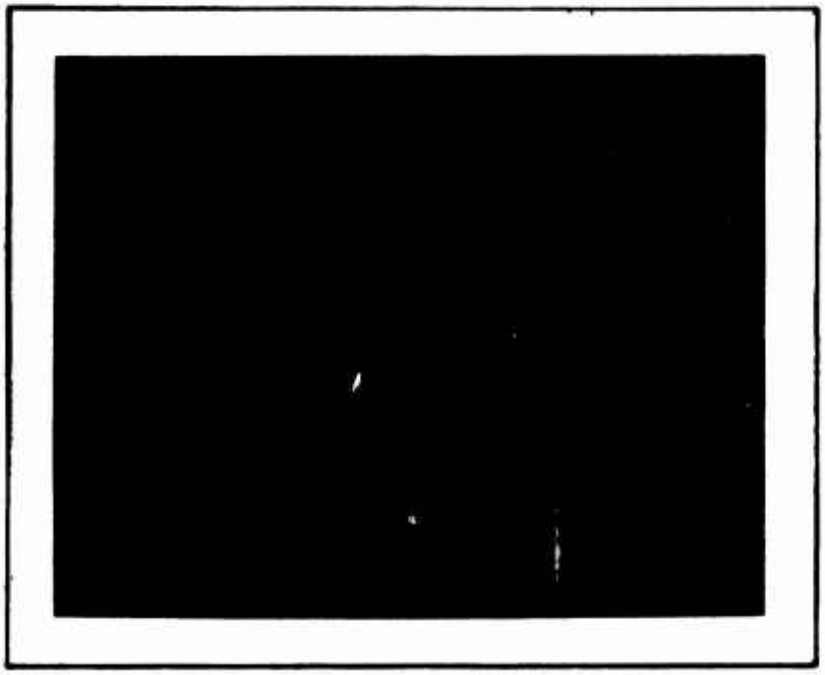

Date: 11 Apr 74

Sample

Snow type: Fresh, cooled

T	(^{o}C)	= -35
d	(cm)	= 12.7
h_o	(cm)	= 2.5
A	(cm^2)	= 126.6
V_o	(cm^3)	= 321.5
W	(g)	= 59
ρ_o	(gcm^{-3})	= .184
h_1	(cm)	= .64
V_1	(cm^3)	= 81
ρ_1	(gcm^{-3})	= .728

Test No. 56 Rate of deform. ($cm\ sec^{-1}$) = 27

Load: Vert. scale: 1 div. = 227.5 (kg)
Stroke: Horiz. scale: 1 div. = .635 (cm)

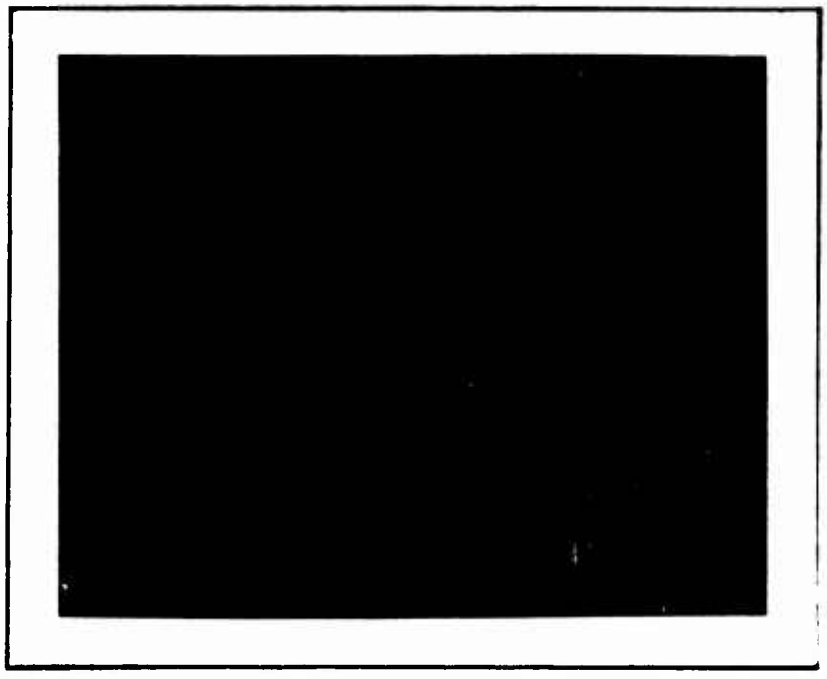

Date: 11 Apr 74

Sample

Snow type: Fresh, cooled

T	(^{o}C)	= -35
d	(cm)	= 12.7
h_o	(cm)	= 2.5
A	(cm^2)	= 126.6
V_o	(cm^3)	= 321.5
W	(g)	= 58
ρ_o	(gcm^{-3})	= .181
h_1	(cm)	= .63
V_1	(cm^3)	= 79.7
ρ_1	(gcm^{-3})	= .728

Test No. 57 Rate of deform. ($cm\ sec^{-1}$) = .027

Load: Vert. scale: 1 div. = 227.5 (kg)
Stroke: Horiz. scale: 1 div. = .635 (cm)

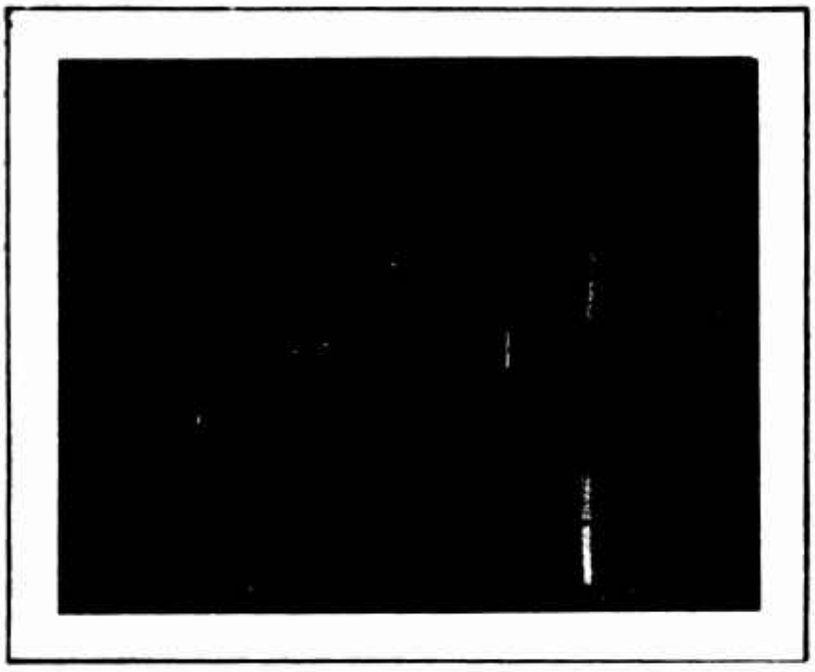

Date: 11 Apr 74

Sample

Snow type: Old

T	(^{o}C)	= -20
d	(cm)	= 12.7
h_o	(cm)	= 2.5
A	(cm^2)	= 126.6
V_o	(cm^3)	= 321.5
W	(g)	= 84
ρ_o	(gcm^{-3})	= .261
h_1	(cm)	= .87
V_1	(cm^3)	= 110
ρ_1	(gcm^{-3})	= .764

Test No. 58 Rate of deform. ($cm\ sec^{-1}$) = 27

Load: Vert. scale: 1 div. = 2275 (kg)
Stroke: Horiz. scale: 1 div. = .635 (cm)

Date: 11 Apr 74

Sample

Snow type: Old

T	(^{o}C)	= -35
d	(cm)	= 20.3
h_o	(cm)	= 7.5
A	(cm^2)	= 323.3
V_o	(cm^3)	= 2421
W	(g)	= 347
ρ_o	(gcm^{-3})	= .143
h_1	(cm)	= 1.6
V_1	(cm^3)	= 517.5
ρ_1	(gcm^{-3})	= .671

Test No. 59 Rate of deform. ($cm\ sec^{-1}$) = 27

Load: Vert. scale: 1 div. = 227.5 (kg)
Stroke: Horiz. scale: 1 div. = .635 (cm)